

# **Characterisation of hair follicle stem cell function in epidermal regeneration and tumourigenesis**

Inaugural-Dissertation

zur

Erlangung des Doktorgrades

der Mathematisch-Naturwissenschaftlichen Fakultät

der Universität zu Köln

vorgelegt von

Monika Petersson

aus Düsseldorf

Köln 2010

Berichterstatter:

Prof. Dr. Jens Brüning

Prof. Dr. Dr. h.c. Thomas Krieg

Tag der mündlichen Prüfung: 02.07.2010



# Table of Contents

<b>1</b>	<b>Introduction.....</b>	<b>1</b>
1.1	Organisation of the skin.....	1
1.2	The epidermis.....	2
1.2.1	The interfollicular epidermis (IFE) .....	2
1.2.2	The hair follicle (HF) .....	2
1.2.3	The sebaceous gland (SG) .....	4
1.3	Epidermal homeostasis.....	5
1.3.1	SC characteristics and identification .....	5
1.3.2	Assays to test SC identity.....	5
1.3.3	Epidermal SC compartments .....	6
1.3.3.1	SCs in the IFE .....	6
1.3.3.2	SCs of the HF bulge .....	6
1.3.3.3	SC/progenitor reservoirs of the isthmus .....	7
1.3.4	Bipotent progenitors at the JZ .....	8
1.3.5	Epidermal regeneration .....	10
1.3.5.1	Regeneration of the IFE .....	10
1.3.5.2	Cyclic regeneration of the HF .....	10
1.3.5.3	Homeostasis of the SG.....	11
1.4	Regulation of epidermal regeneration .....	12
1.4.1	Wnt/ $\beta$ -catenin signalling .....	12
1.4.2	Impaired Wnt/ $\beta$ -Catenin signalling results in a disturbed tissue homeostasis .....	14
1.4.3	Deregulated Wnt/ $\beta$ -catenin signalling causes skin cancer .....	15
1.5	The rationale of cancer stem cells .....	16
1.5.1	Characteristics of CSC .....	16
1.5.2	Identification of CSC.....	17
1.5.3	Controversies .....	17
1.6	Objectives.....	18

<b>2</b>	<b>Material and Methods</b>	<b>19</b>
<b>2.1</b>	<b>Chemicals and reagents</b>	<b>19</b>
<b>2.2</b>	<b>Molecular Biology</b>	<b>19</b>
2.2.1	Isolation of genomic DNA (gDNA)	19
2.2.2	PCR	20
2.2.3	qRTPCR	21
2.2.4	Agarose gel electrophoresis and DNA gel extraction	22
2.2.5	Cloning procedures	22
2.2.5.1	Transformation and isolation of plasmid DNA	22
2.2.5.2	Cloning of pK15CreER(G)T2	22
2.2.5.3	Purification of K15CreER(G)T2 for microinjection	23
2.2.5.4	Cloning of pK15 $\Delta$ NLef1	23
2.2.5.5	Purification of K15 $\Delta$ NLef1 for microinjection	24
2.2.5.6	DNA sequencing	24
<b>2.3</b>	<b>Cell biology</b>	<b>25</b>
2.3.1	Histological analyses	25
2.3.1.1	Immunofluorescent stainings	25
2.3.1.2	Antibodies	25
2.3.2	$\beta$ -Galactosidase staining <i>in vivo/in vitro</i>	26
2.3.3	Isolation of primary keratinocytes	26
2.3.4	Cultivation of cells	27
2.3.5	Passaging of cells	27
2.3.6	FACS-sorting	27
2.3.7	Transfection of primary keratinocytes	28
2.3.8	Tamoxifen treatment <i>in vitro</i>	28
<b>2.4</b>	<b><i>In vivo</i> studies</b>	<b>28</b>
2.4.1	Mouse models	28
2.4.1.1	Generation of K15CreER(G)T2	28
2.4.1.2	Generation of K15 $\Delta$ NLef1	29
2.4.1.3	Cre-reporter lines	29

2.4.1.4	K14 $\Delta$ NLef1 .....	29
2.4.2	Tumour experiments .....	29
2.4.3	Tamoxifen treatment .....	29
2.4.4	Generation of label retaining cells (LRC) .....	30
2.4.5	Tissue harvesting .....	30
2.4.5.1	Isolation of epidermal whole mounts .....	30
<b>2.5</b>	<b>Statistical analysis .....</b>	<b>31</b>
<b>3</b>	<b>Results .....</b>	<b>32</b>
<b>3.1</b>	<b>Epidermal regeneration during skin homeostasis .....</b>	<b>32</b>
3.1.1	Stem cell and progenitor niches within the epidermis .....	32
<b>3.2</b>	<b>Generation of K15CreER(G)T2 transgenic mice .....</b>	<b>35</b>
3.2.1	Cloning of pK15CreER(G)T2 .....	36
3.2.2	Functionality of pK15CreER(G)T2 <i>in vitro</i> .....	37
3.2.3	Identification of K15CreER(G)T2 founder lines .....	39
3.2.4	Specific targeting of bulge cells using K15CreER(G)T2 mice .....	40
3.2.4.1	Optimisation of the application and detection protocol using K14CreER(G)T2 mice .....	40
3.2.4.2	Identification of two specific K15CreER(G)T2 founder lines .....	41
<b>3.3</b>	<b>Characterisation of targeted bulge SC .....</b>	<b>44</b>
3.3.1	Genetically labelled cells co-localise with SC markers of the HFSC compartment .....	44
3.3.2	Multipotency of targeted HFSC .....	45
3.3.3	HFSC-derived progeny drives SG regeneration during resting phase of the hair cycle .....	48
<b>3.4</b>	<b>Renewal of the SG is a continuous process .....</b>	<b>50</b>
<b>3.5</b>	<b>Regeneration of the HFSC compartment and the SG in long-term studies .....</b>	<b>52</b>
<b>3.6</b>	<b>Transition of bulge-derived progeny through different epidermal progenitor niches .....</b>	<b>54</b>
<b>3.7</b>	<b>HFSC-derived progeny expresses marker molecules for sebaceous lineage commitment .....</b>	<b>56</b>
<b>3.8</b>	<b>Ectopic SG formation is driven by HFSC .....</b>	<b>58</b>

3.8.1	Expression of SC and progenitor markers in K14 $\Delta$ NLef1 mice .....	58
<b>3.9</b>	<b>Bulge-derived progeny is involved in ectopic SG formation.....</b>	<b>59</b>
<b>3.10</b>	<b>Development of ectopic SG is accompanied by the establishment of new progenitor niches .....</b>	<b>61</b>
<b>3.11</b>	<b>HFSC-derived progeny contributes to epidermal tumourigenesis .....</b>	<b>63</b>
<b>3.12</b>	<b>Lineage tracing of different keratinocyte populations within the K14<math>\Delta</math>NLef1-tumour model.....</b>	<b>65</b>
<b>3.13</b>	<b>HFSC-derived progeny contributes to sebaceous tumourigenesis.....</b>	<b>67</b>
<b>3.14</b>	<b>Manipulation of Lef1-signalling in the HFSC niche .....</b>	<b>69</b>
3.14.1	Generation of K15 $\Delta$ NLef1 transgenic mice .....	70
3.14.2	Impaired epidermal differentiation and tumour formation in K15 $\Delta$ NLef1-mice .....	72
<b>4</b>	<b>Discussion .....</b>	<b>75</b>
<b>4.1</b>	<b>Development of a transgenic mouse model to trace the fate of HFSC-derived progeny on a single cell level .....</b>	<b>76</b>
<b>4.2</b>	<b>Multipotency of individually labelled bulge cells.....</b>	<b>77</b>
<b>4.3</b>	<b>HFSC contribute to epidermal homeostasis .....</b>	<b>77</b>
4.3.1	Regeneration of the SG.....	77
4.3.2	Regeneration of the IFE .....	79
<b>4.4</b>	<b>A hierarchy of stem and progenitor cells drives epidermal renewal ....</b>	<b>80</b>
<b>4.5</b>	<b>Signalling cues governing epidermal homeostasis .....</b>	<b>82</b>
<b>4.6</b>	<b>Implications for ageing.....</b>	<b>83</b>
<b>4.7</b>	<b>The HFSC niche exhibits a heterogeneous population.....</b>	<b>84</b>
<b>4.8</b>	<b>Impaired Lef1 signalling in the epidermis controls sebaceous commitment of HFSC-derived progeny .....</b>	<b>86</b>
4.8.1	Composition of the HFSC niche .....	86
4.8.2	Ectopic SG originate from HFSC.....	86
4.8.3	Establishment of new progenitor niches.....	87
<b>4.9</b>	<b>Role of HFSC in epidermal tumourigenesis .....</b>	<b>88</b>
<b>4.10</b>	<b>Manipulating Lef1 signalling in the HFSC niche.....</b>	<b>90</b>
4.10.1	Impaired epidermal differentiation .....	90
4.10.2	Sebaceous tumourigenesis in K15 $\Delta$ NLef1 mice .....	91

4.11	Perspectives.....	91
5	Summary .....	92
6	Zusammenfassung.....	93
7	References .....	95
8	Figure index .....	103
9	Table index.....	105
10	List of abbreviations .....	106
11	Curriculum vitae .....	111

# 1 Introduction

## 1.1 Organisation of the skin

The skin epithelium forms the largest organ of the body and has crucial barrier functions. It protects the body from dehydration and environmental assaults (such as pathogens, UV radiation and mechanical stress). In addition, the skin plays a key role in thermoregulation and sensory perception (Segre, 2006). Mammalian skin is a complex organised and multilayered tissue consisting of an epidermis, a dermis and a subcutaneous layer (hypodermis) (Fig 1A). The epidermis is a stratified epithelium comprising the interfollicular epidermis (IFE) and associated hair follicles (HF) and sebaceous glands (SG). The underlying mesenchymal connective tissue (dermis) supplies the epidermis with nutrients and stimulates proliferation. The subcutis is comprised of adipocytes and serves as a nutrient storage for the epidermis and dermis (cutis). Furthermore, it connects the cutis with underlying tissues (e.g. muscle) (Alberts, 2002; Montagna and Parakkal, 1974).

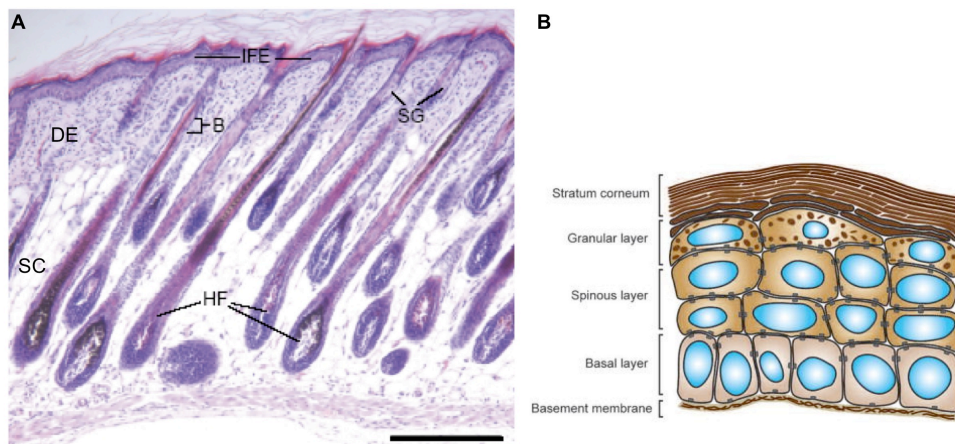


**Fig1: Organisation of the skin**

(A) H/E stained section of the skin showing the epidermis, dermis (DE) and the subcutis. The epidermis consists of an IFE and associated HF and SG (Niemann and Watt, 2002).

(B) Scheme depicting different layers of the interfollicular epidermis (Fuchs and Nowak, 2008).

## **1.2 The epidermis**

The epidermis forms the outermost layer of the skin and is directly exposed to various environmental assaults. Therefore, a highly compartmentalised and multi-layered epithelium has been evolved.

### **1.2.1 The interfollicular epidermis (IFE)**

Murine IFE is composed of 4 cell layers: the stratum basale, stratum spinosum, stratum granulosum and stratum corneum (Fig 1B). Epidermal homeostasis underlies a strict spatial control of proliferation and differentiation. Proliferating keratinocytes are confined to a single basal layer, stratum basale, which is attached to the basement membrane (BM). A reciprocal exchange of signals with the underlying mesenchyme (dermis) is required to induce proliferation of the epidermis (Watt and Hogan, 2000). Keratinocytes destined to differentiate detach from the underlying BM and leave the basal layer. Major structural changes at basal to spinous layer transition are accompanied by a switch in keratin expression, from Keratin (K) K14/K5 (Nelson and Sun, 1983) in basal layer to K1/K10 suprabasally (Fuchs and Green, 1980). Differentiating keratinocytes traverse the distinct epidermal layers, before finally shedding from the epidermal surface as flattened cornified cells. In murine epidermis, the outermost layer, stratum corneum, is arranged in stacks of large hexagonal cells with deposited lipids which are essential for barrier acquisition (Blanpain and Fuchs, 2009; Fuchs and Nowak, 2008; Jones et al., 2007).

### **1.2.2 The hair follicle (HF)**

Similar to the IFE, differentiation and proliferation of the HF are confined to distinct compartments. Proliferating keratinocytes are found in the outer root sheath (ORS), the secondary hair germ (HG) and the hair bulb (at the base of the HF). Terminal differentiation is restricted to the concentric inner layers including the inner root sheath (IRS) and the hair shaft (HS). Basically, the HF is partitioned in a permanent and a cycling portion, resulting in an accessory temporal control of HF renewal (Fig 2A) (Hardy, 1992; Niemann and Watt, 2002).

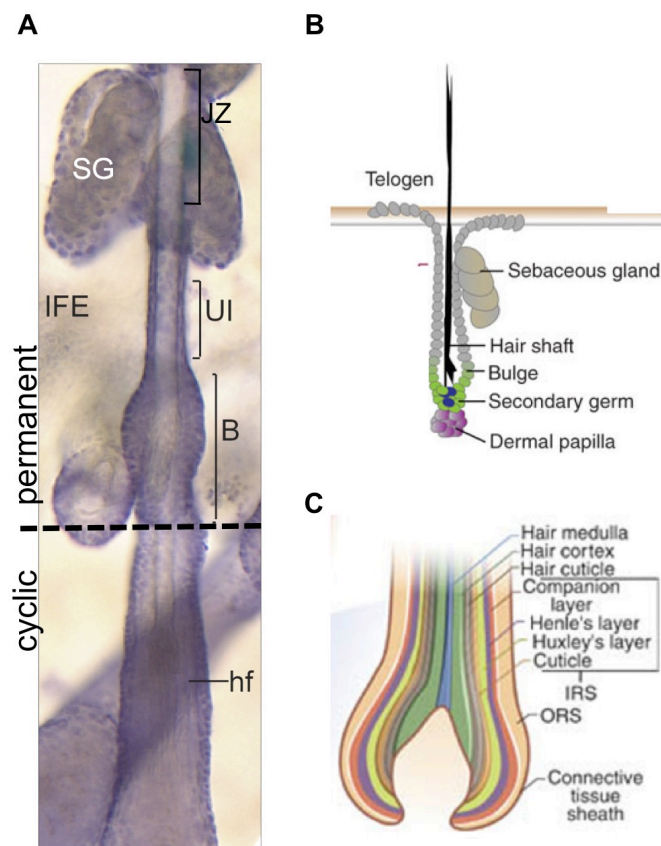


**Fig 2: Structure of the pilosebaceous unit**

(A) The pilosebaceous unit is formed by HF and its attached SG. HF have a permanent and a cycling portion. The permanent part contains the HFSC niche (bulge, B), the secondary hair germ (HG) (B; Jaks et al., 2008) the upper isthmus (UI) and SG, whereas the lower cycling portion produces new hair including all the different lineages of the HS and IRS (C; Cotsarelis, 2006).

During HF growth period, cell type specification of rapidly dividing TA-matrix cells is executed at the basis of the HF, called bulb. This process involves 7 terminal differentiation programs including 3 cell lineages for the HS and 4 for the IRS (Fig 2C) (Cotsarelis, 2006; Krause and Foitzik, 2006; Rogers, 2004; Schneider et al., 2009). The IRS rigidly supports and guides the HS during maturation. Layers of HS and IRS extrude their organelles and are composed of tightly packed bundles assembled by keratin filaments supporting tensile strengths of the hair fibres. The HG and the bulb region are located in close proximity to a cluster of cells called dermal papillae (DP) (Fig 2B). DP cells provide signals to stimulate hair growths during morphogenesis and normal development (Rendl et al., 2005).

In addition to the cyclic part the HF also encompasses a permanent portion including the HFSC niche (bulge), the upper isthmus (UI), the junctional zone (JZ) and the



opening of the hair channel being connected to the IFE, called infundibulum (INF) (Blanpain and Fuchs, 2009; Cotsarelis, 2006).

### 1.2.3 The sebaceous gland (SG)

Functional SG are important for barrier acquisition and protection against pathogens and environmental assaults (Schneider and Paus, 2009; Thody and Shuster, 1989). During late embryonic morphogenesis of the HF, SG develop as outgrowths of the ORS between the infundibulum and the UI. Fully developed SG has been classified into three distinct regions, the peripheral, the maturation and the necrosis zone (Fig 3). At the peripheral basal layer, small undifferentiated and mitotically active cells assure maintenance of the gland. Upon maturation, sebocytes accumulate lipid droplets and are displaced towards the centre of the gland (necrosis zone). Finally, cells disintegrate and lipid containing sebum is lubricated into the hair channel. The sebaceous duct (SD) directly connects the uni- or multilobular organised SG to the hair channel thereby facilitating the holocrine secretion of the sebum (Zouboulis et al., 2008b).

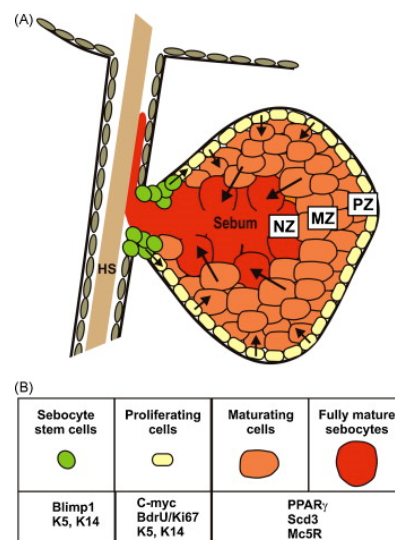


**Fig 3: Structure of the SG**

SG consists of 3 different zones: The growth is comprised of proliferating cells. Upon differentiation basal cells migrate towards the maturation zone (MZ). They accumulate lipids and are displaced into the centre (necrosis zone). Finally, these cells burst and sebum is released into the hair channel (Schneider and Paus, 2009).

Differentiated sebocytes are characterised by SCD1 (stearyl-coenzyme A desaturase1) (Binczek et al., 2007; Ntambi, 1995; Sampath et al., 2009; Zheng et al., 1999), MC5R (Melanocortin5 receptor) and PPAR $\gamma$  (peroxisome proliferator activator

receptor  $\gamma$ -expression (Zhang et al., 2006). Lipid droplets of fully matured cells can be visualised by the use of lipid dyes (OilRedO, NileRed). Notably, several malfunctions have been associated with deregulated sebaceous differentiation including Acne vulgaris and sebaceous tumourigenesis (Zouboulis, 2004).

The existence of multiple compartments within the epidermis indicates that a complex organised signalling network is required to control regeneration of each integral part of the epidermis.

## **1.3 Epidermal homeostasis**

Mammalian epidermis is regenerated constantly throughout the entire life. This continuous replacement of damaged or dead cells guarantees homeostasis of the epidermal tissue. Indeed, epidermal homeostasis is a highly dynamic process, which is maintained by multiple stem (SC) and progenitor cell populations (Blanpain and Fuchs, 2006; Jaks et al., 2008; Jaks et al., 2010).

### **1.3.1 SC characteristics and identification**

SC are defined as a population of long-lived multipotent cells that have been associated with infrequent cell cycling. Upon stimuli from the surrounding microenvironment (SC niche), SC become mobilised and are activated to divide. It is thought that one of the two daughter cells is utilised to replenish the SC pool. The 2<sup>nd</sup> daughter called transit amplifying (TA) cell undergoes distinct rounds of replications and is destined to a particular cell lineage (Fuchs and Segre, 2000). Several studies have taken advantage of the slow cycling nature of the SC (Bickenbach et al., 1986; Cotsarelis et al., 1990; Morris and Potten, 1994; Potten et al., 1974). They have administered the nucleotide analogon <sup>3</sup>H-thymidine or BrdU for a prolonged period to assure uptake in all tissue cells capable to divide. Following a certain chasing time, replicating cells dilute the label, whereas cells with an infrequent cell cycle retain the <sup>3</sup>H-thymidine or BrdU.

### **1.3.2 Assays to test SC identity**

The proliferative potential and differentiation capacity of epidermal SC populations can also be tested *in vitro* (colony forming assay). Therefore, growth and morphology of a certain number of seeded cells is monitored over a period of 2-4 weeks. Multicompetent SC give rise to large colonies (holoclones), whereas TA cells

generate colonies of moderate size (meroclones). Cultivation of more differentiated cells leads to the formation of small abortive clones (paraclones) (Barrandon and Green, 1985, 1987; Jones and Watt, 1993; Morris and Potten, 1994). In addition, SC identity can be assayed by skin reconstitution assays (e.g. graft chamber assay). Transplantation multipotent epidermal SC into nude mice lead to a regeneration of the entire epidermis including IFE, SG and HF (Blanpain et al., 2004).

Until now, several distinct SC and progenitor population and marker molecules have been identified for almost each integral part of the epidermis (see Table 1), provoking the question if the different SC compartments are somehow interconnected.

### 1.3.3 Epidermal SC compartments

#### 1.3.3.1 SC in the IFE

Previously, it has been shown that the IFE has its own SC reservoir (reviewed in (Jones and Simons, 2008)). Indeed, LRC have been found in the IFE (Braun et al., 2003; Lavker and Sun, 1983) and human keratinocytes derived from the IFE exhibiting high  $\beta 1$ -integrin levels have a high proliferative potential *in vitro* (Jones et al., 1995; Jones and Watt, 1993).

#### 1.3.3.2 SC of the HF bulge

The best characterised compartment of HFSC is the HF bulge (Fig 4), which belongs to the permanent portion of the HF and is most likely established after morphogenesis of the HF (Nowak et al., 2008). HFSC divide infrequently as demonstrated by label retention approaches (Cotsarelis et al., 1990; Lavker et al., 2003). This pulse-chase concept was adapted to a tetracycline-inducible, GFP-tagged Histone-2B version and has not only confirmed the slow cycling nature of bulge cells. The fact that some cells retained the label over months indicates that they subsisted in a more quiescent state or were not actively involved in hair regeneration. These data imply that bulge cells represent a more heterogeneous population with regard to their proliferative features (Sotiropoulou et al., 2008; Tumber et al., 2004; Waghmare et al., 2008). SC identity of HF bulge cells has been assessed by *in vitro* studies and clonal analysis of bulge-derived progeny (Table 1). Indeed, several potential HFSC bulge marker have been described including Keratin 15 (K15), CD34, Tcf3 (T-cell factor3), NFATc1 (Nuclear factor of activated T-cells, cytoplasmic1), Lhx2

(LIM/homeobox protein2) and Sox9 (SRY box9) (Liu et al., 2003; Lyle et al., 1998; Merrill et al., 2001; Nguyen et al., 2006; Nowak et al., 2008; Rhee et al., 2006; Trempus et al., 2003; Vidal et al., 2005).

HFSC from the bulge region have been purified based on CD34+/Itga6<sup>high</sup>-expression. Transplantation of these isolated bulge cells resulted in reconstitution of all epidermal lineages including HF, SG, and IFE (Blanpain et al., 2004). The contribution of bulge cells to HF regeneration has been well documented by a series of lineage tracing experiments *in vivo* (Table 1). Genetic targeting of the entire HF bulge by a K15 regulatory sequence revealed that K15<sup>+</sup> cell populations were competent to regenerate the entire hair follicle (Morris et al., 2004). A more distinct cell population located at the lower tip of the HF bulge giving rise to the HG was monitored for either Lgr5 (leucine-rich repeat-containing G-protein coupled receptor) expression (Jaks et al., 2008) or by analysing label retention (Greco et al., Zhang et al., Legue et al., 2010).



**Fig 4: The HFSC niche and its markers**

The HF bulge region (B) is the best characterised SC niche and positive for K15, LRC, CD34, Lhx2, Tcf3, NFATc1, Sox9, Lgr5 and Itga6<sup>high</sup> signal. Lineage tracing experiments were performed with the molecules highlighted in bold.

### 1.3.3.3 SC/progenitor reservoirs of the isthmus

The upper isthmus, a region between the bulge and the SG, was identified to comprise CD34 negative, K15 negative, Scal negative SC/progenitor cells which are clonogenic in culture (Fig 5, Jensen et al., 2008). The UI is recognised by the MTS24 antibody (mouse thymic stroma24, Nijhof et al., 2006). The corresponding epitope for MTS24, Plet1 (glycoylphosphatidylinositol-anchored glycoprotein1) (Depreter et al., 2008), has recently been identified and is also expressed in more differentiated keratinocytes of the hair lineages (Raymond et al., 2010). Residing in the more central isthmus, genetically labelled Lgr6<sup>+</sup>ve cells have recently been traced towards

the IFE and the SG. Interestingly, Lgr6<sup>+</sup>ve keratinocytes do not express the molecular signature of bulge SC and only partially overlap with other epidermal SC/progenitor marker (MTS24/Plet1 or Lrig1) (Snippert et al., 2010).

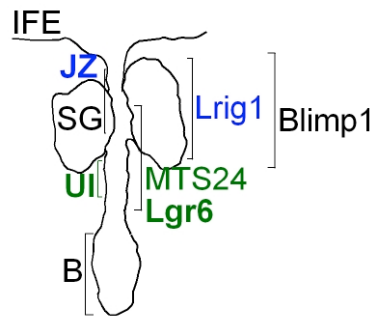


**Fig 5: Epidermal SC/ progenitor niches of the UI and JZ**

The UI (green) contains progenitors which are MTS24/Plet1 and Lgr6<sup>+</sup>ve. The JZ (blue) and the periphery of the SG is characterised by Lrig1 expression. Blimp1 seems to mark unipotent progenitors at the junction of SG and HF. Lineage tracing experiments were performed with the molecules highlighted in bold.

### 1.3.4 Bipotent progenitors at the JZ

The region of the JZ is comprised of bipotent Lrig1<sup>+</sup>ve cell population that seem to contribute to both, SG and IFE renewal (Fig 5 and Jensen et al., 2009).

**Table 1: Identification of several marker molecules at different epidermal SC/progenitor compartments**

Niche	marker	proof of SC identity			potency	regulation	reference
		lineage tracing	Transplantation	clonogenic in vitro			
entire bulge	K15	x	x	x	multi-potent	VitDR, $\beta$ -catenin	Liu et al., 2003; Morris et al., 2004
	LRC	x	x	x	multi-potent		Cotsarelis et al., 1990; Tumber et al., 2004
	CD34		x	x	multi-potent		Trempe et al., 2003; Blanpain et al., 2004
	Lhx2						Rhee et al., 2006
	Tcf3					Wnt	Nguyen et al., 2006
	NFATc1					BMP	Horsley et al., 2008
lower bulge	Lgr5	x	x	x	multi-potent	Wnt	Jaks et al., 2008
central isthmus	Lgr6	x	x		bi-potent		Snippert et al., 2010
upper isthmus	MTS24/Plet1			x			Nijhof et al., 2006; Jensen et al., 2008; DePreter et al., 2008, Raymond et al., 2010
junctional zone	Lrig1		x	x	bi-potent	EGFR?c-myc	Jensen et al., 2009
SG	Blimp1	x		x	uni-potent	c-myc	Horsley et al., 2006
IFE	LRC	x		x			(Ghazizadeh and Taichman, 2001)

The discovery of diverse SC/progenitor populations in the epidermis (summarised in Table1) raises important questions: What is the functional significance of the different progenitor pools within the epidermis? What are the underlying signalling networks maintaining and controlling these different compartments?

### **1.3.5 Epidermal regeneration**

#### **1.3.5.1 Regeneration of the IFE**

Different models have been postulated how the IFE is regenerated. Originally, it was hypothesised the IFE is organised into columns termed epidermal proliferative units (EPU) consisting of about 10 basal cells comprised of a single central SC (LRC) surrounded by TA cells and differentiating columnar stacks of cells extending from the stratum basale to the stratum granulosum (Mackenzie and Bickenbach, 1985; Potten, 1974).

In contrast, it has recently been postulated that a single cell population which neither shares SC nor TA cell characteristics contributes to the homeostasis of the IFE (Clayton et al., 2007; Doupe et al., 2010; Jones and Simons, 2008). Instead, resident and more committed progenitors (CP) give rise to the IFE.

#### **1.3.5.2 Cyclic regeneration of the HF**

Murine HFs undergo a cyclic regeneration and renew within a time frame of about 4 weeks (Fig 6). Since the first and the second postnatal hair cycles are synchronised, the HF represents an excellent system to study the regulation of SC activation and quiescence during skin homeostasis. HF regeneration is separated into distinct phases of resting (telogen), activation (telogen to anagen transition), growth (anagen) and regression (catagen) (Lavker and Sun, 1983; Lavker et al., 2003; Millar, 2002; Muller-Rover et al., 2001). During telogen, HFSC of the bulge are in quiescent state. Upon mesenchymal stimuli sent from the DP (Driskell et al., 2009; Enshell-Seijffers et al., 2010; Rendl et al., 2008), HFSC are activated and more primed SC from the HG are mobilised. This two-step mechanism involves proliferation and migration of more activated SC from the HG along the ORS towards a newly forming hair matrix to support hair growth (anagen phase), before activated bulge SC replenish lost HG cells (Greco et al., 2009; Jaks et al., 2008; Legue et al., 2010; Zhang et al., 2009). The new HF forms adjacent to the old (club) hair that eventually will be shed (Milner et al., 2002). Anagen is followed by catagen, where the lower cycling part of the HF is regressed, mainly by apoptosis. Additionally, HS differentiation terminates concomitant with club hair formation thereby preparing the DP and the permanent part of the HF for the next telogen (Alonso and Fuchs, 2006; Cotsarelis, 2006).

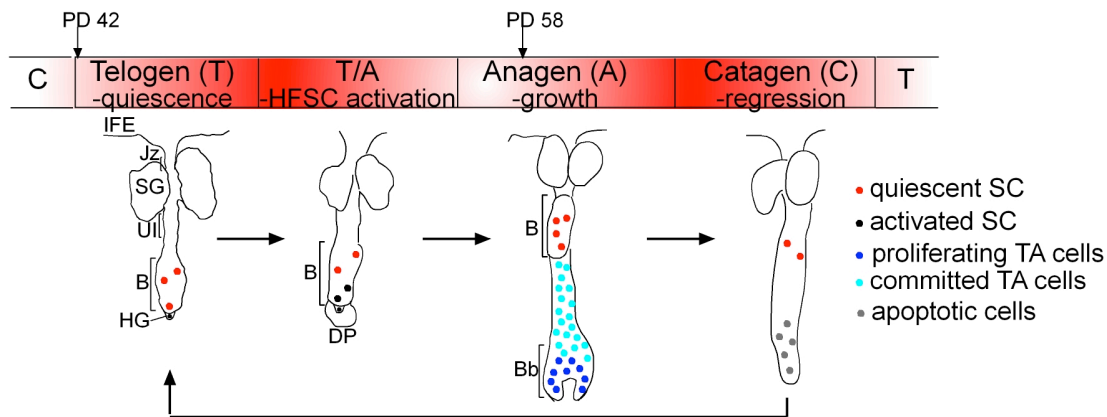


**Fig 6: Cyclic renewal of the HF**

Upon mesenchymal stimuli (telogen to anagen transition), HFSC residing in the bulge (B) and HG are mobilised to promote hair growth (anagen). Activated SC from the HG migrate and generate proliferating TA cells located in the hair matrix which eventually result in the terminally differentiated HS to generate a new hair. Activated HFSC replenish the lost HG cells. During catagen phase, the lower part of the HF regresses and the HF enters the resting phase (telogen).

To date, it has been well documented that SC from the HF bulge are involved in cyclic HF regeneration. So far, it is not absolutely clear, whether HFSC can also contribute to other epidermal compartments like the IFE or the SG during skin homeostasis.

### 1.3.5.3 Homeostasis of the SG

The high turn-over of the SG requires a constant renewal of cells, suggesting SC or progenitor cells to be involved in SG homeostasis. The source of the SC regenerating the SG still remains to be identified.

(1) Currently, two hypotheses exist how the SG are regenerated on a cellular level: Stem cells or progenitors from different epidermal compartments are mobilised and contribute to SG homeostasis (Blanpain et al., 2004; Jensen et al., 2009; Panteleyev et al., 2000; Snippert et al., 2010; Taylor et al., 2000).

(2) Unipotent progenitors residing at the periphery of the SG are committed to sebaceous lineage. Initial long-term retroviral-mediated clonal analyses revealed that a noticeable number of exclusively labelled SG persisted, albeit other compartments such as the HF or the IFE remained negative. This observation suggested that the SG comprises a resident SC population (Ghazizadeh and Taichman, 2001). Recent



studies indicate that unipotent progenitors are located at the junction of the SG and the HF and are characterised by the expression of Blimp1 (B lymphocyte induced maturation protein-1). Fate mapping analyses suggest that Blimp1<sup>+</sup>ve progenitors are capable to maintain the SG (Horsley et al., 2006). In contrast, in human skin or tumour samples Blimp1 marks more matured sebocytes (Sellheyer and Krahel, 2009). However, a remaining issue to be investigated is: what is the origin of cells giving rise to unipotent Blimp1<sup>+</sup>ve progenitors?

Ablation of Blimp1 leads to SG hyperplasia and an increased proliferation in the HF bulge indicating that HFSC respond to this signals if homeostasis is disturbed (Horsley et al., 2006).

Furthermore, it has been well documented that upon wounding, SC/progenitor populations from the hair matrix, the HF bulge, the central isthmus or the JZ are recruited to the injured tissue, indicating a tremendous plasticity of epidermal SC to ensure rapid repair of the damaged tissue (Ito et al., 2005; Ito et al., 2007; Langton et al., 2008; Levy et al., 2005; Levy et al., 2007). This also implies that a fast response of the underlying signalling networks is required to mobilise and direct these SC/progenitor populations towards the site of primary injury.

## **1.4 Regulation of epidermal regeneration**

A complex network consisting of various signalling cascades has been evolved to control epidermal morphogenesis and homeostasis. Several lines of experiments have provided evidence that gradients of Wnt and BMP signalling are essential for controlling SC quiescence, activation and cell type specification by HFSC (DasGupta et al., 2002; Kobiela et al., 2007; Li and Clevers, 2010; Lo Celso et al., 2004; Millar, 2002).

### **1.4.1 Wnt/ $\beta$ -catenin signalling**

In the absence of a Wnt signal,  $\beta$ -catenin is phosphorylated and targeted for proteasomal degradation by a destruction complex consisting of CK1, GSK3 $\beta$ , Apc and Axin among other proteins (Fig 7). Upon binding of Wnt to its receptor Frizzled and its co-receptor LRP5/6, Dishevelled binds to Frizzled and recruits the destruction complex to the membrane through interactions with Axin. Cytoplasmatic  $\beta$ -catenin is now stabilized, accumulates and translocates to the nucleus and binds to TCF/LEF1

transcription factors thereby displacing a complex repressing transcription (Groucho and CBP). Expression of target genes including cell cycle regulators (CyclinD1), adhesion molecules (E-Cadherin) is induced but also a feedback loop of components of Wnt-pathway including Wnt-inhibitors (Nusse, 2005).

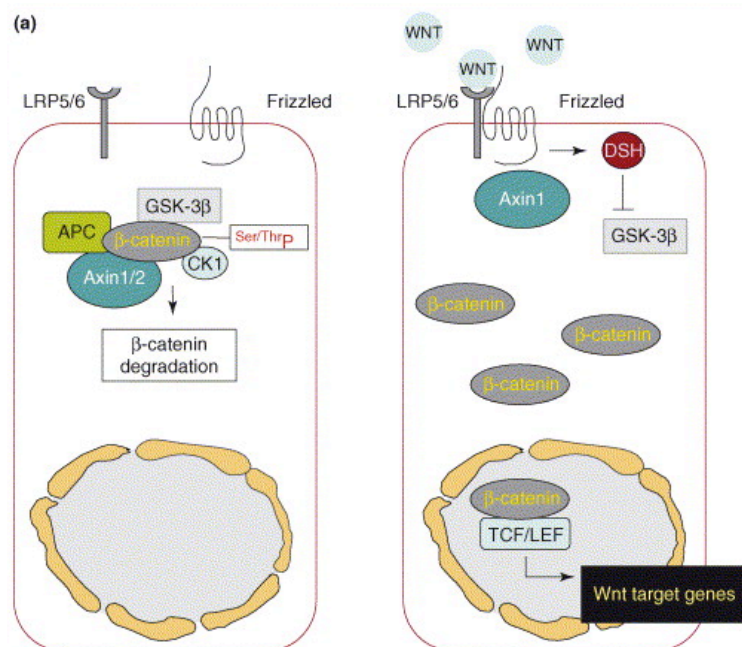


**Fig 7: Scheme depicting the Wnt/β-catenin pathway in repressed (left) and active state (right) (Fodde and Brabletz, 2007)**

Consistent with the observation in other epithelial systems, such as the intestine (Barker et al., 2010; Barker et al., 2007; Sato et al., 2009), quiescence of HFSC is achieved by the secretion of Wnt-inhibitory signals by the mesenchyme (DP). Simultaneously, during refractory stage of telogen, the DP promotes the BMP pathway; thereby activating NFATc1 (nuclear factor of activated T cells c1). NFATc1 represses CDK4 (cyclin dependent kinase 4) and stimulates the expression of cell cycle inhibitors. The mirror image is observed in the SC activation phase. The HFSC niche deciphers BMP inhibitory signals from the DP which in turn leads to the inactivation of NFATc1 followed by cell cycle progression (Horsley et al., 2008). Additionally, Wnt-signalling is induced thereby promoting SC activation and HF growth. Once a bulge SC becomes activated, the expression of downstream effectors such as Sonic hedgehog (Shh) is induced to control proliferation and differentiation at the basis of the HF (Chiang et al., 1999; St-Jacques et al., 1998). The fate decision of matrix cells is dependent on Wnt-mediated Lef1 (lymphoid enhancer factor1) signalling determining lineage commitment towards HS differentiation (Merrill et al.,

2001), whereas BMP signalling stimulates expression of GATA3 thereby inducing differentiation into the IRS (Kobielak et al., 2003)

In addition to the Wnt and BMP pathways, an important function for Hedgehog, c-myc and Notch signalling during epidermal regeneration has been reported (Blanpain et al., 2006; Estrach et al., 2008; Niemann et al., 2003; St-Jacques et al., 1998; Watt et al., 2008; Watt and Jensen, 2009).

A deregulation of these signalling networks has major implications for epidermal homeostasis and cancer.

#### 1.4.2 Impaired Wnt/ $\beta$ -Catenin signalling results in a disturbed tissue homeostasis

Previously, it has been shown that the manipulation of the Wnt/ $\beta$ -catenin pathway causes perturbations of the epidermal differentiation programme (Fig 8).

Overexpressing an active mutant of  $\beta$ -catenin *in vivo* leads to an unscheduled *de novo* formation of hair follicles (Gat et al., 1998; Lo Celso et al., 2004; Lowry et al., 2005).

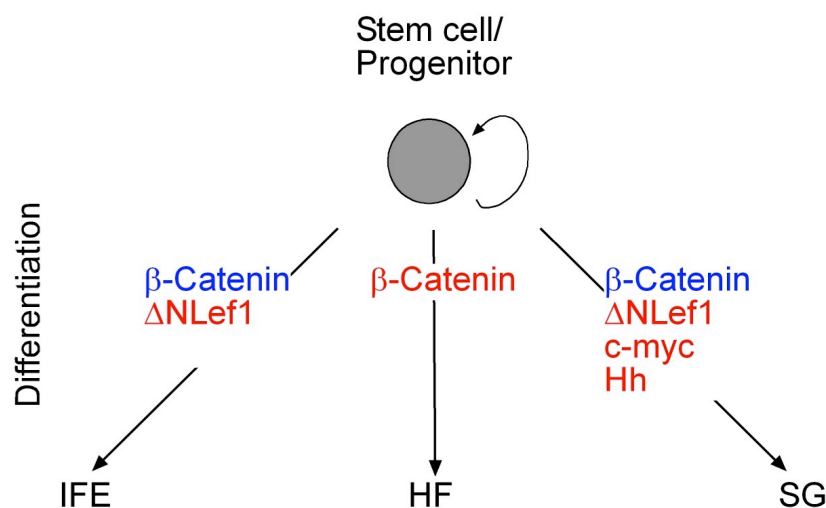


**Fig 8: Manipulation of canonical Wnt signalling affects epidermal homeostasis.**

Overexpression of active  $\beta$ -catenin (red) determines fate decision towards the hair lineages, whereas repression (blue) promotes differentiation cell type specification of keratinocytes towards lineages of the SG and IFE. SG and IFE specification can also be stimulated by the expression of  $\Delta$ NLef1. Over-expression of Hh and c-myc also stimulates sebaceous commitment.

Impairment of signalling by Lef1, which together with  $\beta$ -catenin is crucial for appropriate HF development, promotes sebaceous fate and squamous differentiation (Merril et al, 2001; Niemann et al., 2002).

Recently, it has been demonstrated that epidermal expression of dominant negative Lef1 (K14 $\Delta$ NLef1, Fig 9A) drives the formation ectopic SG (Fig 9B, nSG) along deformed HF. Epidermal fate is also stimulated resulting in cyst development. Additionally, the SG are enlarged (Niemann et al., 2002; Braun et al., 2003). These findings provoked the question whether formation of these ectopic SG originated from an unbalanced fate decision of HFSC or more committed TA cells.

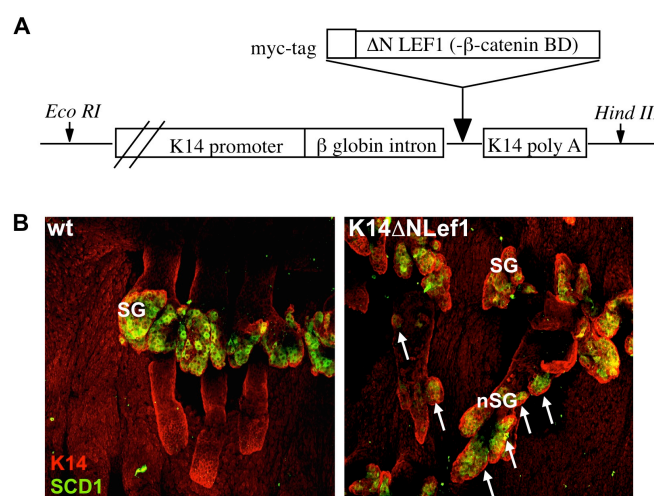


**Fig 9: Formation of ectopic SG in K14 $\Delta$ NLef1 mice**

(A) Schematic presentation of the K14 $\Delta$ NLef1 construct (Niemann et al., 2002).

(B) Development of ectopic SG (nSG) along deformed HF shown by staining for sebocyte differentiation marker SCD1 (Fehrenschild et al., submitted)

### 1.4.3 Deregulated Wnt/ $\beta$ -catenin signalling causes skin cancer

Several studies provide evidence that de-regulated  $\beta$ -catenin signalling causes a variety of epithelial cancers, including skin tumours (Gat et al., 1998; Niemann and Watt, 2002; Owens and Watt, 2003; Polakis, 2000; Taipale and Beachy, 2001). Activating mutations have been found at a high frequency in human pilomatricomas (Chan et al., 1999) and the corresponding mouse models exhibit hair tumours (trichofolliculomas and pilomatricomas) (Gat et al., 1998). Conversely, mutations in the  $\beta$ -catenin binding domain of Lef1 have been found in a high frequency in human sebaceous tumours, indicating that also a repression of  $\beta$ -catenin-mediated Lef1 signalling results in cancer development (Takeda et al., 2006). Interestingly, repressed  $\beta$ -catenin signalling in K14 $\Delta$ NLef1 mice results to the development of

spontaneous sebaceous adenomas and papillomas with sebocyte differentiation tumours (Niemann et al., 2002). These tumours can also be induced: A single application of a sub threshold dose of a carcinogen (DMBA), leading to mutations in *Ha-Ras*, resulted in the formation of macroscopically visible sebaceous tumours within a time frame of 4 weeks (Niemann et al., 2007). The fast and defined development of sebaceous tumours provides an excellent tool to study early stages of tumour formation.

Until now, it is not known which cell population is targeted by transformational events and gives rise to sebaceous tumours in K14 $\Delta$ NLef1 mice.

## **1.5 The rationale of cancer stem cells**

Previous studies have described that tumours are comprised of heterogeneous cell populations which differ in their phenotype and their proliferative capacity. It has been proposed that tumour growth is initiated by a subpopulation of cells, which are biologically different with respect to their functional abilities from the remaining bulk of the tumour. Therefore, a model has emerged to envision cancer as a hierarchical disease in which tumour growth is sustained by a population of cancer stem cells (CSC) (Lobo et al., 2007; Visvader and Lindeman, 2008; Wang and Dick, 2005).

### **1.5.1 Characteristics of CSC**

Like tissue SC, CSC are multipotent and therefore could give rise to multiple cell lineages resulting in the heterogeneity observed in many tumours. CSC have the ability to self-renew and divide infrequently. This would explain the re-occurrence of tumours after chemotherapy, as proliferating (TA) cells are targeted and not transformed CSC sustaining tumour growth. In addition, CSC exhibit an unlimited proliferative potential and are able to recapitulate the cell types found in the originally tumour. Despite ongoing debates about the existence of true CSC (Adams and Strasser, 2008; Kelly et al., 2007), it is controversially discussed whether CSC arise from a transformed long-lived tissue SC accumulating mutations. Potentially, more committed or mature cells could be targeted by transformational events and acquire self-renewing potential thereby being transformed into CSC (Gupta et al., 2009).

### **1.5.2 Identification of CSC**

First evidence supporting the CSC hypothesis came from the hematopoietic system investigating acute myeloid lymphomas (AML) (Bonnet and Dick, 1997) and was followed by the identification of tumour-initiating cells in a variety of solid tumours including tumours in the central nervous and the respiratory system, the mammary gland, prostate, colon, head and neck squamous cell carcinomas and human melanomas (Al-Hajj et al., 2003; Collins and Maitland, 2006; Kim et al., 2005; O'Brien et al., 2007; Prince and Ailles, 2008; Schatton et al., 2008).

Interestingly, there are first indications for the existence of CSC in skin tumours (Ambler and Maatta, 2009; Mancuso et al., 2006). It was found that tumourigenic CD34-expressing keratinocytes reside in murine squamous cell carcinomas (SCC) (Malanchi et al., 2008). More recently, lineage tracing experiments utilising a Cre-sensitive tumour-mouse model for basal cell carcinoma (BCC), revealed that progenitor cells from the basal layer of the IFE and not from the HFSC niche contribute to BCC formation (Donovan, 2009; Youssef et al., 2010).

It still remains elusive how the surrounding microenvironment effects the conversion of a cell to a CSC. Furthermore, the identification of the cell of origin giving rise to a particular type of epidermal tumours will have major therapeutic implication to prevent and to treat cancer.

### **1.5.3 Controversies**

In contrast to the hierarchical CSC model with a unique self-renewing cell type a 2<sup>nd</sup> model for tumour propagation has been postulated (Adams and Strasser, 2008; Kelly et al., 2007). This “clonal evolution” model proposes that most of the tumour cells sustain tumour growth and have self-renewing capacity. Tumour heterogeneity in this context is ascribed not only to differentiation but also to intraclonal genetic and epigenetic variation and influences from the microenvironment. The clonal evolution model more attributes much of the intratumour variation to subclonal differences in mutational profile and all except the terminally differentiated cells may have some self-renewing capacity. Indeed, a collaborative action of both models is conceivable.

## 1.6 Objectives

The multilayered epithelium of mammalian epidermis comprises the IFE, HF and SG. Functional SG release sebum into hair shaft and are important for barrier function and protection against pathogens and environmental assaults. The high cellular turnover of the SG requires a constant renewal of cells, suggesting stem or progenitor cells to be involved in SG homeostasis. To date, the cellular mechanism of SG regeneration still remains elusive. Although multiple SC/progenitor reservoirs have been defined within the epidermis, a functional relationship or hierarchy between the different niches is yet not fully understood. To assess whether multipotent SC from the underlying HFSC compartment regenerate the SG and give rise to these different SC/progenitor populations, an inducible Cre mouse model was generated during this PhD thesis to map the fate of individual HFSC-derived progeny. From these lineage tracing studies we aim to gain new insights into temporal and spatial control of SG renewal and epidermal regeneration during skin homeostasis.

In addition, deregulated homeostasis leads to a variety of diseases including cancer. Previous studies have demonstrated that manipulation of Lef1, a key regulator of epidermal fate decision, drives ectopic SG formation resulting in sebaceous adenoma formation. Since mutant Lef1 in all keratinocytes of the basal layer promotes sebaceous commitment on expenses of HF regeneration, one objective of this thesis is to investigate whether an altered fate decision of HFSC-derived progeny drives the formation of ectopic SG. An additional issue is to identify the cells of origin contributing to the development of sebaceous tumours. Therefore, a major focus of the present study was to perform fate mapping analyses of HFSC-derived progeny during different stages of tumourigenesis. Over-expression of mutant Lef1 in the HFSC compartment will elucidate if deregulated Lef1 signalling in the HFSC niche is sufficient to drive tumour formation.

## 2 Material and Methods

### 2.1 Chemicals and reagents

Chemicals and reagents were purchased from Sigma-Aldrich, Merck or Roth unless stated otherwise. Enzymes used for experimental procedures are listed in Table 2. Oligonucleotides were synthesised by MWG Biotech.

**Table 2: Molecularbiological enzymes**

enzyme	company
Eppendorf 5'prime DNA Taq polymerase	Eppendorf
RedTaq DNA polymerase	Sigma-Aldrich
High Fidelity Taq DNA polymerase	Qiagen
Phusion-Taq polymerase	NEB
T4 DNA ligase	NEB
restriction enzymes	NEB
Alkaline Phosphatase, Calf Intestinal CIP	NEB

### 2.2 Molecular Biology

Unless designated otherwise, standard molecular procedures were carried out according to established protocols (Celis, 2006; Sambrook and Russel, 2001).

#### 2.2.1 Isolation of genomic DNA (gDNA)

Tail biopsies of 3-week old mice were incubated in lysis buffer containing 0,2 M NaCl, 0,1 M Tris/HCl, pH 8,5; 5 µM EDTA; 0,2 % SDS and 100 µg/ml proteinase K (Sigma [39 U/mg]) for 3-4 hours at 55 °C. After a centrifugation step, 2 volumes isopropylalcohol were added to the supernatant to precipitate gDNA. 150 µl H<sub>2</sub>O (DNase free) was added to the pellet and subsequently, gDNA was dissolved o/n at RT.



## 2.2.2 PCR

PCR was used to amplify DNA fragments for plasmid construction or to determine the genotype of the different mouse strains.

For cloning procedures, fragments from plasmid DNA (see also Table 3) were amplified using either High fidelity Taq polymerase (cloning of K15 $\Delta$ NLef1) of Phusion taq polymerase (cloning of K15CreER(G)T2 ).

For cloning purposes, 50-200 ng plasmid DNA template was used and PCR reaction were performed and conditions optimised according to manufacturer's guidelines.

**Table 3: Used plasmids**

plasmid	reference
pEGFP	Clontech
pK15CVM	Liu et al., 2003
pK14CreER(G)T2	Indra et al., 1999
pSK2198 $\Delta$ NLef1	(Behrens et al., 1996)

A maximum of 500 ng gDNA isolated from tail biopsies was employed for genotyping. The typical PCR sample contained within 25  $\mu$ l volume 10 pmol of the two primer (Table 4), 25  $\mu$ mol dNTPs, 1 U of RedTaq DNA polymerase and 1x Red taq Reaction buffer. The following PCR conditions were applied: 5 min, 94 °C initial denaturation, 30 sec, 94 °C cyclic denaturation, 60 sec cyclic annealing at the appropriate temperature; 45 sec, 72 °C, cyclic elongation for a total of 30-35 cycles followed by a 72 °C elongation step for 5 min. All PCR reactions were carried out either in T-Gradient Thermocycler or Personal Thermocycler (Biometra).

PCR amplification products were analysed by agarose gel electrophoresis.

**Table 4: Oligonucleotides used for genotyping**

Mouse strain		oligonucleotide (5'-3')
K15CreER(G)T2	b-globfor	GGA CAT CTT CCC ATT CTA AAC AAC ACC CTG
	K15for	AGG TGG GCG GGC AGC TGT GTT TGT
K14 $\Delta$ NLef1 (Niemann et al., 2002) and K15 $\Delta$ NLef1	dNLef1for	TGT CCC TTG TAT CAC CAT GGA CC
	dNLef1rev	CCA AAG ATG ACT TGA TGT CGG CT
R26RLacZ (Soriano et al., 1999) and R26REYFP (Srinivas et al., 2001)	YFP_1neu	CCA AAG TCG CTC TGA GTT GTT ATC
	YFP_2	GCG AAG AGT TTG TCC TCA ACC
	YFP_3 wt	GGA GCG GGA GAA ATG GAT ATG
K14CreER(G)T2 (Indra et al., 1999)	SC1	GTC CAA TTT ACT GAC CGT ACA C
	SC3	CTG TCA CTT GGT CGT GGC AGC

### 2.2.3 qRT-PCR

For quantitative real-time PCR experiments, total RNA of primary keratinocytes isolated from K14 $\Delta$ NLef1 and control mice was purified using RNeasy Plus Mini-Kit (Qiagen, Germany). For FACS-sorted cells, TRIZOL-reagent (Invitrogen) was used for RNA purification. QuantiTect Reverse Transcriptase Kit (Qiagen, Germany) was employed for cDNA-synthesis according to the manufacturer's instructions. Quantitative PCR analyses were conducted using RT<sup>2</sup> RT SYBR Green qPCR Master Mix (SuperArray Bioscience Cooperation, USA) and a StepOnePlus real time PCR system (Applied Biosystems). Particularly, the following PCR conditions were applied: 10 min 95 °C initial denaturation, cyclic denaturation at 95 °C for 15 sec followed by an annealing step at 60 °C for 1 minute. Primer pairs were designed as shown in Table 5. Fold differences between primary keratinocytes derived from K14 $\Delta$ NLef1 mice and age and sex-matched wild-type control animals were calculated based on the  $\Delta\Delta C_t$  method, adjusted to GapDH expression and are depicted as fold change normalized to wt expression. For analysis of mRNA expression levels of FACS-sorted cells changes were adjusted to 18S RNA expression and normalised to Itga6 positive keratinocytes.

**Table 5: Oligonucleotides used for qRT-PCR**

gene	for oligo 5'-3'	rev oligo 5'-3'
mc-myc	mcmcyfor- TGAGCCCCTAGTGCTGCATGAG	mcmcyrev- ATGGAGATGAGCCCGACTCCGAC
mNucleolin	mNucleolinEx2for- AAAACCCACGGTGAGGCCAA	mNucleolinEx3rev- CACCTTCTTTGCTGGGGTTGTG
mSCD1	mSCD1for- GCTTCCACAACCTACCACCACACCT	mSCD1rev- TGTGACTCCCGTCTCCAGTTCTCT CAATCC
mBlimp1	mBlimp1Ex2for- GGCATCCTTACCAAGGAACCTGC	mBlimp1Ex3rev- GATGAGGGGTCCAAAGCGTG
mKeratin6a	mK6aEx5for- ATCGCTGAGGTCAAGGCCAGTA	mK6aEx6rev- GCTTGGTGTTCGCTAGGTCTG
mLgr6	mLgr6Ex15for- AGGGAACCTTGGCCCTGTCTC	mLgr6Ex16rev- GGATGAAAGTCCTCGGCCTG
mCD34	mCD34Ex2for- GGACAGCAGTAAGACCACACCAGC	mCD34Ex3rev- AGGCAGTATGCCAGTTGGGGA
mK15	mK15Ex3for- TGGAGATGCAGATTGAGCAGCTGAA	mK15Ex4rev- TGCTCCCTCATCTCTGCCAGCA
mItga6	ma6ItgEx4for- AAGTTTGGCTCCTGTCAGCAAGG	ma6ItgEx5- CTGTTAGCAGGAACGGGCACGA
mTenascinC	mTenascinCEx6for- TACCGCCAACTGGCCTTGCTC	mTenascinCEx7rev- TGAACCAGGTGATCAGTGCTGTGG
mNFATC1	mNFATc1for TGCTGAGCAGTATCTGTGGGTGC	mNFATc1rev TGTGGTGAGACTTGGGCTGC
mGapDH	mGapDHfor- ACCTTTGGCATTGTGGAAGG	mGapDHrev- ACACATTGGGGGTAGGAACA
m18S	m18Sfor- CCTGCCCTTTGTACAC	m18Srev- CGATCCGAGGGCCTCAC

## 2.2.4 Agarose gel electrophoresis and DNA gel extraction

Following PCR amplification or treatment of DNA with restriction enzymes resulting DNA fragments of different sizes were separated by agarose gel electrophoresis (0.2-2 % (w/v) agarose in 1xTAE electrophoresis buffer).

For cloning purposes, large DNA fragments ranging from 1.5-8 kb were excised and DNA was eluted using NucleoGelExtractionII kit (Macherey&Nagel).

Alternatively, small PCR-amplified or digested DNA fragments (up to 1 kb) were purified using NucleoSpinExtractionII kit (Macherey&Nagel).

The right size of the isolated DNA fragments was always verified by an analytical agarose gel electrophoresis (100V). The concentration of the DNA was determined by measuring the sample absorption at 260nm with a spectrophotometer (Eppendorf). Purity of the DNA was assessed by calculating the ratio of absorption at 260nm versus 280nm.

## 2.2.5 Cloning procedures

### 2.2.5.1 Transformation and isolation of plasmid DNA

Ligated plasmid DNA was introduced into chemo competent bacteria (TZ101 $\alpha$  Trenzyme) using heat shock transformation. Plasmid DNA was isolated either using QiagenMiniPrep or Maxiprep kit.

### 2.2.5.2 Cloning of pK15CreER(G)T2

To generate the plasmid pK15CreER(G)T2, a 5 kb K15 promotor fragment (Liu et al., 2003) was cloned into the K14CreER(G)T2 vector (Indra et al., 1999) after the K14 regulatory sequence had been removed by *Sall* digest (Fig 10). In particular, the K14CreER(G)T2 vector is comprised of an inducible Cre recombinase, a rabbit  $\beta$ -globin Intron II sequence enhance transgene expression and a polyAAA tail to prevent exonucleatic RNA degradation. The K15 promotor fragment was PCR-amplified from pBK15CVM plasmid (Liu et al., 2003). The addition of *Sall* restriction sites introduced by both primers allowed the insertion of the K15 promotor fragment into the CreER(G)T2 vector. Ligated vector (CreER(G)T2) and insert (K15) was introduced into chemo-competent bacteria TZ101 $\alpha$  (Trenzyme) using heat shock transformation. To allow growth of bacteria transformed with pK15CreER(G)T2 special media conditions were employed (LB medium containing 0.05 % glucose and: 100  $\mu$ g/ml ampicillin for selection). Positive clones were identified using *XhoI* / *PacI*

double digests. Right nucleotide sequence was proven by sequencing (performed by the CMMC service unit).

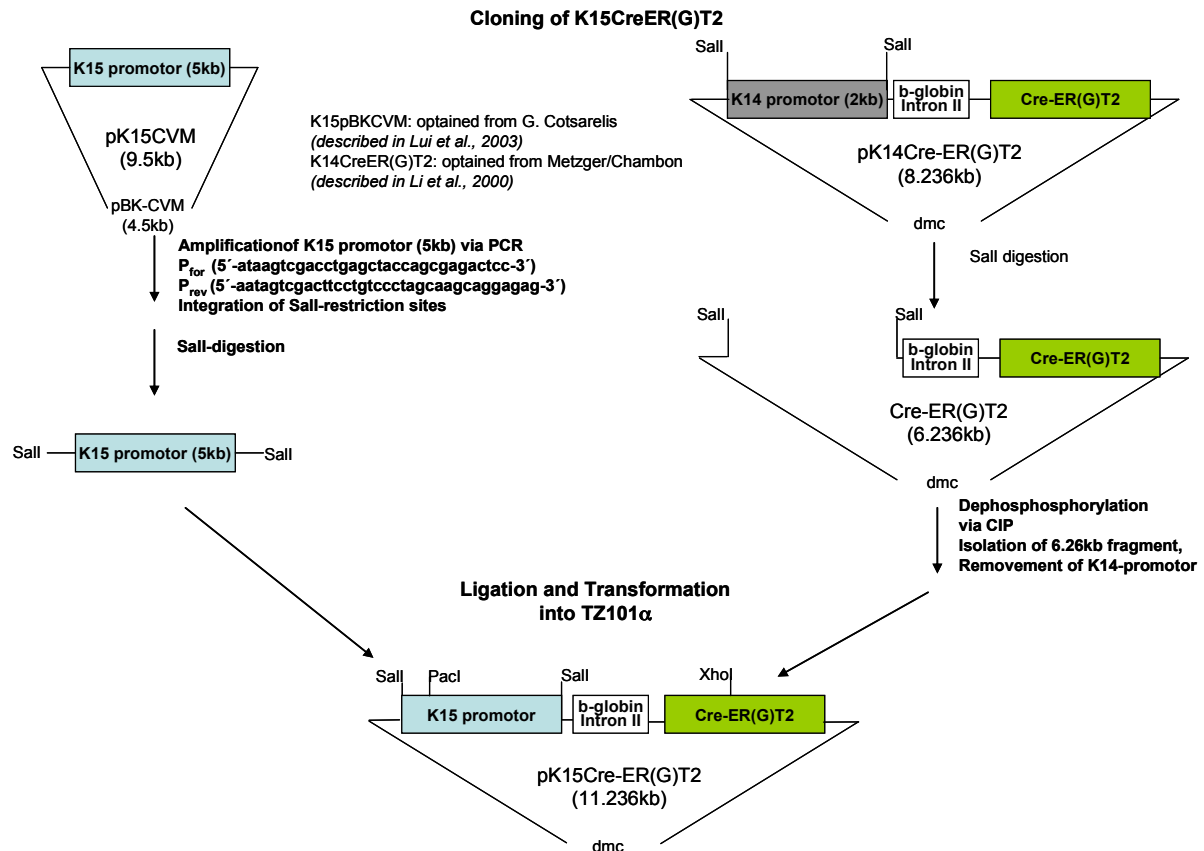


**Fig 10: Scheme depicting cloning procedure for generating pK15CreER(G)T2 (see also text)**

### 2.2.5.3 Purification of K15CreER(G)T2 for microinjection

*NotI* digestion was performed to linearise the construct and to delete vector backbone not required for successful microinjection. The resulting 8 kb DNA fragment was purified using gel extraction and strained through a 0.45µm filter (Millipore) to ensure high quality for microinjection.

### 2.2.5.4 Cloning of pK15ΔNLeF1

To generate the plasmid pK15ΔNLeF1, pK15CreER(G)T2 was partially digested with *EcoRI* to remove CreER(G)T2 (Fig 11). Accessorily to the amplification of myc-tagged ΔNLeF1, *EcoRI* restriction sites were added for subsequent ligation into *EcoRI*-digested pK15CreER(G)T2. Using heat shock transformation, DNA was introduced into chemo competent bacteria (TZ101α, Trenzyme). Again, 0.05% glucose and 100 µg/ml ampicillin was added to the medium. Plasmid DNA of 150

clones was isolated and PCR was performed amplifying K15 or  $\Delta$ NLef1 fragment to identify positive clones that carried pK15 $\Delta$ NLef1. Plasmid DNA was sequenced to confirm the right nucleotide sequence of positive clones (performed by the CMMC service lab).

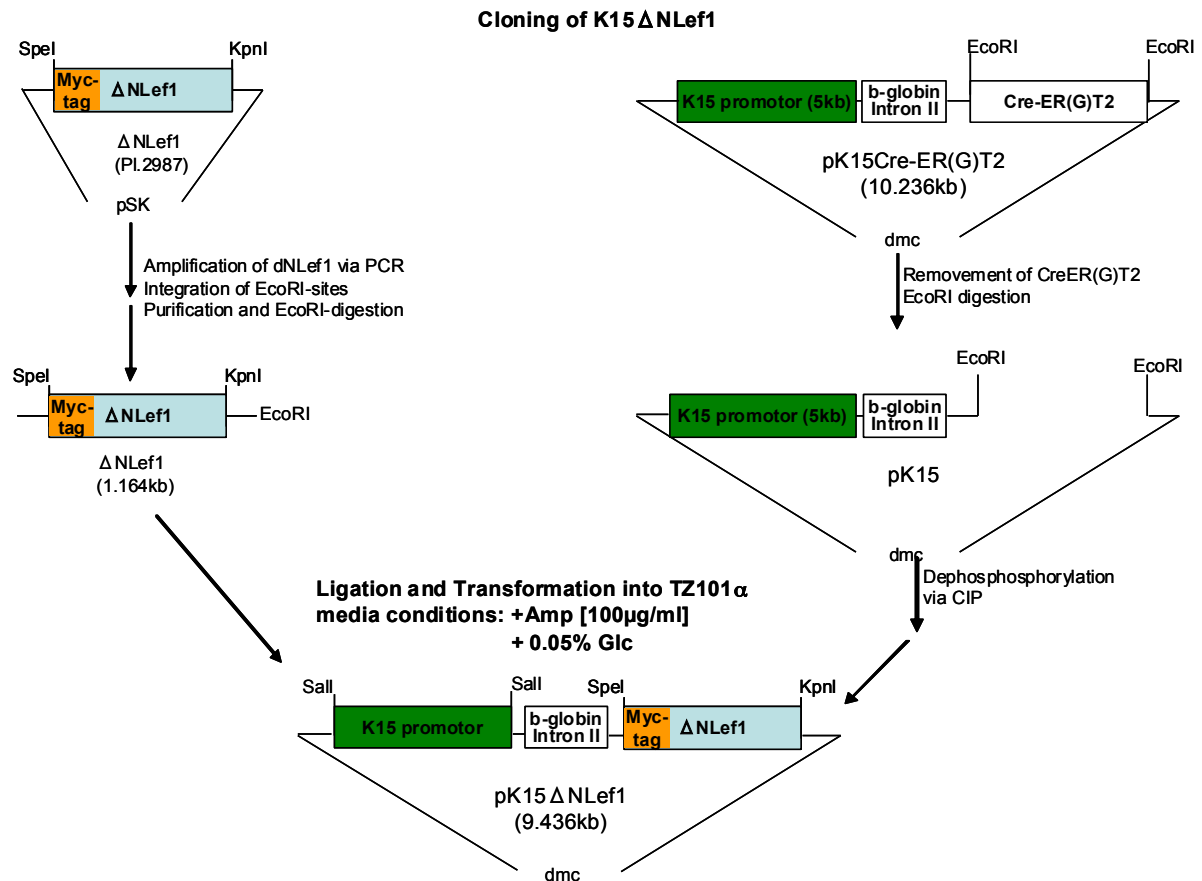


**Fig 11: Schematic representation of cloning procedures for generating pK15 $\Delta$ NLef1**

#### 2.2.5.5 Purification of K15 $\Delta$ NLef1 for microinjection

*NotI* digestions were carried out to linearise and a 7 kb DNA fragment containing the K15 $\Delta$ NLef1 expression cassette was purified by agarose gel extraction. DNA was additionally strained through a 0.45 $\mu$ m filter (Millipore) to ensure high quality of the construct for microinjection (Millipore columns).

#### 2.2.5.6 DNA sequencing

Plasmid DNA was sequenced using a ABI Big Dye Terminator Sequencing Kit (Applied Biosystems) according to the manufacturer's instructions. The fluorescently labelled DNA was analysed with an ABI Prism3730 DNA analyser (Applied Biosystems).

## 2.3 Cell biology

### 2.3.1 Histological analyses

Sections of formaline-fixed and paraffin-embedded back or tail skin and tumour tissue (7-10  $\mu\text{m}$ ) were dehydrated. Subsequently, hematoxylin/eosin (H/E) staining was performed according to the standard protocols. Alternatively, skin sections (4-7  $\mu\text{m}$ ) of OCT-embedded frozen tissue were fixed with 4 % (w/v) PFA and subjected for further immunofluorescent analyses.

#### 2.3.1.1 Immunofluorescent stainings

Fixed epidermal sheets were blocked for 1 h with PB buffer containing 0.5 % milk powder, 0.25 % fish skin gelatine and 0.5 % TritonX-100 in TBS (20 mM HEPES, pH 7.2, 0.9 % NaCl) (Braun et al., 2003). Following o/n incubation with primary antibodies at RT (gentle agitation), whole-mounts were washed with PBS-0.2 % Tween-20 for 4 h. Secondary antibodies were then applied o/n at RT and washing steps were repeated for 4 h. Epidermal sheets were rinsed with distilled water before mounting with Mowiol/DABCO. To detect EYFP expression in skin sections, tissue was fixed with 4% PFA for 3 hours at RT. After an incubation with 30% sucrose (o/n, 4°C), skin was OCT-embedded and cryo sections (5-50 $\mu\text{m}$ ) were analysed for YFP expression.

#### 2.3.1.2 Antibodies

The antibodies listed in Table 6 were used applying protocols described previously (Braun et al., 2003).

**Table 6: Used antibodies**

antibody	host	dilution	reference
K15	mouse IgG2a	1:1000	Neomarkers
K15	guinea pig	1:1500	Progen
GFP	rabbit	1:2500	Molecular Probes
Cre	rabbit	1:750	Covance
SCD1	goat	1:150	Santa Cruz
Itga6	rat	1:3000	BD Bioscience
CD34	rat	1:50	E-Bioscience/Natutec
MTS24	rat	1:100	Gill et al., 2002
NG2	rabbit	1:250	Calbiochem
Scal-PE	rat	1:250	BD Bioscience
Sox9	rabbit	1:150	Santa Cruz

All secondary antibodies Alexa-488, -594, Cy3 were obtained from Molecular Probes. In some cases, propidium iodide (PI, 1:2000) or DAPI (1:2000) was used for nuclear counterstain. Immunostainings were analysed and images taken applying confocal microscopy (Zeiss LSM711). For 3-dimensional evaluation of epidermal whole mounts, 15-30 stacks of 2.5µm size were taken and projected in a maximum intensity using ImageJ (NIH).

### 2.3.2 $\beta$ -Galactosidase staining *in vivo* / *in vitro*

$\beta$ -galactosidase staining was conducted as described earlier (Morris et al., 2004). Skin tissue and epidermal whole-mounts were fixed with 0.2 % glutaraldehyde/2 % formaldehyde for 1.5 h. Alternatively, a fixation of keratinocytes with 4 % PFA was followed by a permeabilisation step (washing buffer). After a washing step with potassium phosphate-buffer (KPP) containing EGTA [0.05M],  $MgCl_2$ [0.02M] and 0.02 % NP-40, samples were incubated with X-Gal staining solution (0.5 mg/ml X-Gal, 10 mM  $K_3[Fe(CN)_6]$ , 10 mM  $K_4[Fe(CN)_6]$  in KPP 0.1 M, pH 7.4; 0.02 % NP-40) o/n at RT. Following a washing step o/n, RT, X-Gal treated paraffin and cryo sections (4-10 µm) or whole-mounts were counterstained with hematoxylin and analysed by light microscopy (LeicaDM4000B).

### 2.3.3 Isolation of primary keratinocytes

The skin of 3-4 days old mice was harvested and subsequently digested with 0.25 % trypsin/EDTA 0.02 % o/n at 4°C. Epidermis was separated from underlying dermal tissue and minced (Rheinwald, 1989; Rheinwald and Green, 1975; Watt, 1994).

Primary keratinocytes of adult back skin were isolated as described earlier (Blanpain et al., 2004; Jensen et al., 2009). Briefly, subcutaneous and fat tissue of 6-8 weeks old mice was removed manually and back and tail skin were digested with 0.25 % trypsin (without EDTA, GIBCO/Invitrogen) for 2-2.5 h at 37 °C, 5 %  $CO_2$ . Subsequently, epidermis was peeled off, minced and gently agitated for 20 min at RT in defined keratinocyte medium (chapter 2.3.4 and (Watt, 1994) at RT).

After straining through a 70 µm filter, cell suspensions derived from 2-4 days old and adult mice were centrifuged (1000 x g, 15 min, 4 °C). Resuspended keratinocytes were seeded on Collagen G coated [0.04mg/ml] 10 cm plates. Keratinocytes were grown in co-cultures with mitomycin [4µg/ml]-treated anti-proliferative J2 3T3 feeder

cells (Swiss Albino) (Rheinwald and Green, 1975; Watt, 1994). K14, Itga6 staining (FACS-analysis, immunostainings) were performed to confirm epidermal deprivation of the isolated cells.

### 2.3.4 Cultivation of cells

Primary keratinocytes were co-cultured with anti-proliferative J23T3 cells in defined low calcium keratinocyte medium containing DMEM/Ham's F12 (3:1) ( $<50 \mu\text{M Ca}^{2+}$ , Biochrom) supplemented with penicillin (100 IU/ml), streptomycin (100  $\mu\text{g/ml}$ ), adenine ( $1.8 \times 10^{-4} \text{ M}$ ), glutamine (2 mM), hydrocortisone (0.5  $\mu\text{g/ml}$ ), epidermal growth factor (EGF) (10 ng/ml), cholera enterotoxin ( $10^{-5} \text{ M}$ ), and insulin (5  $\mu\text{g/ml}$ ) and 10 % fetal calf serum (FCS Gold) at 32 °C in an atmosphere of 5 %  $\text{CO}_2$  in a humidified incubator (Carroll et al., 1995; Morris et al., 1987; Rheinwald, 1989; Rheinwald and Green, 1975). To avoid differentiation of keratinocytes which can be induced by  $\text{Ca}^{2+}$ , FSC was treated with Chelex-100 resin (BioRad) o/n, RT, pH 7.0 and was strained through a sterile filter prior to use.

J23T3 fibroblast were cultured in DMEM supplemented with 10 % FCS, penicillin (100 U/ml) and streptomycin (100  $\mu\text{g/ml}$ ) at 37 °C and 5 %  $\text{CO}_2$ .

### 2.3.5 Passaging of cells

Medium was changed every 2-3 days. When keratinocyte reached confluency of 80-90 %, cells were washed with PBS-0.02 % EDTA and incubated with 0.05 % (w/v) trypsin/0.02 % (w/v) EDTA (Gibco/Invitrogen) at 37 °C until the anti-proliferative feeder cells detached. Cells were passaged 1:2 on collagen-coated culture dishes. To freeze keratinocytes, cell suspensions were mixed with 10 % (v/v) DMSO in FSC-Gold+Chelex and were gradually frozen down using a "Cryo 1°C freezing container" (Nalgene). For long-term storage, keratinocytes were transferred into liquid nitrogen. J23T3 feeder cells were passaged by washing with PBS at RT and incubation with 0.05 % (w/v) trypsin/0.02 % (w/v) EDTA for 2 min at 37 °C. For co-culturing with primary keratinocytes, J23T2 cells were treated with mitomycin [4 $\mu\text{g/ml}$ ] for 1.5 hours to stop proliferation.

### 2.3.6 FACS-sorting

Keratinocytes were isolated as described above (2.3.3). For Lrig1-staining, epidermis of back skin was harvested and digested using thermolysin (Sigma-Aldrich) (Jensen



et al., 2009). Single cell suspensions were incubated with the following antibodies in 5 % FCS/PBS for 45 min at 4 °C: phycoerythrin (PE)-conjugated  $\alpha$ 6-integrin (CD47f, BD Pharmingen; 1:25), Alexa488-coupled CD34 (Ram34, eBioscience; diluted 1:10), Lrig1 (R&D Systems; 1:20). Cell viability was assessed by propidium iodide (PI) labelling. Subsequent cell sorting for RNA isolation and expression analysis were carried out using a FACSVantage SE System (BD Bioscience).

### **2.3.7 Transfection of primary keratinocytes**

Transfection of primary keratinocytes was carried out using lipofectamin2000 (Invitrogen) according to the manufacturer's instructions. DNA amount and relationship between lipofectamin and DNA was optimised using a pEGFP vector. Maximal transfection efficiency ranged from 15-20 % when using 1-4  $\mu$ g of DNA.

### **2.3.8 Tamoxifen treatment *in vitro***

Primary keratinocytes derived from R26RLacZ or wt mice were transfected with pK14CreER(G)T2 or pK15CreER(G)T2-DNA (2.3.7). Cre recombinase was induced in transfected keratinocytes with the incubation of 0.2  $\mu$ M 4-hydroxytamoxifen (4-OHT, Sigma-Aldrich, dissolved in EtOH) for 12 h. Cells were analyzed for Cre reporter gene expression 24 h after transfection. For appropriate induction of Cre recombinase, it is essential to use Optimem or SFM defined keratinocyte (Invitrogen), media that do not contain any pH-indicators or colorants, since these might lead to unspecific Cre-activation.

## **2.4 *In vivo* studies**

All experimental procedures applying different mouse models were performed in according to institutional guidelines and animal license given by the State Office North Rhine Westphalia.

### **2.4.1 Mouse models**

All mouse strains used were backcrossed or maintained on a C57Bl/6 background.

#### **2.4.1.1 Generation of K15CreER(G)T2**

8 ng/ $\mu$ l of linearised and purified K15CreER(G)T2-DNA was introduced into 250 fertilised oocytes (performed by the CMMC microinjection lab). Subsequent

transplantation of the micro-injected oocytes into different pseudo-pregnant foster mice resulted in the birth of 34 founder animals. Vitality and quality of the micro-injected oocytes was confirmed by light microscopy.

#### **2.4.1.2 Generation of K15 $\Delta$ NLef1**

A 7 kb DNA fragment containing the K15 $\Delta$ NLef1 expression cassette [5 ng/ $\mu$ l] was injected into the pronucleus of fertilised oocytes. The transplantation of 300 of these oocytes into different fosters generated 54 F0-mice.

#### **2.4.1.3 Cre-reporter lines**

To monitor and visualise specificity of Cre recombination and enzyme activity *in vivo*, inducible Cre-strains were either crossed with R26RLacZ (Soriano, 1999) or to R26REYFP Cre-reporter mice (Srinivas et al., 2001). To maximise visualisation of positive recombination, Cre-reporter lines were kept in a homozygous background.

#### **2.4.1.4 K14 $\Delta$ NLef1**

To study effects of impaired Lef1 signalling on the fate of labelled bulge cells, K15CreER(G)T2 (A\_C\_line)/ R26REYFP were crossed with K14 $\Delta$ NLef1 mice (Niemann et al., 2002).

### **2.4.2 Tumour experiments**

To initiate tumourigenesis, 7 week old K14 $\Delta$ NLef1, K15 $\Delta$ NLef1 mice and wt control littermates were treated once with a sub-critical threshold dose (100 or 150 nM dissolved in 200 ml acetone) of 7,12-dimethylbenz(a)anthracene (DMBA, Sigma-Aldrich). 3-4 weeks after topical DMBA application tumors developed as described earlier (Niemann et al., 2002).

### **2.4.3 Tamoxifen treatment**

Tamoxifen substance (Sigma-Aldrich) was dissolved in 200  $\mu$ l sun flower oil for 1 hour under vigorous shaking (Indra et al., 1999). A dose of 2.5 mg/day was injected intraperitoneally at three consecutive days. In alternative experiments, a single dose of 4 mg tamoxifen was used. Intraperitoneal injections were more efficient than topical application of the same dose of tamoxifen. To apply the tamoxifen in the appropriate phase of the hair cycle, animals were shaved, the current hair cycle phase was determined (according to (Muller-Rover et al., 2001) and Cre

recombinase was induced in early telogen (PD42-52), telogen to anagen transition (PD53-55) and anagen (PD56-71).

#### **2.4.4 Generation of label retaining cells (LRC)**

To generate LRC (Bickenbach et al., 1986; Bickenbach and Chism, 1998), mice (PD9/10) were injected with 50 mg/kg bodyweight 5-bromo-2'-deoxyuridine (BrdU, Sigma-Aldrich, Germany) every 12 h for a total pulse of four intraperitoneal injections (Braun et al., 2003). Mice were analysed for LRC 6-8 weeks post injection. For short-term labelling, a dose of 100 mg/kg BrdU was used. Tissue was harvested 1.5 h post injection.

#### **2.4.5 Tissue harvesting**

Mice were sacrificed and tail, back skin or tumour tissue was dissected as described (Paus et al., 1999). Tissue was either fixed directly (1.5 h, 4 % formaldehyde or 0.2% glutaraldehyde/2% formaldehyde at RT) for paraffin embedding or stored at -80°C embedded in tissue Tec OCT (tissue freezing medium, Sakura) to perform cryosections.

Additionally, samples were directly transferred into liquid nitrogen for RNA or protein analyses.

##### **2.4.5.1 Isolation of epidermal whole mounts**

Epidermal whole-mounts of tail skin were isolated as described before (Braun et al., 2003). Briefly, tail skin was incubated in 5 mM EDTA, 37 °C for 4 h and epidermis was separated from the underlying dermis. To prepare whole mounts from early lesions and epidermal tumours, early lesions and sebaceous tumours from K14ΔN<sup>Lef1</sup> mice were dissected and fat tissue and most of the connective tissue was removed using forceps. Following an EDTA [20 mM] -treatment at 37 °C for 3.5 to 4.5 h, the epidermis was gently peeled off using forceps.

Epidermal sheets of tail, back and early sebaceous tumours were fixed in 3.4% formalaldehyde or in 0.2 % glutaraldehyde/2 % formaldehyde for 2 h at RT.

Fixed whole mounts were stored at 4 °C in PBS.

## **2.5 Statistical analysis**

Epidermal whole-mounts of induced A\_K15CreER(G)T2/R26RLacZ were analysed for LacZ positive cells at different tracing time points (day 1 to 7 after Cre induction). After counting a minimum of n=120 telogen HF of 3 independent mice per tracing time point, we classified the LacZ positive cells concerning their expression pattern, namely bulge (B) bulge only; B, B + SD + SG (more complex pattern) and SG + SD. S.D. was calculated. To test the significance between labelled bulge cells per pilosebaceous unit between d3 and 6months of tracing (n=3 mice/time point), students t-test was employed to determine the p-value.

### 3 Results

#### 3.1 Epidermal regeneration during skin homeostasis

Mammalian epidermis is a highly dynamic epithelium comprising the IFE, HF and associated SG. Tissue integrity and the individual cellular turn over of each of these compartments is maintained by multiple SC and progenitor populations (Blanpain and Fuchs, 2009, Jaks et al., 2010).

##### 3.1.1 Stem cell and progenitor niches within the epidermis

In a first set of experiments, the expression pattern of different described SC/progenitor markers was analysed by immunofluorescent studies on epidermal tail whole-mounts. The whole-mount technique provides an excellent tool to screen and visualise large areas of tail epidermis in a three dimensional (3D) fashion (Braun et al., 2003). Physiologically, pilosebaceous units of tail skin are organised in triplicates and comprise two SG attached to one HF.

First, we investigated the HFSC niche (HF bulge) (Fig 12A), which was recognised by K15 (Fig 12B), CD34 (Fig 12E), Itga6 (Fig 12D) antibodies. Notably, LRC were not only detected in the bulge of telogen HF (Fig 12C, arrowhead), but the BrdU label was also diluted along the UI and the SG (Fig 12C, arrows) and downwards to the HF indicating a contribution of HFSC from the bulge to these compartments. The transcription factor Sox9 showed a heterogeneous expression in the bulge region (Fig 12F, arrowheads) and Sox9<sup>+</sup>ve cells were seen in the developing HF (Fig 12F, arrows).

Additional SC and progenitor cell populations of the pilosebaceous unit have been identified residing above the HF bulge (Fig 12G). The region of the UI, located between the HFSC niche and the SG, shows low Itga6 expression and lacks CD34 and Scal (Fig 12 D,E,K and Jensen et al, 2008). The UI is positive for the MTS24 antigen (Nijhof et al., 2006), which is a progenitor marker for the thymic epithelium (Gill et al., 2002) and has recently been identified to correspond to Plet1 (Depreter et al., 2008, Raymond et al., 2010). Besides a positive signal in the UI, MTS24 antigen<sup>+</sup>ve cells were also detected at the outer periphery of the SG (Fig 12H).

The JZ, just adjacent to the SG, has recently been reported to contain bipotent Lrig1<sup>+</sup>ve SC giving rise to the IFE and the SG. Consistent with previous reports

(Jensen et al., 2009) the transmembrane protein Lrig1 was detected within the JZ and periphery of the SG (Fig 12I, arrow).

Next, we analysed Blimp1 expression, a transcription factor that has been proposed to mark unipotent progenitor cells at the SG in murine epidermis (Horsley et al., 2006). In contrast, a recent study analysing human skin and tumour tissue revealed that Blimp1 expression was restricted to more differentiated sebocytes (Sellmeyer and Krall, 2009). Although Blimp1 antibody showed a positive signal in the SG in epidermal tail whole-mounts (Fig 12J), no expected nuclear staining was seen.

NG2 (chondroitin sulfate proteoglycan) was described to be a surface marker for progenitors in human IFE (Ghali et al., 2004; Legg et al., 2003). In murine tail epidermis, a NG2<sup>+</sup>ve signal was not only observed in the IFE but also in the HF and UI, indicating that NG2 in murine tail epidermis does not restrictively mark progenitors of the IFE (Fig 12L).

Taken together, we were able to detect a series of SC/progenitor markers in epidermal whole-mounts of tail skin, thereby providing the tools to study the dynamics of spontaneous epidermal regeneration.

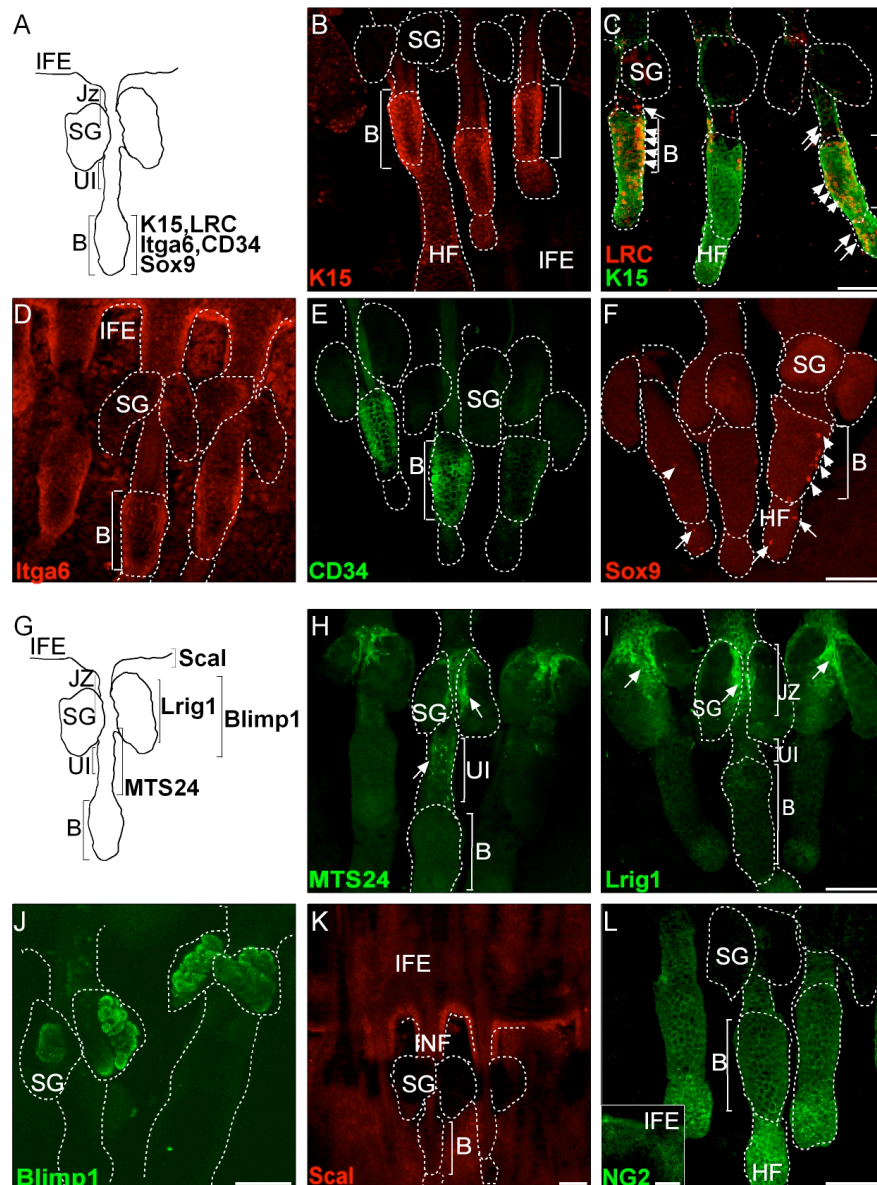


**Fig 12: Different SC/progenitor compartments within the epidermis**

Immunofluorescent studies on epidermal whole-mounts from 7-8weeks old wt mice (early anagen/anagen) using the indicated antibodies against SC/progenitor markers.

(A) Localisation and markers of the HF bulge. (B-F) Expression of K15, LRC, Itga6<sup>high</sup>, CD34 and Sox9 in the HF bulge. Note that LRC were diluted towards the HF and UI/SG (C, arrows). Sox9<sup>+</sup>ve cells were also detected at the HF (F, arrows). (G) Markers for SC/progenitor niches lying above the HF bulge. (H) MTS24 antigen is expressed at the UI and the periphery of the SG. (I) Lrig1 detected the JZ and periphery of the SG. (J) Blimp1 antibody recognised cells localised to the SG, but no nuclear signal was seen. (K) Scal is confined to the INF and IFE interspersing the pilosebaceous units. (L) NG2 marked the HF and IFE. HF-hair follicle, UI-upper isthmus, JZ-junctional zone, SG-sebaceous gland, B-bulge, INF-infundibulum, IFE-interfollicular epidermis. Scale bars in C,F,I,J represent 80  $\mu$ m, in K and L (inset) 40  $\mu$ m.

### 3.2 Generation of K15CreER(G)T2 transgenic mice

To investigate a potential contribution of HFSC to epidermal regeneration and tumourigenesis, we have generated K15CreER(G)T2 transgenic mice (Fig 13). This mouse model expresses a tamoxifen-inducible CreER(G)T2-system (Indra et al., 1999) under the control of the Keratin 15 (K15) regulatory sequence. This 5 kb K15 promotor fragment has previously been shown to specifically target HFSC from the bulge region and K15<sup>+</sup>ve progenitors contribute to HF regeneration (Liu et al., 2003, Morris et al., 2004). With the site-specific targeting of CreER(G)T2 under the control of the K15 promotor, we aim to conditionally induce Cre-recombinase in HFSC of the bulge region. The CreER(G)T2 system consists of a Cre-recombinase fused to a modified ligand binding domain of the human estrogen receptor (ER(G)T2), which carries a triple mutation in G400V/M543A/L544A (Indra et al., 1999).

Upon application of the estrogen analogon tamoxifen to K15CreER(G)T2 mice, Cre-recombinase is translocated to the nucleus and therefore becomes active. Crossing K15CreER(G)T2 mice to Cre-sensitive reporter lines (Rosa26RLacZ, Soriano, 1999; R26REYFP, Srinivas et al., 2001) provides an excellent tool to trace all cell lineages descending from the originally labelled HFSC (HFSC-derived progeny). This involves Cre-mediated removal of a loxP-flanked transcriptional termination sequence in front of the reporter genes (such as LacZ or EYFP) leading to a constitutive expression of LacZ or EYFP. As a result, not only HFSC but also HFSC-derived progeny could be visualised and traced over a certain period of time.



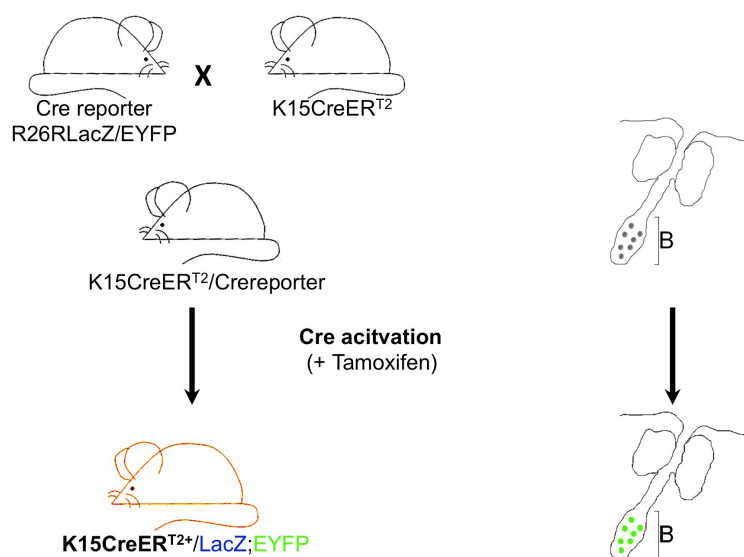


**Fig 13: Generation of K15CreER(G)T2 mice to target HFSC and to map HFSC-derived progeny**

Tamoxifen treatment of K15CreER(G)T2 mice leads to the activation of Cre recombinase in keratinocytes carrying the K15 promoter fragment. By crossing K15CreER(G)T2 to R26REYFP/LacZ Cre reporter mice, Cre mediated recombination leads to a constitutive reporter gene expression (LacZ or EYFP).

### 3.2.1 Cloning of pK15CreER(G)T2

To generate K15CreER(G)T2 transgenic mice, a 5 kb K15 promoter fragment (Liu et al., 2003) was amplified (Fig 14). The K15promotor fragment was exchanged with the K14promotor fragment of pK14CreER(G)T2 (Indra et al.1999). The pK14CreER(G)T2 vector consists of a rabbit  $\beta$ -globin intronII sequence downstream of the promoter to enhance transgene expression and a polyAAA tail to prevent exonucleatic RNA degradation (Fig 14); detailed cloning procedure in 2.2.5.2.).



**Fig 14: Scheme depicting the K15CreER(G)T2 construct**

A 5 kb K15 promoter fragment was used to drive an inducible CreER(G)T2. The CreER(G)T2 vector is comprised of an inducible CreER(G)T2, an enhancer ( $\beta$ -globin intronII) and a polyAAA tail. *NotI* restriction sites were used to linearise the construct for microinjection .

Next, we analysed if cloned pK15CreER(G)T2 DNA exhibited the correct size, orientation and sequence. Therefore, plasmid DNA isolated from potential pK15CreER(G)T2 clones was digested with *PacI* enzyme which linearised the construct resulting in a fragment of an expected size of 11 kb (Fig15B). Double digests using *XhoI* (restriction site at +1) and *PacI* (restriction site at +0.8 kb) (Fig 15A) were used to verify the right insertion of the K15 promotor fragment. As expected, fragments of 6 and 4.8 kb were obtained (Fig 15B). Additional sequence analyses (performed by the CMMC service lab) affirmed the correct sequence of pK15CreER(G)T2 plasmid DNA.

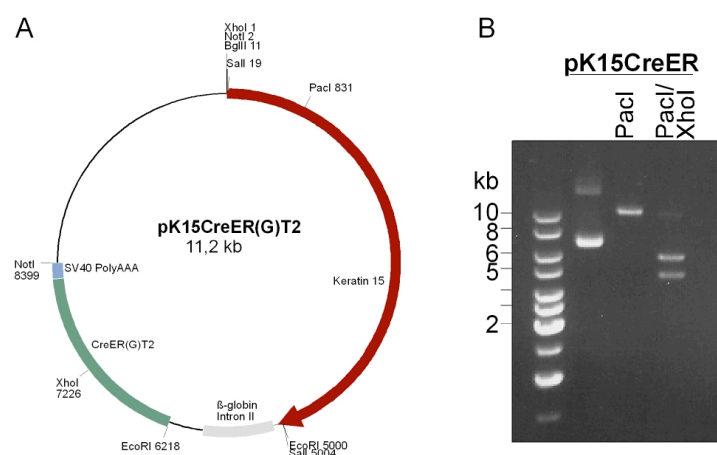


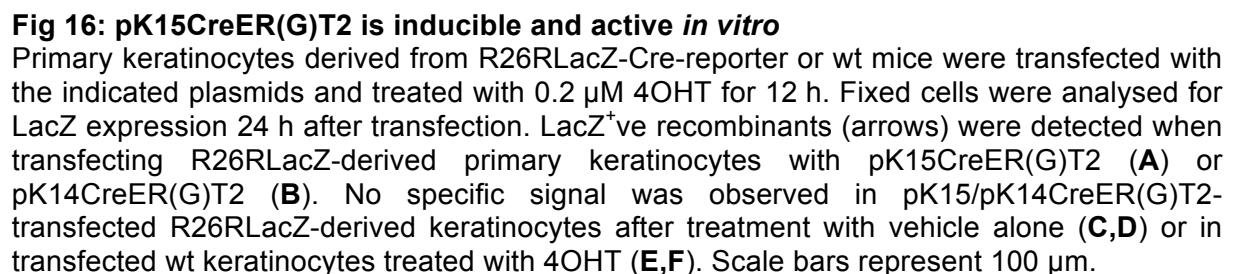
**Fig15: Generation of pK15CreER(G)T2**

(A) Map depicting restriction sites of pK15CreER(G)T2. (B) K15CreER(G)T2-derived plasmid DNA was digested to verify correct size and orientation of the construct. *PacI* linearised the pK15CreER(G)T2 and *PacI* / *XhoI* double digests showed expected fragments of 6 and 4.75kb size.

### 3.2.2 Functionality of pK15CreER(G)T2 *in vitro*

To test whether the pK15CreER(G)T2 construct indeed expresses CreER(G)T2 and if Cre recombinase can be specifically activated by the application of tamoxifen, primary keratinocytes derived from LacZCre-reporter mice (R26RLacZ) were transfected with pK15CreER(G)T2. Subsequently, Cre recombinase was induced by adding 0.2  $\mu$ M 4-hydroxytamoxifen (4OHT) for 12 hours. 24 hours following transfection, Cre-mediated recombination was visualised and quantified by the detection of LacZ. 2 % of pK15CreER(G)T2 transfected keratinocytes exhibited  $\beta$ -Galactosidase activity (Fig 16, arrows), respectively. Transfections using pK14CreER(G)T2 (targets basal keratinocytes) revealed 25 % of the counted cells to be LacZ<sup>+</sup>ve and served as positive control (Fig 16B), since K14 is more widely

These data demonstrate that Cre recombinase of pK15CreER(G)T2 could be specifically activated by the application of 4-hydroxy-tamoxifen and was functional *in vitro*.



### 3.2.3 Identification of K15CreER(G)T2 founder lines

Having verified the functionality *in vitro*, pK15CreER(G)T2-DNA was linearised and purified for microinjection. Therefore, *NotI* digest was performed to exclude sequences of the vector backbone not required for transgene expression. A 8 kb DNA fragment was isolated and purified. An additional purification step was performed to ensure a high quality of the DNA fragment. Quality, size and quantity were determined by a subsequent analytic agarose gel electrophoresis.

Linearised DNA of K15CreER(G)T2 [8ng/μl] was introduced into the pronucleus of approximately 250 fertilised oocytes. Subsequently, oocytes were transplanted into 40 pseudo-pregnant foster mice (performed by the CMMC microinjection lab). Genomic DNA isolated from the offspring (F0-generation) was analysed for K15CreER(G)T2 expression. Conventional PCR analysis amplifying a fragment of 290bp size covering a sequence from the K15 promotor and the  $\beta$ -globin intronII revealed that 8 out of 34 mice carried the transgene (Fig 17, highlighted in bold). The transgene could also be amplified using genomic gDNA derived from F1-generation, demonstrating germline transmission of the transgene. All founder mice showed a normal postnatal development, although 2 founder lines (founder F and H line) were infertile.

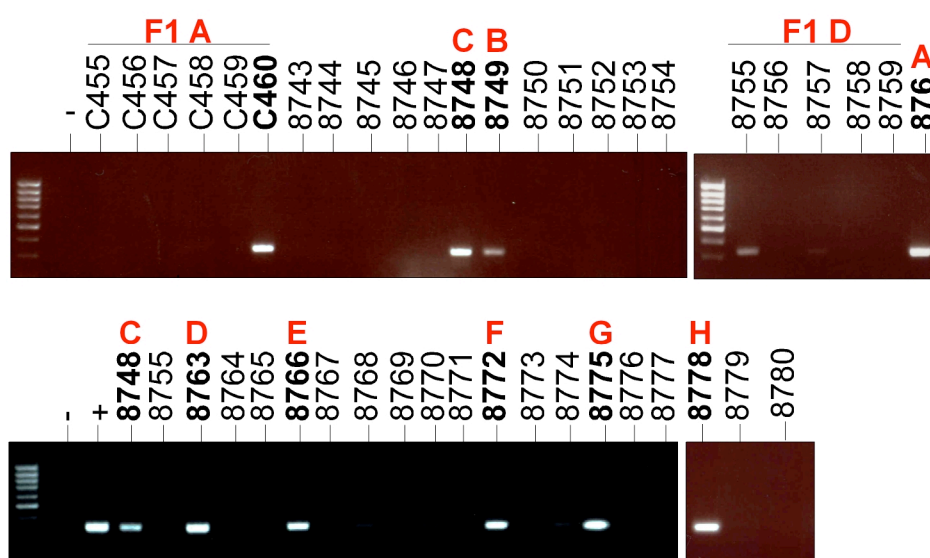


**Fig 17: Identification of K15CreER(G)T2 founder lines**

Performing PCR on genomic DNA isolated from tail biopsies, 8 positive founder lines could be identified (highlighted in bold, referred to A-H line). No signal was observed in the negative control (-), whereas in the positive control (+, pK15CreER(G)T2) an amplicon at the right size (290bp) could be detected.

To test whether Cre recombinase can specifically be activated in K15<sup>+</sup>ve cells from the HFSC *in vivo*, the F1-generation of each founder line was crossed to Cre-reporter mice (either R26RLacZ or R26REYFP).

### **3.2.4 Specific targeting of bulge cells using K15CreER(G)T2 mice**

#### **3.2.4.1 Optimisation of the application and detection protocol using K14CreER(G)T2 mice**

In a first set of experiments, K14CreER(G)T2 mice (targeting all proliferating (TA) cells of the basal layer, (Fig 18B) crossed to Cre-reporter were used as positive control to optimise the dose and duration of tamoxifen-treatment as well as the detection method to specifically visualise positive recombinants in epidermal tail whole-mounts and back skin sections. The following Cre-reporter lines were tested: Rosa26LacZ (Mao et al., 1999), ACZL (Akagi et al., 1997) and R26RLacZ (Soriano, 1999) for LacZ detection and RA/EG (Constien et al., 2001) and R26REYFP (Srinivas et al., 2001) for the detection of EYFP<sup>+</sup>ve cells. To this end, applying a dose of 2.5mg of tamoxifen for three consecutive days resulted in maximal detection of active and nuclear Cre-recombinase in K14CreER(G)T2 (Fig 18C). R26RLacZ or R26REYFP Cre-reporter were utilised for further lineage tracing experiments, since these strains showed the most specific LacZ or EYFP signal. As expected, EYFP (Fig 18E) or LacZ (Fig 18F) of induced K14CreER(G)T2 mice could be detected in the IFE, the ORS of the entire HF and periphery of the SG at day 3 following tamoxifen treatment. Vehicle controls (oil) remained negative for LacZ (Fig 18G) or EYFP and Cre recombinase was expressed in a diffuse cytoplasmic fashion (Fig 18D).



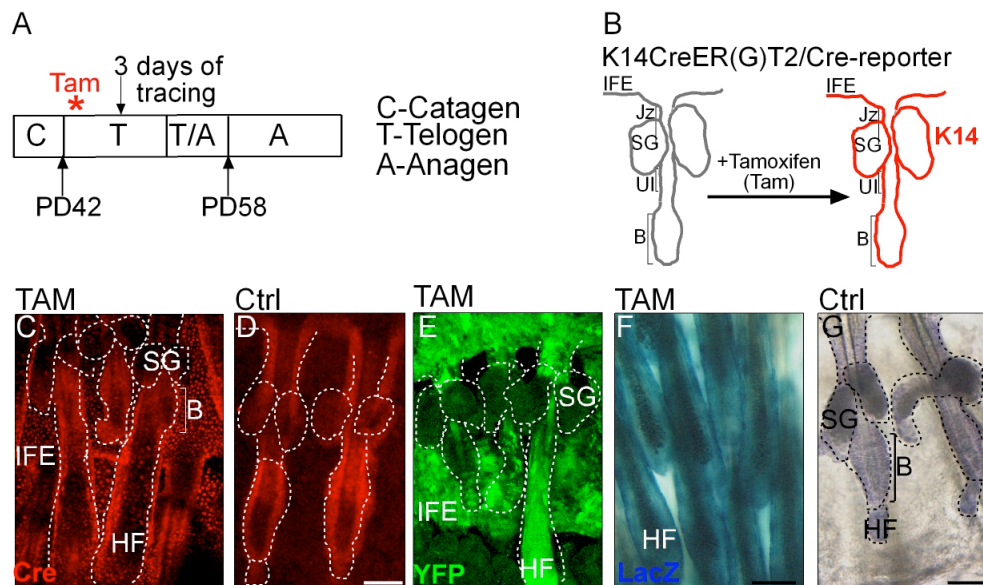


**Fig 18: Optimisation of tamoxifen application procedure and detection methods**

(A, B) K14CreER(G)T2 crossed to Cre-reporter mice were treated with tamoxifen (Tam) during resting phase of the hair cycle (telogen) to target all basal cells of the epidermis. Specific detection of nuclear Cre recombinase (C), EYFP (E) and LacZ (F) in the IFE, ORS of the HF and SG at 3 days of chase. Genotype-matched vehicle treated control mice showed a diffuse cytoplasmic localisation of Cre recombinase (D) and no LacZ signal (G) was detected. Scale bars represent 80µm.

### 3.2.4.2 Identification of two specific K15CreER(G)T2 founder lines

Following optimisation of the tamoxifen treatment and the detection methods for EYFP, LacZ and Cre, all K15CreER(G)T2 founder lines were subjected for further analyses (Fig 19). K15CreER(G)T2 (founder lines A-E and G; F,H were infertile) were crossed to R26RLacZ or EYFP Cre-reporter mice and Cre-recombinase was induced during quiescent state of the hair cycle (beginning of 2<sup>nd</sup> telogen, PD53) (Fig 19A). For each founder line different dose and duration of tamoxifen treatments were assayed to ensure the maximal labelling efficiency and specificity. Nuclear Cre, LacZ or EYFP signal was monitored in epidermal whole-mounts and back skin sections day 1 to 5 following Cre activation (minimum 3 mice/tracing time point). Localisation and number of labelled bulge cells of each of the K15CreER(G)T2 founder line was examined as summarised in Table 7. Mice of B\_D\_G\_K15CreER(G)T2 founder lines showed a broad expression of Cre recombinase and reporter gene activation. These lines were not suitable for further investigations of HFSC function in tissue regeneration. E\_K15CreER(G)T2 mice showed a moderate and exclusive labelling in the bulge region (5-10 cells), but unfortunately exhibited unspecific background activity in the vehicle controls.

**Table 7: Analysis of Cre expression, number of labelled cells and intensity of Cre-reporter gene activation in K15CreER(G)T2/Cre reporter mice**

founder_line		n=	bulge specificity	amount of labelled bulge cells	intensity
<b>A</b>	<b>TAM</b>	<b>30</b>	<b>high</b>	<b>low 1-4</b>	<b>high</b>
	<b>Ctrl</b>	<b>22</b>	%	%	%
B	TAM	5	low	low	low
	Ctrl	4	%	%	%
D	TAM	5	low	low	low
	Ctrl	3	%	%	%
G	TAM	5	low	low	low
	Ctrl	3	%	%	%
<b>C</b>	<b>TAM</b>	<b>44</b>	<b>high</b>	<b>high 20-40</b>	<b>high</b>
	<b>Ctrl</b>	<b>21</b>	%	%	%
E	TAM	9	low	moderate 5-10	high
	Ctrl	5	low	moderate 5-10	high

Eventually, two specific founder lines were identified (referred to as A\_and C\_line) which differed in the number of labelled bulge cells:

- i. Almost the entire HF bulge of tamoxifen treated C\_K15CreER(G)T2 R26RLacZ mice comprised nuclear Cre (Fig 19C) and LacZ (Fig 19E) positive cell populations. Vehicle (oil) treated genotype-matched littermate controls remained negative for LacZ (Fig 19F) or EYFP (data not shown) and Cre recombinase was expressed in a diffuse cytoplasmatic fashion (Fig 19D). These data are in line with previous observations that the K15 promotor fragment targets the entire HF bulge (Morris et al., 2004). Thus, this high expressing C\_K15CreER(G)T2 line could be utilised to genetically manipulate the entire HFSC compartment.
- ii. In contrast, individual bulge cells could be targeted using the low-expressing A\_line (Fig 19G-J). Single LacZ (Fig 19J), EYFP (Fig 19H) and nuclear Cre (2-5 <sup>+</sup>ve cells, Fig 19A) could be targeted at early time points (day 1-3) after tamoxifen treatment. In addition, single EYFP/Cre double positive cells could be detected the bulge region (Fig 19I), whereas the vehicle controls remained negative for EYFP or LacZ (Fig 19K). Therefore, the A\_K15CreER(G)T2 line provides an powerful tool to map the fate of single bulge-derived progeny.

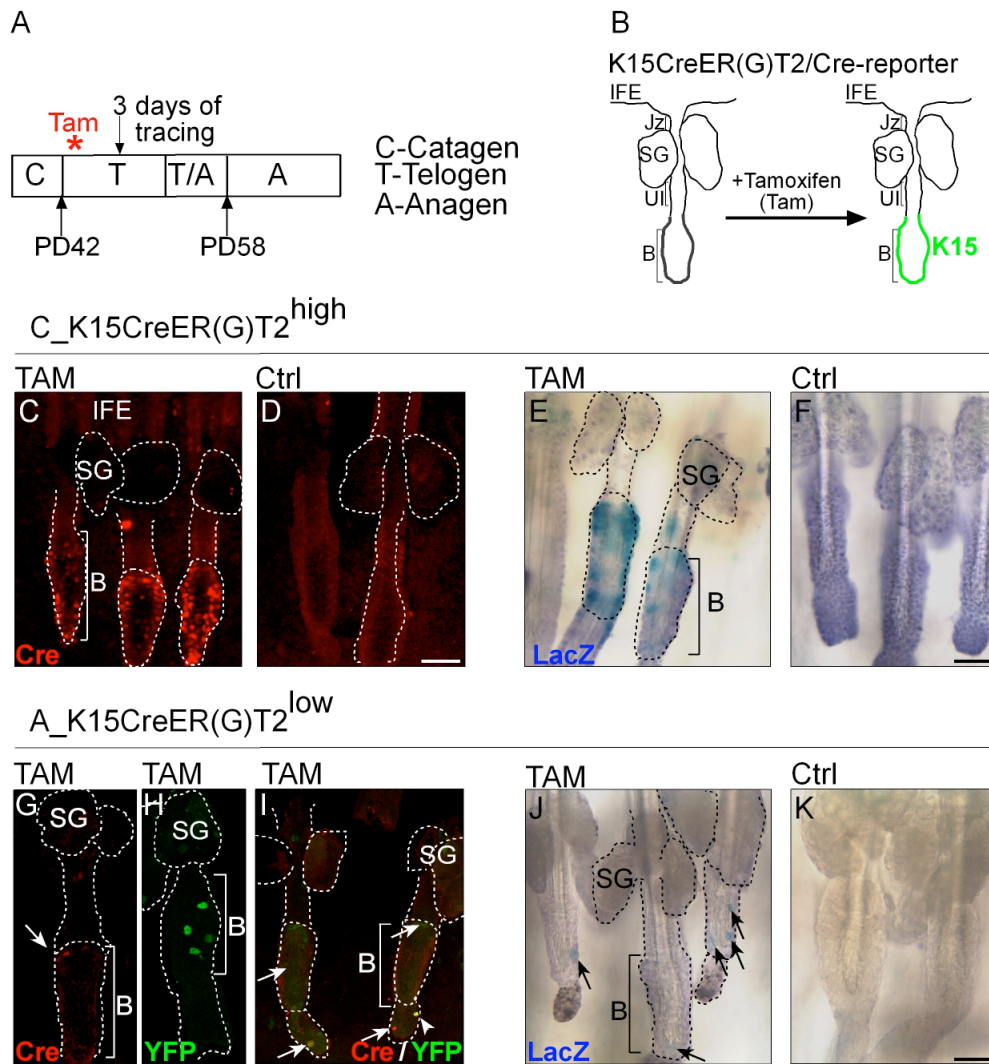


**Fig 19: Targeting of bulge cells using K15CreER(G)T2**

K15CreER(G)T2/R26RLacZ/EYFP mice were treated with tamoxifen during resting phase of the hair cycle (telogen, T) (**A**, **B**). Specific detection of bulge cells (**B**) in tamoxifen-treated K15CreER(G)T2 (Founder C and A) was demonstrated by nuclear Cre LacZ or EYFP stainings. Note that in C\_K15CreER(G)T2 almost the entire bulge region was stained (**C**, **E**), whereas in the A\_K15CreER(G)T2 line, individual bulge cells were targeted (**G-J** arrows). Vehicle controls (Ctrl) were always negative for LacZ (**F**, **K**) or nuclear Cre signal (**D**). Scale bars represent 80  $\mu$ m.



### 3.3 Characterisation of targeted bulge SC

#### 3.3.1 Genetically labelled cells co-localise with SC markers of the HFSC compartment

To examine if the genetically labelled cells of K15CreER(G)T2-mice were indeed localised to the HFSC compartment, co-immunofluorescent studies of labelled keratinocytes with established HFSC/progenitor markers were conducted (Fig 20A). Cre recombinase of A\_K15CreER(G)T2/R26REYFP mice was activated during resting phase of the hair cycle (telogen, PD53), where HFSC are thought to be quiescent. Initially, day 1-2 after tamoxifen treatment, labelled cells co-localised with established HF bulge markers such as K15, LRC and exhibited a high *Itga6* expression (Fig 20B-D), demonstrating that labelled cells were confined to the HFSC compartment.

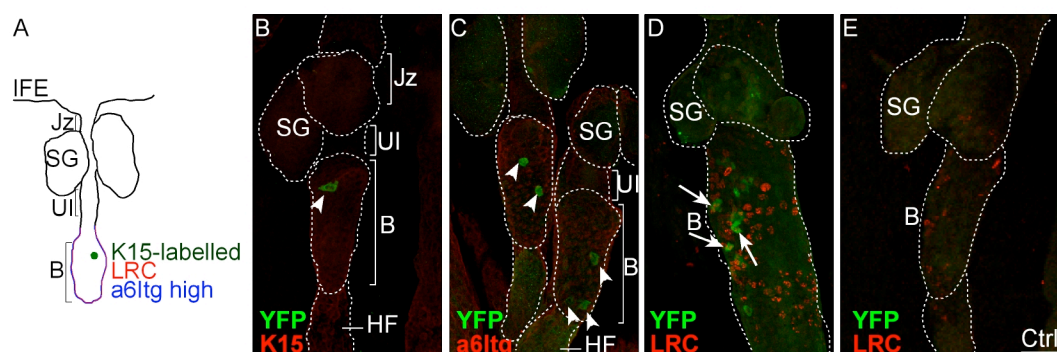


**Fig 20: Genetically targeted cells co-localise with established HFSC/progenitor markers** Tamoxifen was applied to A\_K15CreER(G)T2/EYFP mice during telogen. Co-immunofluorescent studies of EYFP and bulge markers (A) were carried out 3 days following Cre activation. (B) Single EYFP<sup>+</sup> cells (arrow) co-localised with K15. (C) Labelled cells co-expressed a high *Itga6* signal. (D) Individual EYFP<sup>+</sup> keratinocytes were LRC (arrows). EYFP was not detected in vehicle (oil) treated littermate controls (E). Scale bar represents 50µm.

### 3.3.2 Multipotency of targeted HFSC

Next, we tested whether the labelled bulge cells were multipotent *in vivo*.

To date, it is well established that HF regeneration requires a cyclic activation of HFSC in late telogen. This mechanism involves an activation and a mobilisation of HFSC before proliferation is induced to sustain hair growth (anagen phase) (Greco et al., 2009; Legue et al., 2010; Zhang et al., 2009). Applying tamoxifen to A\_K15CreER(G)T2 mice during this HFSC activation phase (telogen to anagen transition, Fig 21A), a trail of single K15-derived progeny was detected along the forming HF (Fig 21C,E) (day 3 after Cre activation). Analysing anagen HF by 6 days of chase, the newly regenerated HF comprised K15-derived progeny and EYFP signal was frequently found in all different hair lineages including layers of the IRS (Fig 21G), the hair matrix (Fig 21G), the bulb and the precortex (Fig 21H). These findings were consistent with previous reports (Morris et al., 2004), demonstrating that targeted cells were multipotent and competent to sustain hair growth.

In comparison to the tracing analyses performed in telogen, tamoxifen treatment during telogen to anagen transition resulted in an increased number of labelled cells at day 3 following Cre activation. An enhanced mobilisation of targeted cells and elevated cellular turn-over at this time point of the hair cycle might be a possible reason for this finding.

To analyse whether targeted cells were long-living SC, lineage tracing analyses were performed following the next hair cycle (day 28 of chase). These experiments revealed that labelled bulge cells still contributed to HF regeneration, but were also detected exclusively in the HFSC compartment (Fig 21D). This data clearly show that no exhaustion of genetically marked bulge cells took place within one month of tracing.

Taken together, these results imply that the genetically targeted K15<sup>+</sup>ve cells were indeed multipotent *in vivo* and will therefore be termed HFSC and all descending cell lineages will be defined as HFSC-derived progeny in the following experiments.

Pilot studies were performed to test the proliferative capacity of labelled HFSC compared to K14<sup>+</sup>ve cells *in vitro*. First, epithelial character of primary keratinocytes derived from adult back skin was confirmed. The isolated cells were positive for K14, Itga6 and K17 and a minority was CD34 or K15<sup>+</sup>ve as verified by immunofluorescent stainings or FACS analyses (data not shown). Furthermore, 2500

initially seeded keratinocytes (passage 2) were competent to form large colonies (holoclones) by 2 weeks of cultivation (data not shown) indicating that a certain number of SC was present within the isolated keratinocyte pool. In a second set of experiments, C\_K15CreER(G)T2 (high expressing line) and K14CreER(G)T2 mice crossed to LacZ-Cre-reporter mice were treated with tamoxifen at early telogen (PD53) and primary keratinocytes were isolated day 3 following Cre-activation. Cells of the 3<sup>rd</sup> passage were analysed for LacZ expression (Fig 21K,L). Interestingly, almost all K15CreER(G)T2-derived keratinocytes were positive for reporter gene activation, whereas only a minority of K14CreER(G)T2 cells expressed LacZ. These initial experiments suggest that K15-derived keratinocytes exhibited a growth advantage compared to K14CreER(G)T2-derived keratinocytes, indicating an increased proliferative potential *in vitro*.

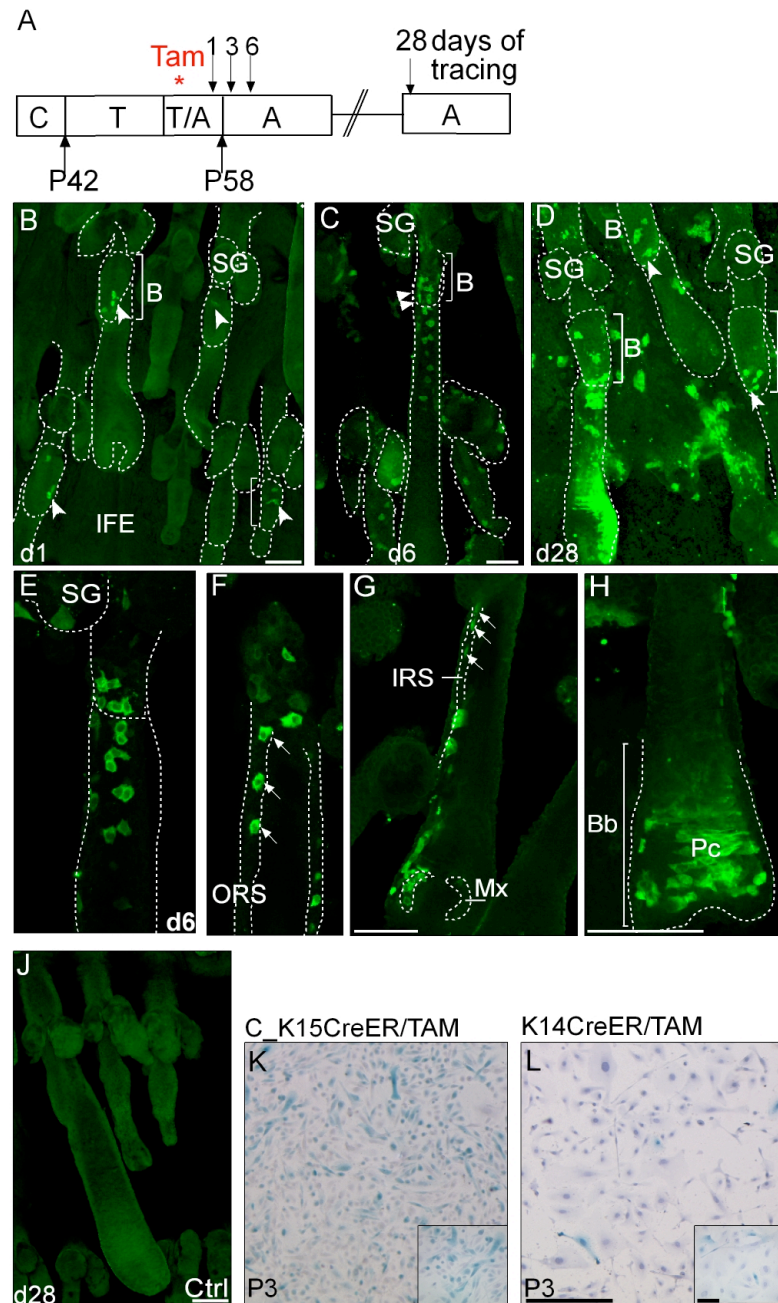


### Fig 21 Targeted bulge cells are capable to regenerate all hair lineages

(A) Cre recombinase of A\_K15CreER(G)T2 mice was activated during telogen to anagen transition. (B) Single EYFP<sup>+</sup> cells appeared in the bulge region at day 1 following Cre activation. Bulge-derived progeny was detected along the developing HF (C) and at all different hair lineages including ORS (E,F), IRS, matrix (Mx) (G), bulb (Bb) and precortex (Pc) (H) at 6 days of chase (n=3 mice). Vehicle controls were negative for EYFP (J). Tracing labelled cells for 28 days, EYFP<sup>+</sup> keratinocytes were found almost at the entire HF. Note single cells in the bulge (D). Primary keratinocytes derived from K14CreER(G)T2/ or C\_K15CreER(G)T2/ R26RLacZ skin (isolated at day 3 following tamoxifen treatment) were cultivated for 3 passages. Fixed cells were analysed for LacZ expression (K,L). Scale bars in B-J represent 80  $\mu$ m, in L 100  $\mu$ m.

### 3.3.3 HFSC-derived progeny drives SG regeneration during resting phase of the hair cycle

To follow the fate of HFSC-derived progeny during telogen phase (quiescent state of the hair cycle) on a single cell level, we conducted lineage tracing experiments utilising the low-expressing A\_line. Therefore, A\_K15CreER/R26EYFP mice were treated with tamoxifen (2.5 mg) for 3 consecutive days and skin was analysed for EYFP expression at different time points (Fig 22). In an alternative experimental set-up, a high dose of tamoxifen (4 mg) was applied once. The number of labelled HF of a minimum of 400 analysed pilosebaceous units (n=9 mice) was higher than 50 %. Initially, single labelled HFSC were present in the bulge within 1 to 2 days of chase (Fig 22B). Analysing day 3-5 following Cre activation, genetically targeted cells were also located at the UI and SD (Fig 22C) and HFSC-derived progeny repopulated the lower tip of the SG (Fig 22D). By 7 days of chase, almost the entire SG comprised EYFP<sup>+</sup>ve keratinocytes, implying a contribution of SC from the HF compartment to SG regeneration (Fig 22E,F). The interesting observation that only one of the two SG compassed EYFP<sup>+</sup>ve signal in a high frequency suggests that activation of more than one HFSC is required to renew both SG.

From these experiments we conclude that single labelled HFSC were capable to replenish the SG within 7 days. SG homeostasis is a rather highly dynamic process in contrast to the cyclic HF regeneration, which renews in a time frame of 2 weeks.

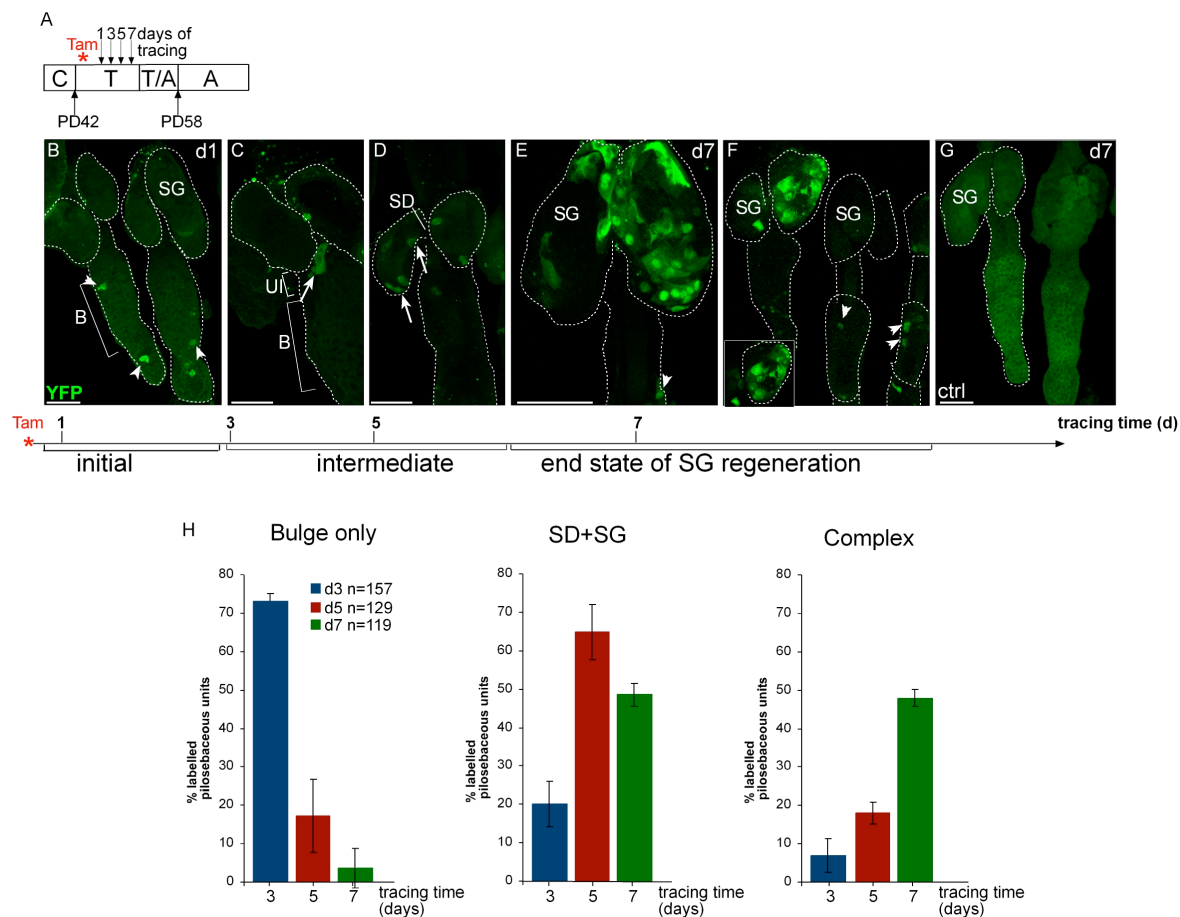


**Fig 22 Commitment of bulge-derived progeny to sebaceous lineage**

(A) Lineage tracing experiments were performed during telogen phase using A\_K15CreER(G)T2/R26REYFP mice. (B) Day 1-3 after Cre induction, single EYFP<sup>+</sup> cells were localised to the HF bulge. Day 3-5 labelled cells were observed at the UI (C, arrow) and the SD (D, arrow), resulting in the detection of EYFP<sup>+</sup> cells at the lower tip of the SG (D, arrow). Almost the entire SG was positive for EYFP by 7 days of chase (E,F). No specific signal was observed in vehicle controls (ctrl) (G). Scale bars represent 50  $\mu$ m. Statistical analyses of K15-traced cells were performed using A\_K15CreER(G)T2/R26RLacZ transgenic mice. LacZ<sup>+</sup>ve cells within the pilosebaceous units (n=3 (d3, d5), n=2 d7 mice/time point) were counted and grouped according to their expression in the bulge only, SD and SG (SD+SG) and a more complex pattern including bulge, SD and SG. S.D. of 3 independent experiments per time point was calculated (H).

Similar results were obtained using a LacZ-Cre-reporter line (data not shown) and no LacZ or EYFP signal was observed in vehicle (oil)-treated littermate controls (Fig 22G). To determine the distribution of labelled cells in more detail, statistical analyses using A\_K15CreER/R26RLacZ mice were carried out (Fig 22H, together with Andreas Kraus, Niemann Lab). Day 3 following Cre activation, the majority (73 %) of labelled cells were confined to an exclusive localisation in the bulge (bulge only pattern), whereas 7 % of the analysed pilosebaceous units showed a more complex pattern labelled in bulge, SD and SG. 20 % of labelled cells were detected in the SD

and SG, most likely because HFSC-derived progeny had already left the HFSC niche. Analysing day 5 and 7 following tamoxifen treatment, a dramatic decrease of cells being exclusively labelled in the bulge is observed (17 % day 5; 4 % day 7, respectively). Concomitant with this finding, the percentage of pilosebaceous units labelled in the B, SD and SG is elevated (18 % day 5; 48 % day 7). Additionally, more LacZ<sup>+</sup>ve keratinocytes are located exclusively in SD+SG (65 % day 5; 49 % day 7).

Taken together, the statistical analyses revealed that HFSC-derived progeny indeed exit the HFSC niche to drive SG renewal. Additionally, few labelled cells remained in the bulge, indicating that they might get mobilised at a later time point or were involved in the renewal of the HFSC pool itself.

### 3.4 Renewal of the SG is a continuous process

On the bases of these results, we addressed the question whether the process of SG regeneration by HFSC was linked to distinct phases of the periodic HF regeneration. Therefore, HFSC and their progeny labelled during HFSC mobilisation phase (telogen to anagen transition) were screened for reporter gene activation at sites of the SG. 3 days following Cre activation, SG were heavily repopulated by EYFP<sup>+</sup>ve keratinocytes, implying that the SG is renewed (Fig 23B). Analysing day 28 following Cre activation, single labelled cells appeared at the lower tips of the SG. In addition, no increase in the number of EYFP<sup>+</sup>ve cells at the SG was detected, indicating that our observations did not result from activation of progenitor cells residing within the SG (Fig 23D).

As expected, HFSC-derived progeny was mobilised for HF renewal during telogen to anagen transition, but intriguingly, EYFP<sup>+</sup>ve keratinocytes were detected in clusters emanating from the JZ towards the IFE (Fig 23B). These clones did not persist after a tracing period of 28 days and no increase of EYFP signal in the IFE was observed. Interestingly, the contribution of HFSC-derived progeny to IFE renewal was enhanced compared to telogen tracing experiment.

Next, we labelled HFSC at the beginning of anagen when activation of bulge SC for HF growth had completed (Fig 23F). Starting with single LacZ<sup>+</sup>ve cells in the bulge region at day 1 (Fig 23G), individually labelled keratinocytes appeared at the lower tip of the SG 3 days following Cre induction (Fig 23H). This culminated in the entire SG (SCD1<sup>+</sup>ve) being positive for activated Cre-reporter gene at day 5-7 of chase (Fig 23I). In this set of experiments, no contribution of genetically labelled cells to HF



regeneration was observed as activation of HFSC had occurred earlier and vehicle treated control mice remained negative for reporter gene activation (Fig 23J).

From this fate mapping studies we have learned that the process of SG renewal was not connected to the cyclic activation of HFSC for HF renewal, but rather occurred continuously. Furthermore, genetically targeted HFSC were competent to regenerate all epidermal lineages including the HF, SG and the IFE.

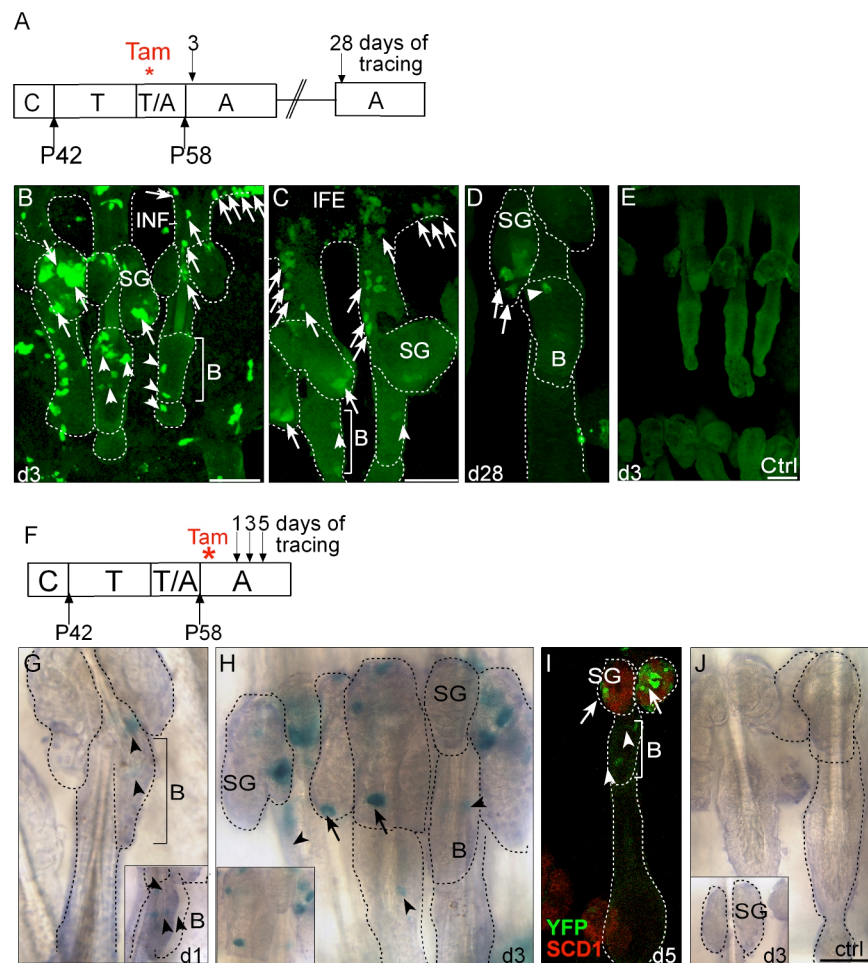


**Fig 23: Epidermal regeneration during different stages of the hair cycle**

(A) Fate mapping studies of HFSC-derived progeny labelled at telogen to anagen transition (n=2-3 mice/time point). (B,C) HFSC-derived progeny contributed to HF regeneration. EYFP<sup>+</sup>ve keratinocytes were also detected at the SG, the JZ, the INF and the IFE. (D) Tracing HFSC-derived cells for 28 days, single EYFP<sup>+</sup>ve cells appeared in the SG (arrows). In vehicle treated double transgenic mice no reporter gene activation was found (E,J). (F) Lineage tracing experiments were conducted during anagen phase. Single LacZ<sup>+</sup>ve cells were confined to the bulge at day 1 (G, arrowheads). Day 3 following Cre activation, EYFP<sup>+</sup>ve progeny could be detected at the lower tip (H, arrows). EYFP<sup>+</sup>ve cells co-localised with the sebocyte marker SCD1 at day 5 after tamoxifen treatment (I). Scale bars represent 50µm.



### 3.5 Regeneration of the HFSC compartment and the SG in long-term studies

To investigate if labelled HFSC were competent to replenish the pilosebaceous unit over a long period of time, we activated Cre-recombinase of A\_K15CreER(G)T2/R26RLacZ mice during 2<sup>nd</sup> telogen and traced HFSC-derived progeny for 6 months. Analyses of LacZ<sup>+</sup>ve keratinocytes in epidermal tail whole-mounts revealed that the SG were still repopulated. Similar to the short-term tracing, one of the two SG showed an intense  $\beta$ -galactosidase activity (Fig 24B-D). These data exclude the possibility that HFSC-derived progeny resided within the SG and sustain SG homeostasis, since the number of labelled cells at sites of SG did not increase.

Besides the SG, LacZ<sup>+</sup>ve cells were detected at the HFs including all hair lineages (Fig 24E-G) and hair fibres (Fig 24E-G asterisk). Additionally, the HF bulge itself contained an elevated pool of LacZ<sup>+</sup>ve keratinocytes (Fig 24B,C,J, 3 fold) compared to the number of initially labelled HFSC (day 3 following Cre activation).

These data strongly imply that genetically targeted bulge cells were capable to regenerate the entire pilosebaceous unit and to replenish the HFSC compartment even after a time period of 6 months. The renewal of the SC pool seems to involve a symmetric cell division of the targeted HFSC. Control mice treated with vehicle alone never showed a specific LacZ<sup>+</sup>ve signal even after a time period of 6 months, albeit a slight crystallic residue derived from the dye was observed attached to the HS.

To examine the distribution of HFSC-derived progeny after 180 days of tracing (n=3 mice) closer, statistical analyses were carried out (together with Andreas Kraus, Niemann Lab). Intriguingly, 53% of labelled pilosebaceous units consist of LacZ<sup>+</sup>ve keratinocytes localised to the bulge region, 32 % showed a more complex pattern, namely bulge, SD and SG and 15 % were exclusively labelled in the SD+SG (Fig 24I). The increased number and localisation of LacZ<sup>+</sup>ve keratinocytes in the HF bulge indicates that targeted HFSC resided in the HF bulge.

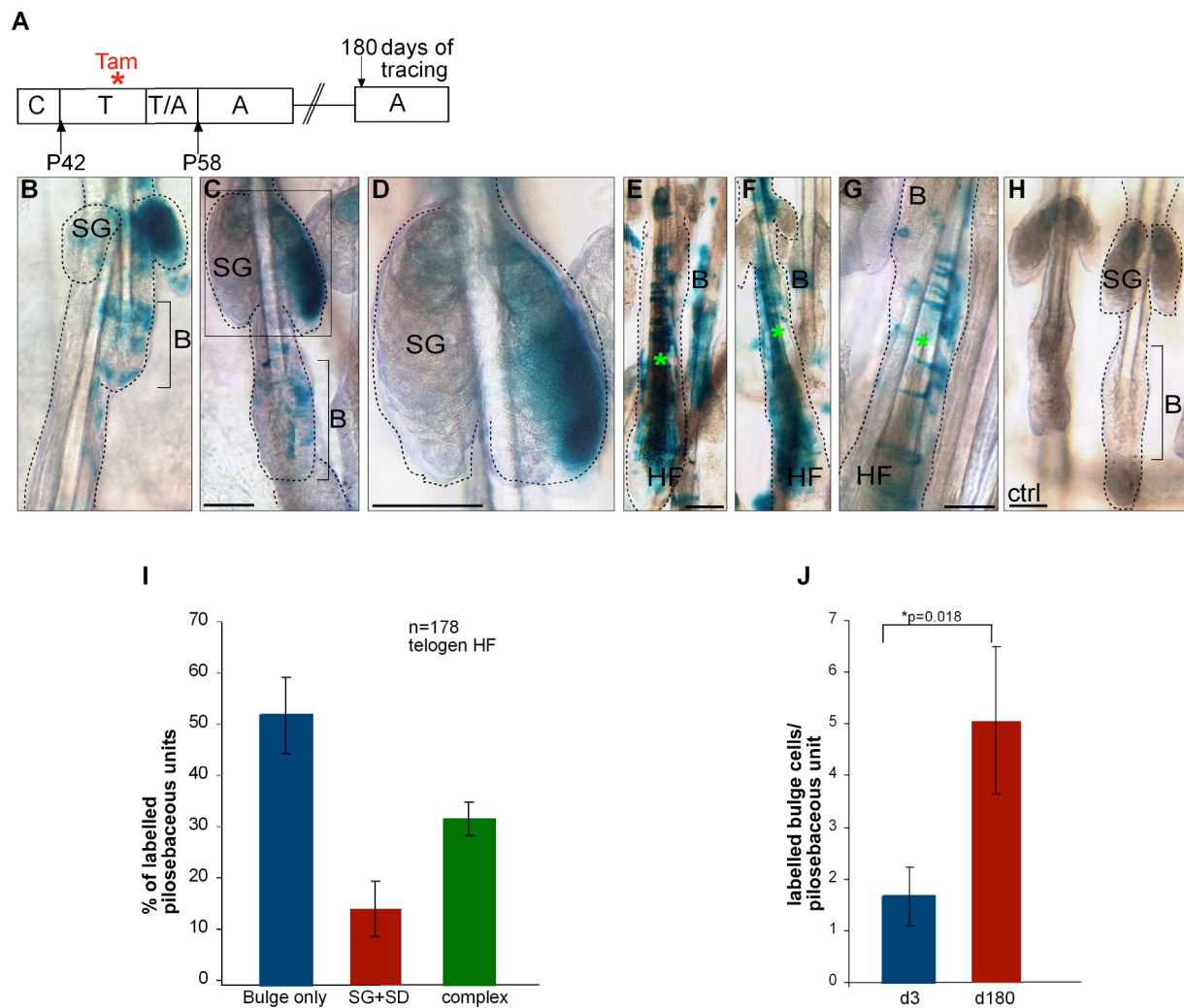


**Fig 24: Labelled bulge-derived progeny is competent to regenerate all epidermal compartments after 6 months of tracing**

(A) Long term analysis of bulge derived progeny labelled during 2<sup>nd</sup> telogen and LacZ<sup>+</sup>ve cells were traced following 180 days (n=3 A\_K15CreER(G)T2/ R26RLacZ mice). The HFSC niche (B) and the SG were replenished (B,C,D). Bulge-derived progeny contributed to all hair lineages. Note that hair fibers (asteriks) were LacZ<sup>+</sup>ve (D,E,F). Vehicle treated control mice showed no specific LacZ signal (H). (I,J) Statistical analyses to quantify the distribution of LacZ<sup>+</sup>ve cells at d180 (n=3mice, 178 analysed telogen HF). Counted cells were grouped concerning their expression in bulge only, SG+SD and B, SD+SG. S.D. was calculated. The number of labelled bulge cells per pilosebaceous unit at d3 and d180 following Cre activation was determined; p-value-0.018. Scale bars represent 50µm.

### 3.6 Transition of bulge-derived progeny through different epidermal progenitor niches

Multiple SC/progenitor compartments residing between the HFSC niche and the follicular infundibulum have been identified recently (Horsley et al., 2006; Jensen et al., 2009; Jensen et al., 2008; Nijhof et al., 2006; Snippert et al., 2010).

To date, it is still unknown whether these different populations act autonomously or are integrated into a hierarchy. What is the functional relevance of these different SC and progenitor cell populations?

Since our results clearly demonstrated that SC-derived progeny from the HF niche migrated upwards the HF to renew the SG, we next aimed to investigate whether labelled HFSC were interconnected with these different SC/progenitor reservoirs thereby creating a hierarchy.

Therefore, EYFP<sup>+</sup>ve cells were analysed for the expression of epidermal SC/progenitor markers during a time frame of 7 days of tracing (Fig 25A,D,H,L).

As expected, a co-localisation of single symmetrically grouped LRC with EYFP was observed in the HF bulge. Additionally, double positive keratinocytes were detected at the UI at 5 days following Cre activation (Fig 25B). The BrdU-label was diluted towards the SG and the INF supporting our initial finding that HFSC-derived progeny was indeed capable to regenerate the SG.

At early tracing time points (day 3 post labelling), genetically labelled EYFP<sup>+</sup>ve cells were negative for MTS24 antigen (Fig 25E) and Lrig1 (Fig 25I), which both mark progenitor cells at the periphery of the SG and at the UI (MTS24, Nijhof et al., 2006) and the JZ (Lrig1, Jensen et al., 2009) (Fig 25D,H). Concomitantly with the observed migration of HFSC-derived progeny towards the SG during tracing (day 5-7), a change in marker expression in EYFP<sup>+</sup>ve keratinocytes was seen. Notably, a minority of genetically labelled cells remained to be positive for bulge markers K15 and Itga6<sup>high</sup> (data not shown). Instead, HFSC-derived progeny was detected at the MTS24<sup>+</sup>ve UI by 5 days following tamoxifen treatment and co-localised with MTS24 antigen at the perimeter of the SG (Fig 25F). In addition, some labelled cells that localised at the SD and inner periphery of the SG co-expressed Lrig1 (Fig 25J, higher magnification in K). Interestingly, the images suggested that Lrig1 marked the trail of HFSC-derived progeny to the lower tip of the SG. By 5 days of tracing, EYFP<sup>+</sup>ve keratinocytes at the lower tip of the SG co-localised with SCD1 (Fig 25N), a marker

for mature sebocytes (Sampath et al., 2009). This co-localisation comprised almost the entire SG 7 days following Cre activation (Fig 25O), showing that HFSC-derived progeny differentiated towards sebocyte lineage.

Taken together, these experiments indicate that targeted HFSC gave rise to MTS24 antigen and Lrig1<sup>+</sup>ve progenitor populations indicating a hierarchy of HFSC and MTS24 antigen and Lrig1<sup>+</sup>ve progeny.

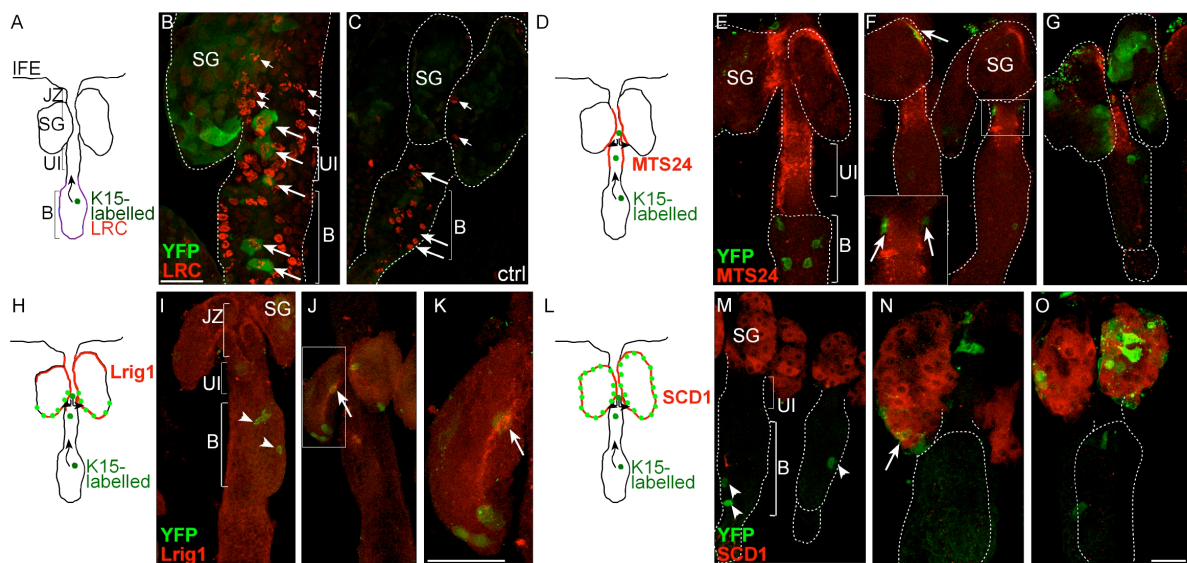


**Fig 25: Traced bulge-derived cells co-express different progenitor markers along their trail to the SG**

Co-immunofluorescent studies of EYFP<sup>+</sup>ve keratinocytes of activated A\_K15CreER(G)T2/R26REYFP-mice and different SC/progenitor markers (**A,D,H,L**) were performed using telogen whole-mounts. 3 days following Cre activation, no EYFP signal was detected in the MTS24 (**E**), Lrig1 (**I**) and SCD1 (**M**) positive cells. EYFP and LRC double positive cells were detected at the HF bulge and the UI at 5 days of chase (**B**). The label was also diluted along the UI in vehicle treated controls, which were negative for EYFP (**C**). Day 5 following Cre activation HFSC-derived progeny is detected in the MTS24 antigen (**F**) and Lrig1 (**J,K**) positive compartment. Single EYFP<sup>+</sup>ve cells located at the lower tip of the SG co-expressed SCD1 (**N**) culminating in almost the entire SG to be double positive at 7 days of chase (**O**). Scale bars represent 50  $\mu$ m.

### 3.7 HFSC-derived progeny expresses marker molecules for sebaceous lineage commitment

Next, we validated whether sebaceous commitment of HFSC-derived progeny was also reflected on a transcriptional level. Therefore, FACS sortings were performed utilising freshly isolated keratinocytes from induced A\_K15CreER(G)T2/R26REYFP telogen back skin (together with Heike Brylka, Niemann lab). Bulge-derived keratinocytes were enriched by sorting for EYFP/Itga6<sup>high</sup> or CD34/Itga6<sup>high</sup> at day 2 following Cre activation (Fig 26A-C). To purify SG-associated cells by 6 days of chase, EYFP/Lrig1 or Lrig1/Itga6<sup>high</sup> +ve populations were sorted (Fig 26D-F).

Subsequently, RNA was isolated from these different populations and used for cDNA synthesis. Expression of SG-associated genes such as Lgr6, Blimp1 and SCD1 was determined using qRT-PCR (Fig 26G). Fold regulation was adapted to 18S expression and normalised to Itga6<sup>+</sup>ve keratinocytes. Comparing bulge-derived (EYFP/Itga6<sup>high</sup> and CD34/Itga6<sup>high</sup>) and SG-derived (EYFP/Lrig1 and Itga6<sup>high</sup>/Lrig1) keratinocytes revealed no major differences in Lgr6 expression levels, suggesting that Lgr6<sup>+</sup>ve SC pool is most likely located in between the bulge-and the SG-sorted populations.

Furthermore, the expression of Blimp1, a proposed marker for unipotent progenitors detected close to the SD (Horsley et al., 2006), was up-regulated in EYFP/Lrig1 and Itga6<sup>high</sup>/Lrig1<sup>+</sup>ve cell populations (7 fold and 12 fold, respectively) when compared to the basal cell pool. The most tremendous change (55 fold) was seen for the sebocyte marker SCD1. Notably, EYFP/Itga6<sup>high</sup> and CD34/Itga6<sup>high</sup> sorted populations shared almost the same expression levels of the analysed marker. As expected, the expressional changes of EYFP/Lrig1 and Itga6<sup>high</sup>/Lrig1 isolated keratinocytes were quite similar.

Thus, sebaceous commitment of HFSC-derived progeny observed in the lineage tracing experiments was also confirmed on the molecular level.

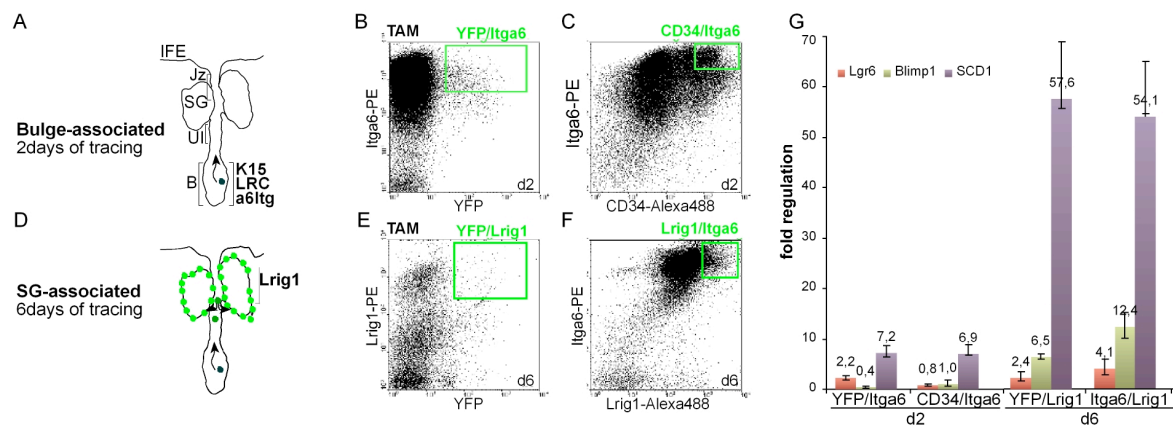


**Fig 26: HFSC derived progeny at the periphery of the SG expressed markers for sebaceous lineage**

A\_K15CreER(G)T2/R26REYFP mice were treated with tamoxifen during 2<sup>nd</sup> telogen phase (2 independent experiments). Primary keratinocytes were isolated and FACS-sorting (n=2 mice/sort) was performed to enrich keratinocytes from the bulge region (2 days of tracing, **A**) and from the JZ and SG (6 days of tracing, **D**). To isolate bulge cells keratinocytes were stained using either the combination of YFP/Itga6<sup>high</sup> (**B**) or CD34/Itga6<sup>high</sup> (**C**). To purify bulge-derived progeny located at the periphery of the SG, YFP/Lrig1<sup>+</sup>ve (**E**) and Itga6<sup>high</sup>/Lrig1<sup>+</sup>ve (**F**) cells were sorted. qRT-PCR analysis of indicated SG-associated genes was performed using cDNA derived from the different populations (**G**). Expression levels were normalised to 18S expression and are depicted as fold regulation compared to Itga6 signal. S.D. was calculated.

### 3.8 Ectopic SG formation is driven by HFSC

Lef1 and  $\beta$ -catenin signalling is crucial for cell fate determination in various epithelial tissues. In the skin, impaired Lef1 signalling promotes sebaceous fate decision (Merrill et al., 2001; Niemann et al., 2002). It has been demonstrated that epidermal expression of dominant negative Lef1 (K14 $\Delta$ NLef1) drives the synthesis of ectopic SG (nSG) along deformed HF (Fig 27B,C). Additionally, SG are enlarged. These findings provoked the question whether formation of these ectopic SG originated from an unbalanced fate decision of HFSC.

#### 3.8.1 Expression of SC and progenitor markers in K14 $\Delta$ NLef1 mice

In a first set of experiments, the localisation and expression levels of HFSC and progenitor markers in K14 $\Delta$ NLef1 epidermis were determined conducting immunostaining and qRT-PCR. In comparison to wt epidermal whole-mounts (Fig 27A), K15 and CD34 protein were confined to a deformed bulge region which was reduced in size (Fig 27B,C). This was consistent with the molecular expression patterns validated by qRT-PCR (together with Peter Schettina, Niemann lab). RNA isolation from freshly isolated keratinocytes of wt and K14 $\Delta$ NLef1-mice was followed by cDNA synthesis. Gene expression was analysed. The results were adopted to GapDH expression and are depicted as fold change compared to wt. A dramatic decrease of 60% in K15 expression could be detected in keratinocytes from K14 $\Delta$ NLef1 mice, whereas CD34, Sox9, Itga6-levels were only slightly reduced. Notably, NFATc1, which is involved in the regulation of SC quiescence, was down-regulated to 20 % (Fig 27D). This suggests that the pool of quiescent HFSC was decreased in K14 $\Delta$ NLef1 mice. Furthermore, the expression levels of SG-associated genes were determined (Fig 27E): Keratin6a (K6a) which is strongly expressed at the SD (Gu and Coulombe, 2008) was more than 5 times up-regulated in K14 $\Delta$ NLef1-derived keratinocytes. Expression of TenascinC -known to be up-regulated in MTS24antigen/Plet1<sup>+</sup>ve progenitors (Nijhof et al., 2006)- was also elevated. Importantly, one of the key regulators determining sebaceous fate decision, c-myc and its target Nucleolin were dramatically down-regulated in K14 $\Delta$ NLef1 epidermis compared to control littermates. This implicates a possible independent regulation of sebaceous differentiation by Lef1 and c-myc.



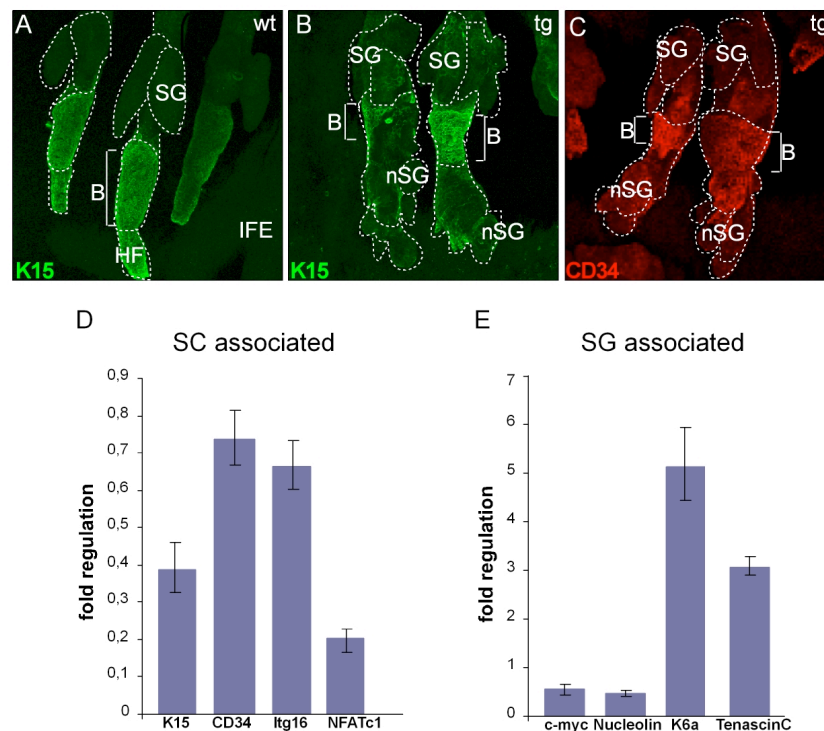


**Fig 27: Epidermal SC and SG-associated markers are differentially expressed in K14ΔNLef1 mice.**

To investigate the localisation and expression of SC and progenitor marker in K14ΔNLef1 tail epidermis, immunostainings were performed analysing the indicated proteins. (A) K15 protein was expressed in wt HF bulge. (B,C) K15 protein and CD34 marked the deformed HF of K14ΔNLef1 epidermis. (D,E) SC and SG associated marker molecules were analysed on a transcriptional level. qRT-PCR was conducted and fold differences between K14ΔNLef1 and wt (n=3mice) were adjusted to GapDH expression and are depicted as fold regulation compared to wt expression. S.D. was calculated.

### 3.9 Bulge-derived progeny is involved in ectopic SG formation

To examine whether HFSC contributed to ectopic SG development in K14ΔNLef1, we performed lineage tracing experiments using A\_K15CreER(G)T2/EYFP mice crossed into the K14ΔNLef1 background (Fig 28A). Cre recombinase was activated at early telogen. By 3 days of chase, a cluster of EYFP<sup>+</sup>ve cells was confined to the deformed bulges (Fig 28B). At this early time-point of labelling, no co-localisation with SCD1, a marker for mature sebocytes, was observed. Intriguingly, HFSC-derived progeny migrated towards ectopically generated SG by 5 days of tracing. In particular, SCD1 and EYFP co-expression was not only restricted to the enlarged upper SG, but also co-localised to the *de novo* formed SG (Fig 28C,D).



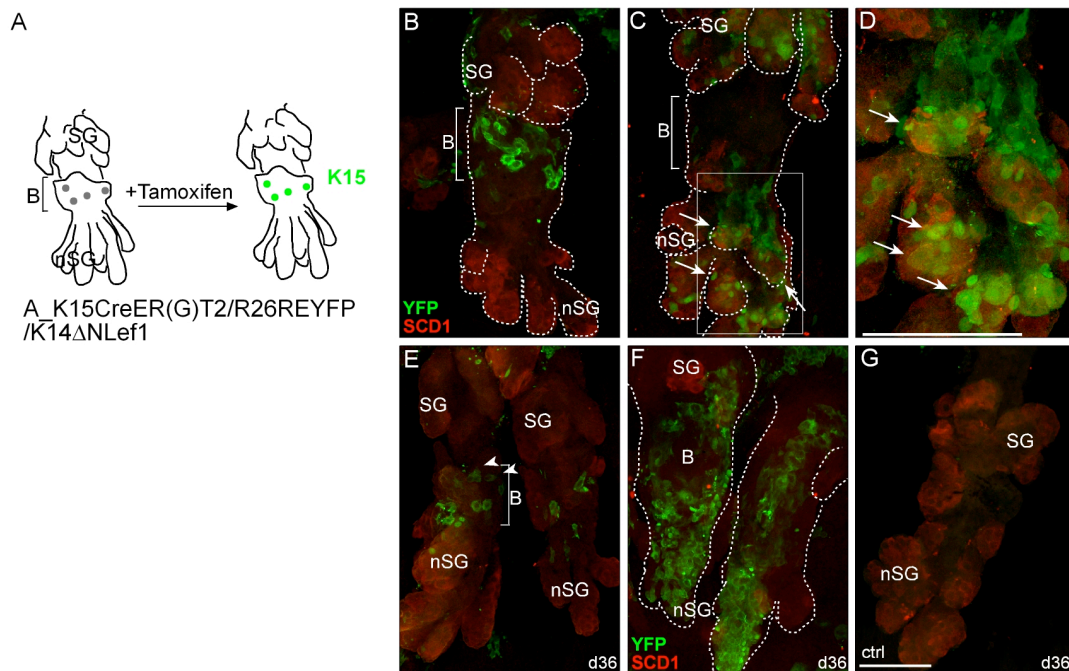


**Fig 28: Bulge-derived progeny contributes to ectopic SG formation in K14ΔNLef1 mice.**

(A) Lineage tracing experiment of K15CreER(G)T2/K14ΔNLef1/R26REYFP mice (n=3 animals/time point) during 2<sup>nd</sup> telogen. Co-immunofluorescent studies of EYFP and SCD1 were performed. A cluster of EYFP<sup>+</sup>ve keratinocytes was detected in the deformed HF bulge at day 3 after Cre activation and labelled bulge cells were negative for SCD1 (B). By 5 days of tracing, bulge-derived progeny was found at the ectopic SG (nSG) (arrows) and coexpressed SCD1 (C and higher magnification in D). (E) Single EYFP<sup>+</sup>ve cells were resident in the bulge region after a tracing period of 36 days (n=2) and clonal expansion of bulge-derived progeny were seen in some of the deformed HF (F). No EYFP signal was seen in vehicle controls (G). Scale bars represent 50 μm.

These observations demonstrate that HFSC-derived progeny contribute to development of ectopic SG in K14ΔNLef1 mice. To test if targeted HFSC reside in the bulge region of K14ΔNLef1 mice, we performed long-term tracing experiments. 36 days (Fig 28E-G) and 90 days (data not shown) following Cre activation, two different staining patterns were observed. First, small aggregates of EYFP<sup>+</sup>ve cells were localised to the deformed bulge region (Fig 28E, arrowheads). Alternatively, large cluster of HFSC-derived progeny were distributed along the deformed pilosebaceous units including the ectopic SG (Fig 28F). Epidermal whole-mounts derived from vehicle control mice did not show a specific EYFP signal (Fig 28G).

These data imply that the HFSC pool of K14ΔNLef1 mice was not exhausted over time.

### 3.10 Development of ectopic SG is accompanied by the establishment of new progenitor niches

The formation of ectopic SG by HFSC-derived progeny raised the interesting question how the SG-associated progenitor markers MTS24 antigen and Lrig1 were expressed in K14 $\Delta$ NLef1 mice. Therefore, immunofluorescent studies were carried out analysing these markers in epidermal whole-mounts derived from K14 $\Delta$ NLef1 mice. In addition to its localisation at the periphery of the enlarged SG and deformed JZ, Lrig1 was also detected at the perimeter of the newly generated SG (Fig 29B). The expression pattern of the UI-marker MTS24 was also altered in K14 $\Delta$ NLef1 tail epidermis. Single cells appeared in close proximity to the deformed bulge and the most intense signal was observed at the branching ducts of the ectopic SG (Fig 29C). These data indicate that concomitantly with the development of ectopic SG new progenitor niches were established.

Next, we analysed the relationship between labelled HFSC-derived progeny and SG-associated progenitor markers in more detail conducting co-immunofluorescent studies on induced A\_K15CreER(G)T2/K14 $\Delta$ NLef1/R26REYFP-epidermis (n=5). Accessorily to the co-localisation of individual EYFP with MTS24 antigen and Lrig1 at sites of the upper SG, the majority of EYFP and MTS24 antigen double positive cells were found at the branching ducts of the *de novo* synthesised SG (Fig 29F). Interestingly, many Lrig1 and EYFP double positive cells were detected at the perimeter of the ectopic SG (Fig 29E). Analysing K15 protein at this stage of tracing revealed that HF with EYFP<sup>+</sup>ve labelled cells restricted to the bulge region still could be found. The majority of HF showed an EYFP<sup>+</sup>ve signal in the deformed HF, *de novo* SG and enlarged SG (Fig 29D), which were negative for K15 antigen.

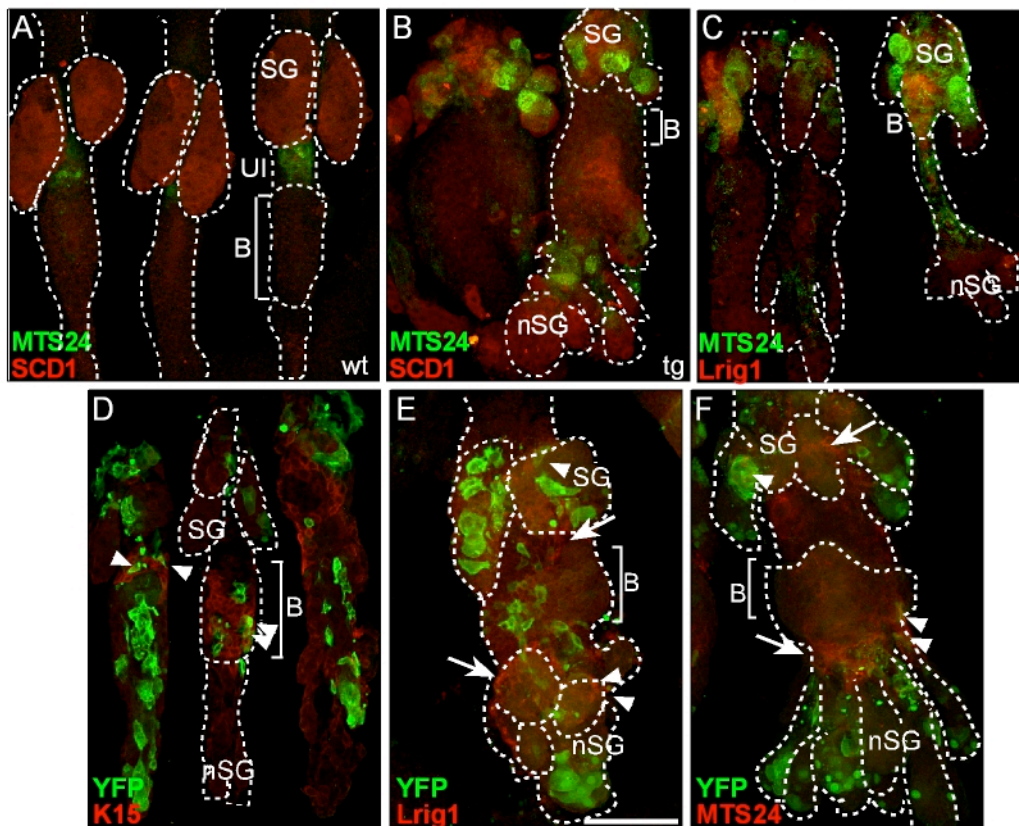


**Fig 29: Ectopic SG formation is accompanied with the establishment of *de novo* progenitor niches**

(A) MTS24 antibody recognises the UI and the periphery of the SG (SCD1<sup>+</sup>ve) in wt tail epidermis. (B,C). MTS24 antigen and Lrig1 were localised at the SG and ectopic SG (nSG) visualized by SCD1 staining in K14ΔNLef1 tail epidermis. (D-E) Co-immunofluorescent studies of SC/progenitor markers and EYFP<sup>+</sup>ve keratinocytes of activated A\_K15CreER(G)T2/ K14ΔNLef1/ R26REYFP tail epidermis (n=5 mice). At 5 days of tracing a clustered EYFP-pattern detected in the deformed hair follicle bulges colocalised with K15 protein (D, arrowheads). EYFP<sup>+</sup>ve keratinocytes co-localised with Lrig1 (E, arrowheads) and with MTS24 antigen (F, arrowheads) at the periphery of nSG. Scale bars represent 50 μm.

## 3.11 HFSC-derived progeny contributes to epidermal tumourigenesis

### 3.11.1 3D-visualization of epidermal tumours

Repression of  $\beta$ -catenin mediated Lef1 signalling in the epidermis not only drives ectopic SG formation, impairs HF differentiation and stimulates transdifferentiation of keratinocytes (Niemann et al., 2002). Furthermore, early lesions develop which are characterised by large cysts attached to a cluster of abnormally differentiated cells (Fig 30A). Intriguingly, K14 $\Delta$ NLef1-mice start to develop sebaceous adenomas and papillomas with sebocyte differentiation starting from 3 months of age. Early sebaceous adenomas appear as small lobules with a proliferative outer layer of keratinocytes (Fig 30B, dashed line) and an enhanced sebocyte (S) differentiation in the centres (Fig 30B). Fully developed sebaceous adenomas are characterised by large and complex organised tumour lobules comprising differentiated sebocytes surrounded by an undifferentiated basal layer (Fig 30C, dashed line). This proliferative layer is Keratin14 (K14) positive, whereas the differentiated sebocytes located at the center of tumour lobules express SCD1. Previous chemical carcinogenesis experiments have clearly shown that sebaceous tumourigenesis in K14 $\Delta$ NLef1 mice can be induced by a single application of a carcinogen (DMBA). DMBA treatment of K14 $\Delta$ NLef1 mice resulted in the development of macroscopically visible tumours within a time frame of 4 weeks (Niemann et al., 2007).

Thus, this inducible K14 $\Delta$ NLef1 model provides a powerful tool to study early steps of tumourigenesis and to investigate the origin and cause of tumour formation. Since bulge-derived progeny contributed to ectopic SG formation in K14 $\Delta$ NLef1 mice, an emerging issue was to investigate a function of HFSC-derived progeny in sebaceous adenoma formation within the K14 $\Delta$ NLef1 inducible tumour model.

To allow a 3D visualisation of single cells within early sebaceous lesions and sebaceous tumours of back skin, we set out to optimise the protocols for the isolation of epidermal whole-mounts derived from tumourigenic lesions. Therefore, K14 $\Delta$ NLef1 mice were treated with DMBA at onset of 2<sup>nd</sup> telogen and whole-mounts were isolated at early (3 weeks) and late stages (6-8 weeks) post tumour initiation. Subsequently, different concentrations and incubation times for EDTA treatment were tested to isolate epidermal whole-mounts up to 0.8 cm diameter in size.

To investigate the morphology of these whole-mounts, immunofluorescent studies were carried out. As expected, K14 was detected along the early lesions (Fig 30D). Analysing later stages following tumour initiation, K14 expression was observed along the lobular structures (Fig 30E), whereas SCD1 marked cells within the centre of the lobules (Fig 30F). This organisation resembled the histology of early tumours seen in H/E stained cross-sections and therefore will be defined as sebaceous tumours in the following lineage tracing analyses. Taken together, the protocol to isolate whole-mounts was adapted to visualise early lesions and sebaceous tumours and now provides a powerful tool to visualise epidermal tumours in a 3D fashion

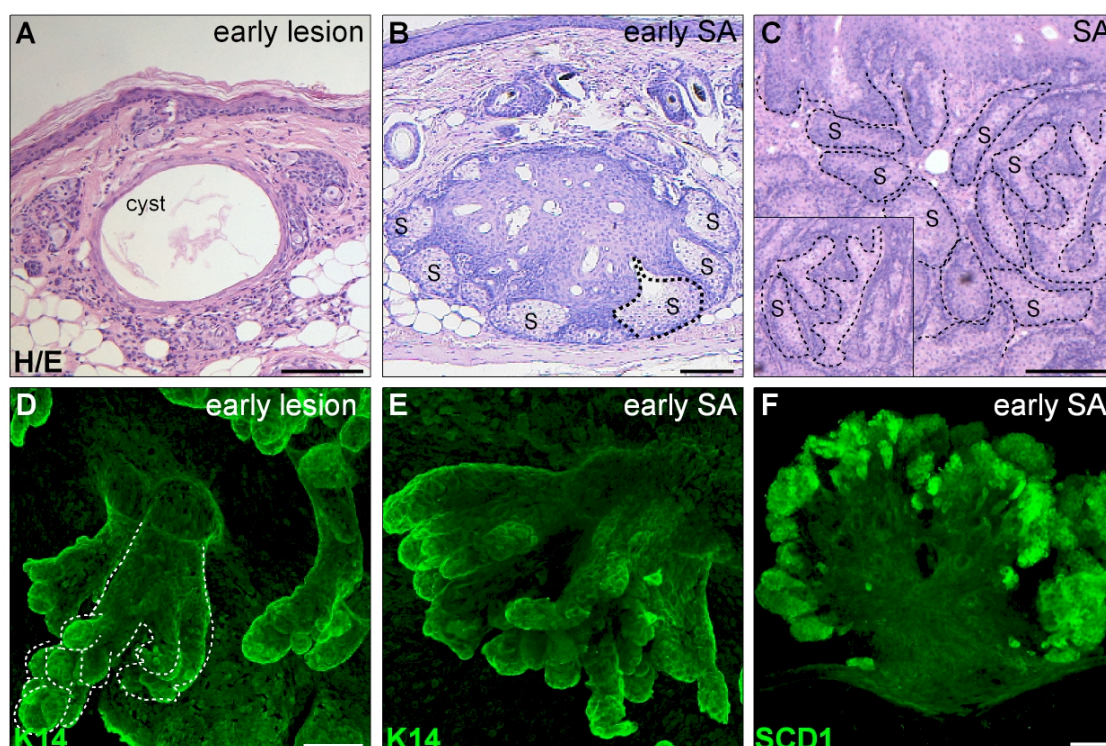


**Fig 30: Development of skin lesions and sebaceous adenomas in K14 $\Delta$ NLef1-mice**

H/E stained cross sections of K14 $\Delta$ NLef1-derived skin and tumours depicts an early lesion comprised of a large cyst attached to a cluster of abnormally differentiated cells (A) and an early sebaceous adenomas (SA) characterised by small lobules with differentiated sebocytes (S) in the center and a basal layer (dashed lines) at the periphery (B). Fully developed SA exhibit complex tumour lobules with sebocyte differentiation (S) surrounded by a basal layer (dashed line) (C). (D-E) K14 immunostaining of whole-mounts isolated from back skin of K14 $\Delta$ NLef1 mice 3 weeks following DMBA-treatment (n=2 mice) visualising compact organised early lesions (D). K14 was expressed at the periphery of densely packed lobular structures derived from K14 $\Delta$ NLef1-back whole-mounts 6 weeks after tumour initiation (n=3 mice) (E). SCD1 marked more differentiated sebocytes (E). Note that these structures (E,F) resemble the lobular organisation of SA as observed in B. Scale bars represent 100  $\mu$ m in A-C and 50  $\mu$ m in D-E.



### 3.11.2 Lineage tracing of different keratinocyte populations within the K14 $\Delta$ NLef1-tumour model

To optimise the application and detection protocols for lineage tracing analyses within the K14 $\Delta$ NLef1-tumour model, K14CreER(G)T2/R26RLacZ/K14 $\Delta$ NLef1 mice (n=6) were utilised as positive control to target keratinocytes from the entire basal layer (Fig 31A) including the IFE, HF, SG and ectopic SG (Fig 31B). Therefore, tail and back skin of triple transgenic mice was treated with DMBA at onset of 2<sup>nd</sup> telogen. At day 3 following tumour initiation, a dose of 2.5 mg tamoxifen was applied daily for the following 3 days (Fig 31A). Epidermal whole-mounts derived from DMBA-treated tail skin were analysed for activated Cre recombinase and reporter gene expression at day 8 and 12 following DMBA treatment. As expected, nuclear active Cre and LacZ signal was monitored in the IFE, HF, SG and ectopic SG, indicating that the experimental set-up was sensitive enough for further fate mapping analyses (Fig 31C,E). Genotype-matched littermate controls treated with DMBA and vehicle (oil) were negative for nuclear Cre or LacZ signal. In some cases, a background activity of LacZ was observed in the IFE and hair channel of acetone and DMBA- and oil treated K14CreER(G)T2/R26RLacZ/K14 $\Delta$ NLef1-epidermis (Fig 31F). In contrast, Cre recombinase in these controls was diffusely distributed in the cytoplasm, indicating that the seen LacZ signal was due to background from the LacZ staining procedure. To investigate whether the improved labelling protocols were suitable to trace descending cell lineages from almost the entire HFSC population within the K14 $\Delta$ NLef1 tumour model, the high-expressing C\_K15CreER(G)T2 strain was subjected to DMBA-treatment and the same application procedures as for the K14CreER(G)T2 mice were used. Analysing tail epidermis at day 10 following DMBA-application revealed that the majority of LacZ<sup>+</sup>ve cells was confined to the upper SG and ectopic SG, whereas only few cells remained to be positive in the bulge. The most prominent LacZ signal was observed at the lower tips of the SG and ectopic SG (Fig 31H). 13 days following DMBA-treatment, LacZ<sup>+</sup>ve keratinocytes were distributed along the deformed pilosebaceous units (Fig 31I), resulting in detection of strong reporter gene activation in early skin lesions by 32 days following tumour initiation (Fig 31J,K). Analysing LRC and Cre expression of DMBA-treated epidermal whole-mounts showed that almost the entire bulge region was negative for nuclear Cre and LRC (Fig 31M), indicating that mobilisation of HFSC had occurred. Instead, nuclear Cre was localised to the SG, nSG and IFE and BrdU label was diluted

towards these compartments. Triple transgenic littermate controls treated with DMBA or acetone and vehicle (oil) were negative for nuclear Cre or LacZ signal (Fig 31L).

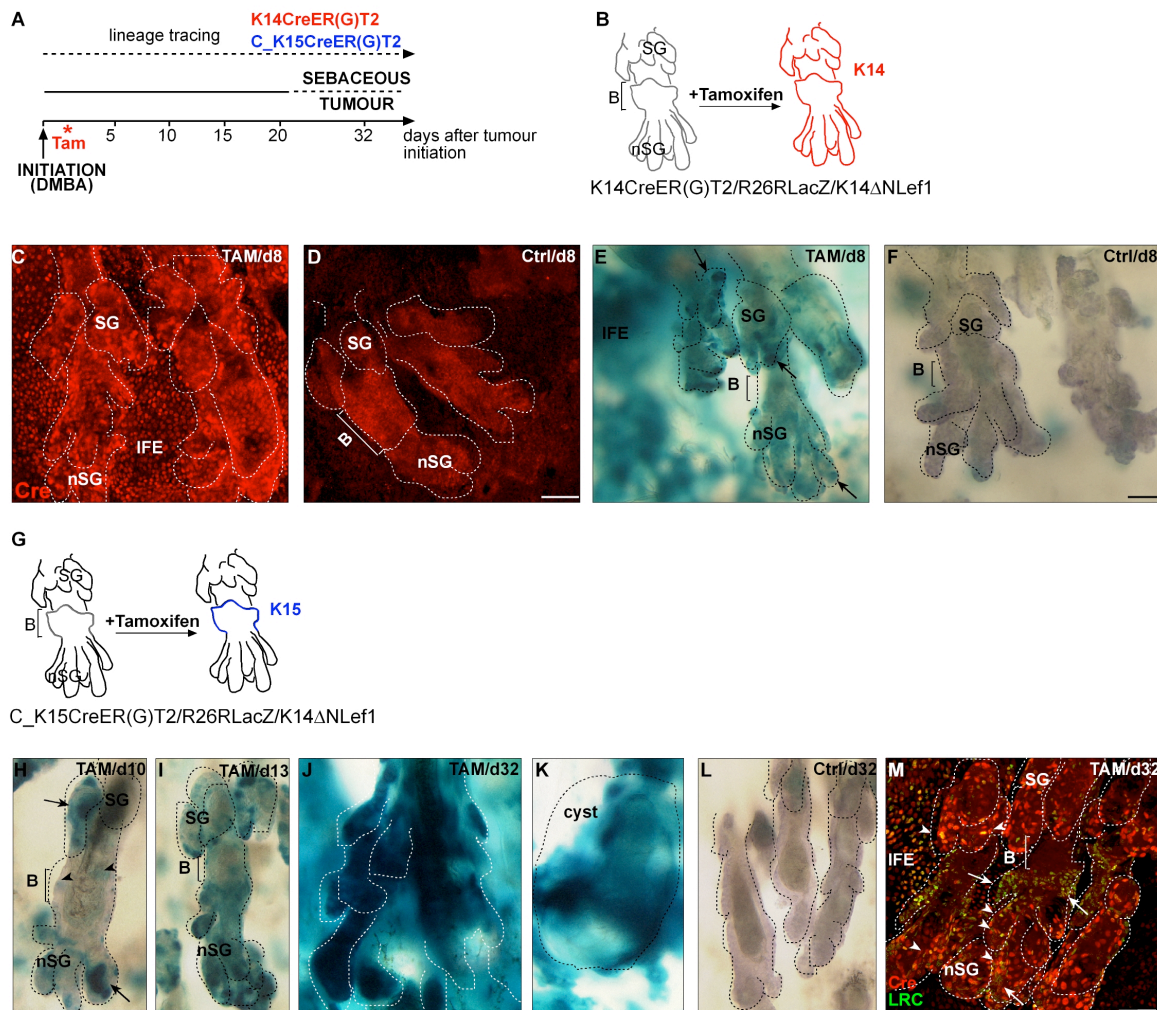


**Fig 31: Optimisation of the detection protocols for lineage tracing experiment during sebaceous tumour formation**

(A) Tumour formation was initiated and Cre recombinase in K14<sup>+</sup>ve (B) or K15<sup>+</sup>ve (H) cell populations was induced day 3 post DMBA treatment. Whole-mounts were analysed for Cre or LacZ expression. (C-F) Nuclear Cre in induced K14CreER(G)T2 mice was detected in the basal layer (C), whereas LacZ<sup>+</sup>ve keratinocytes were localised to the IFE and lower tip of the SG and nSG (E, arrows). LacZ stained vehicle controls occasionally showed a background in the IFE and HS (F), whereas Cre was diffusely distributed (D). (G-M) In activated C\_K15CreER(G)T2 mice, LacZ<sup>+</sup>ve keratinocytes were found in SG and nSG and few positive cells were confined to the bulge 10 days following DMBA treatment (H, arrowhead). The deformed pilosebaceous unit including nSG (I, day 13) and sebaceous lesions (day 32, J,K) were LacZ<sup>+</sup>ve. HF bulge was almost negative for nuclear Cre or LRC, whereas SG and nSG were strongly +ve for Cre and LRC (day 32) (M, arrowheads). DMBA- and vehicle treated C\_K15CreER(G)T2 epidermis was negative for LacZ (L). Scale bars in D, E, M 80μm, H, L 50μm.

From these experiments we conclude that cell populations targeted by the high expressing C\_K15CreER(G)T2 contributed to early skin lesions. The observation that only few LacZ<sup>+</sup>ve cells were detected in the bulge could be due to a fast mobilisation of bulge cells in response to DMBA treatment resulting in a high cellular turn-over. Since Cre recombinase was induced 3 days post DMBA-application, it was restrictive to analyse very early time points. Performing lineage tracing analyses using the high expressing C\_K15CreER(G)T2 strain did not allow fate mapping analyses of individual clones in tail epidermis. To circumvent this limitation, we decided to utilise the low expressing A\_K15CreER(G)T2 mice for further tumour studies.

In addition, we activated Cre recombinase at day1 following DMBA treatment to monitor the fate of HFSC-derived progeny immediately after tumour initiation. To reduce the background of LacZ signal observed in DMBA or acetone-treated K14CreER(G)T2/R26RLacZ/K14ΔNLef1 mice, R26REYFP Cre reporter mice were utilised for further tracing analyses.

### **3.11.3 HFSC-derived progeny drives sebaceous tumourigenesis**

Next, we aimed to examine if individual labelled HFSCs were indeed involved in the process of sebaceous tumourigenesis. Therefore, the low expressing A\_K15CreER(G)T2/R26REYFP/K14ΔNLef1 mice (n=12) were utilised for chemical carcinogenesis experiments and the fate of HFSC-derived progeny was monitored within a time frame of day 5 to day 42 following tumour initiation (Fig 32A,B). Large areas were screened for EYFP expression in whole-mounts derived from DMBA treated back and tail. Analysing early stages of tumour formation (day 5 following DMBA treatment), a clustered EYFP signal was restricted to the bulge region of tail epidermis (Fig 32C). Interestingly, the number of initially labelled cells was increased compared to acetone treated controls (data not shown), indicating an enhanced proliferation caused by DMBA treatment. Consistent with the data from the fate mapping analyses during the development of the K14ΔNLef1 phenotype, HFSC-derived progeny contributed to ectopic SG formation by 7days of chase (Fig 32D). During the process of sebaceous tumourigenesis (day 20 post DMBA-treatment), clonal expansion of EYFP<sup>+</sup>ve keratinocytes was detected along deformed HF (Fig 32E,F). By 42 days of chase, HFSC-derived progeny was found in early lesions derived from back skin (Fig 32G,H), resulting in almost the entire sebaceous tumours



to comprise EYFP<sup>+</sup> cells (Fig 32K). Notably, at sites of early lesions and the tumour lobules, co-localisation of more differentiated SCD1<sup>+</sup> sebocytes and HFSC-derived progeny was observed (Fig 32J,L,M).

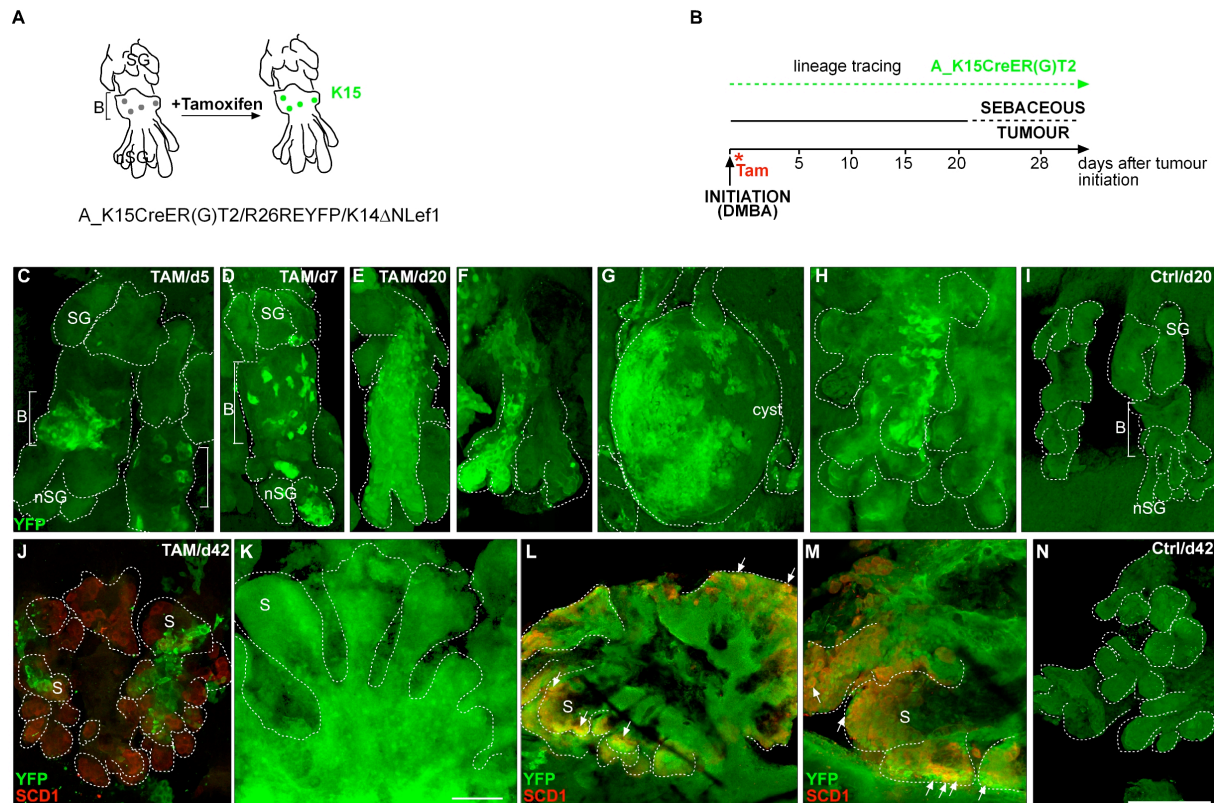


**Fig 32: Bulge-derived progeny contributes to sebaceous adenoma formation**

Lineage tracing experiments were conducted to map the fate of single HFSC-derived progeny within the inducible K14ΔNLeF1 tumour model (A). Epidermal whole-mounts (tail, back, early lesions and tumours) were analysed for EYFP expression at different time points following tumour initiation (DMBA) and Cre induction (Tam) at d1 (B). Starting with a cluster of labelled cells confined to the bulge (C), HFSC-derived progeny was detected at sites of the ectopic SG (nSG) (D). Clonal expansion of EYFP positive cells was observed at day 20 following Cre activation (E,F). By 42 days of chase, EYFP<sup>+</sup> cells were found in early lesions (G,H) and sebaceous tumours (J-M). YFP/SCD1<sup>+</sup> cells were visible in early lesions and in more differentiated parts of the sebaceous tumours (L, M, arrows). DMBA-treated vehicle controls displayed an autofluorescence, but were negative for EYFP (I,N). Scale bars represent 50 μm.

To this end, 12 out of 14 analysed early sebaceous tumours derived from back skin (n=6 mice) and 6 out of 7 early sebaceous tumours isolated from tail epidermis exhibited EYFP<sup>+</sup>ve signal (Table 8).

**Table 8: Detection of EYFP<sup>+</sup>ve keratinocytes in early lesions and sebaceous tumours (n=6 mice)**

	early lesions	sebaceous tumours	
		back epidermis	tail epidermis
TAM	3/4	12/14	6/7
Ctrl	0/1	0/3	0/2

Albeit whole-mounted sebaceous tumours (n=3 for back and 2 for tail whole-mounted tissue) isolated from DMBA-treated vehicle (oil) controls (n=2mice) exhibited an enhanced autofluorescence, no EYFP signal could be detected (Fig 32I,N). As expected, acetone-treated tamoxifen-induced A\_K15CreER(G)T2/R26REYFP/K14ΔN<sup>Lef1</sup> controls never developed tumours and showed EYFP<sup>+</sup>ve keratinocytes at the bulge region but also at sites of the ectopic SG (by 20 or 42 days of chase). Taken together, these experiments clearly demonstrate that tHFSC-derived progeny contributed to tumourigenesis and was indeed committed to sebaceous lineage within the tumours.

### 3.12 Manipulation of Lef1-signalling in the HFSC niche

Spontaneous regeneration in tissue homeostasis requires a tightly regulated balance between SC quiescence and activation. Besides BMP, Notch and Hh, Wnt/β-catenin signalling is essential for epidermal regeneration (Blanpain and Fuchs, 2009). Various reports demonstrated that inhibited Wnt-signalling in the HFSC niche is important for SC quiescence, whereas stimulation of the pathway is thought to play a role in the activation of bulge SC for cyclic HF regeneration (Lowry et al., 2005; Lo Celso et al., 2004). At the base of the HF, within the precortex, an active β-catenin/Lef1 transcriptional complex is crucial for HF differentiation (Andl et al., 2002). Here, we aimed to manipulate Lef1 signalling in the HFSC niche *in vivo* and to study the consequences on epidermal regeneration and differentiation. An important issue was to investigate if the expression of mutated Lef1 in the HFSC compartment is sufficient to drive sebaceous tumourigenesis. Therefore, we have developed a transgenic mouse model expressing mutant Lef1 lacking the β-catenin binding domain under the control of a K15 promoter fragment (K15ΔN<sup>Lef1</sup> mice).

### 3.12.1 Generation of K15 $\Delta$ NLef1 transgenic mice

The 5 kb K15 promoter fragment derived from pK15CreER(G)T2 was used to target N-terminally deleted Lef1 to the HFSC compartment (Fig 33A). Therefore, a partial digestion of pK15CreER(G)T2 was performed to excise CreER(G)T2 thereby allowing the insertion of N-terminally deleted Lef1 (detailed description of the cloning procedures in chapter 2.2.5.4). A myc-tag in front of  $\Delta$ NLef1 enabled transgene detection.

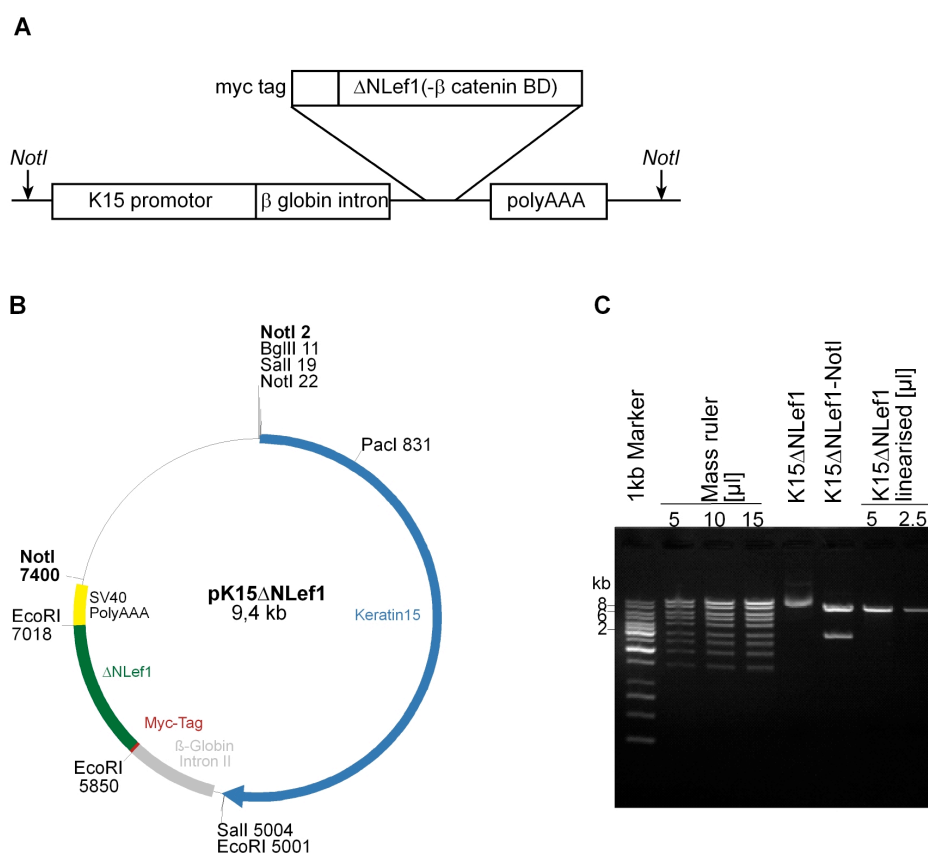


**Fig 33: pK15 $\Delta$ NLef1 was cloned and linearised for subsequent microinjection**

**(A)**  $\Delta$ NLef1 lacking the  $\beta$ -catenin binding domain (BD) was cloned downstream of a 5 kb K15promotor fragment. A myc-tag of  $\Delta$ NLef1 facilitates transgene detection.

**(B)** Restriction map depicting pK15 $\Delta$ NLef1. The plasmid was digested using *NotI* enzyme. A 7 kb fragment of the linearised construct was purified for microinjection. A concentration of 5 ng/ $\mu$ l of the purified construct was estimated by the comparing different amounts of the purified construct with different concentrations of a mass ruler **(C)**.

Having verified the right insertion and sequence of the construct, its functionality was tested *in vitro*. Keratinocytes were transfected with pK15 $\Delta$ NLef1 and subsequently, immunofluorescent studies were performed to detect the myc-tag and transgene

expression. These experiments showed that 2% of the cells expressed the transgene, respectively (done by Gabriel Peinkofer, diploma student, Niemann lab, Peinkofer, 2008) demonstrating that pK15 $\Delta$ NLef1 was functional *in vitro*.

To generate K15 $\Delta$ NLef1 transgenic mice, pK15 $\Delta$ NLef1 was linearised using *NotI* enzyme and a 7 kb fragment was isolated and purified. Purity, quality and concentration were determined by agarose gel-electrophoresis and spectrophotometric analysis (Fig 33B,C).

Subsequently, linearised and purified DNA [5ng/ $\mu$ l] was introduced into the pronucleus of fertilised oocytes (performed by the transgenic core facility at the CBG, Dresden). 300 oocytes were transplanted into different pseudo-pregnant foster animals. Genomic DNA (gDNA) was isolated from tail tissue derived from the offspring (n=47) and was used as template to amplify a fragment either within the  $\Delta$ NLef1 sequence or a region between K15 promotor and the  $\beta$ -globin intronII. Three positive founder lines (referred to as A\_B\_C\_line) were identified. The transgene could also be amplified using gDNA isolated from F1-generation showing germline transmission of the construct.

To determine the copy number of inserted K15 $\Delta$ NLef1, Southern-Blot analyses were employed using gDNA derived from F1-generation. Since a probe was designed recognizing  $\Delta$ NLef1, gDNA derived from K14 $\Delta$ NLef1-mice could be utilised as positive control. Chemiluminiscent intensity of Southern Blots probed with  $\Delta$ NLef1 was measured densitometrically (ImageJ, NIH). The values were adjusted to the intensity of Southern blots probed with IL2R (interleukin 2 receptor), which is integrated once into the murine genome (Carrol et al., 1995).

These analyses revealed that the B\_K15 $\Delta$ NLef1 (n=7) showed the highest, C\_K15 $\Delta$ NLef1 (n=4) a moderate and A\_K15 $\Delta$ NLef1 (n=4) a low integration rate of the transgene. Notably, the copy number of B\_K15 $\Delta$ NLef1-mice constituted one third of the integration rate of mutant Lef1 in K14 $\Delta$ NLef1 (Peinkofer, 2008 and Andreas Kraus, Niemann lab).

### 3.12.2 Impaired epidermal differentiation and tumour formation in K15 $\Delta$ NLef1-mice

K15 $\Delta$ NLef1 mice were born healthy and showed a normal postnatal development. Interestingly, K15 $\Delta$ NLef1 mice (F0-F2-generation, A\_line n=10, B\_line n=11, C\_line n=7) commonly displayed a progressive but reversible hair loss relating to different areas of the body incipient with an age of 7-10 months, whereas age and sex-matched wt controls showed a normal hair coat. The low expressing A\_K15 $\Delta$ NLef1 line displayed the mildest phenotype, which might be due to a dose-dependent effect. Detailed histological and immunofluorescent analyses of epidermal whole-mounts and skin sections at different ages were carried out (by Heike Nöbel, diploma student, Niemann lab, Nöbel, 2009) to investigate whether morphogenesis and epidermal differentiation were affected in K15 $\Delta$ NLef1 mice.

Initial histological examination of skin sections derived from 2.5 months old K15 $\Delta$ NLef1 mice (A\_ and C\_line, n=4) showed a thickening of the IFE and a development of cysts. In addition, SGs were enlarged and HF s occasionally elongated.

Further immunological characterisation of the IFE revealed an elevated expression level of several lineage markers for the IFE (such as K10 and Loricrin). Concomitantly, the expression of Ki67, a marker for cell proliferation, and K6, a marker for hyperproliferation in the IFE, were increased. These data suggest that the over-expression of mutant Lef1 in the HF bulge stimulates cell fate specification towards the IFE.

Interestingly, SG differentiation was also altered in K15 $\Delta$ NLef1 mice. Typically, two SG are attached to one HF in wt tail epidermis. In contrast, 3.5 months old K15 $\Delta$ NLef1 not only exhibited enlarged SG, but also displayed multiple sebaceous lobules attached to one HF (n=2 mice/line). Surprisingly, with an increase in age an augmentation in the number of sebaceous lobules per pilosebaceous unit was seen (A\_line n=3; B\_line n=5; C\_line n=2). Up to seven SG lobules were detected in epidermal whole mounts of B\_ and C\_K15 $\Delta$ NLef1 mice. This phenotype correlated with the transgene copy number integrated since only a mild increase in number of SG lobules could be seen within the low expressing A\_K15 $\Delta$ NLef1-line.

Accessorily to the increase in SG differentiation in 7-19 months old B\_ and C\_K15 $\Delta$ NLef1 tail skin, the bulge region of the HF appeared more compact and thickened. HF were occasionally degenerated and deformed (Fig 34). In some cases, invaginations along the HF were observed, presumably resemble cyst like structures or ectopic SG (Nöbel, 2009). Notably, the typical pattern of HF triplets was frequently lost in epidermal whole-mounts derived from B\_ and C\_K15 $\Delta$ NLef1 tail epidermis. Taken together, these results indicate that mutant Lef1 in the HF bulge directs the migration of HFSC and lineage commitment towards the IFE and SG.

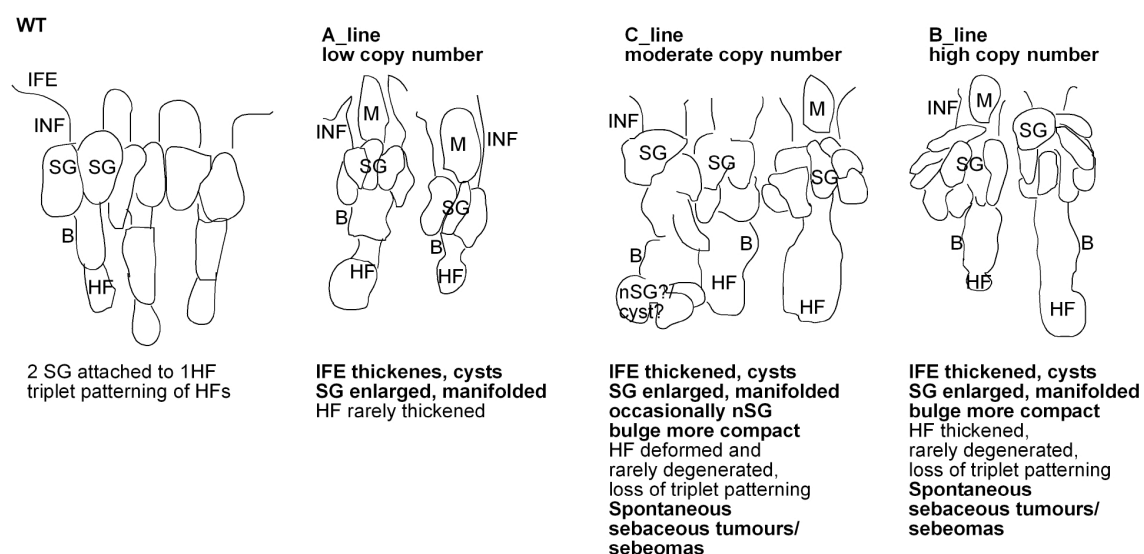


**Fig 34: Characterisation of K15 $\Delta$ NLef1-mice (F0-F2 generation)**

Epidermal tail whole-mounts isolated from K15 $\Delta$ NLef1 mice show an altered differentiation. SG are enlarged and amplified. B\_C\_K15 $\Delta$ NLef1 mice display shortened HF. Occasionally invaginations at the deformed HF (nSG/cyst) are found. The HF bulge seems to be more compact.

Expression of the transgene was analysed conducting immunofluorescent studies on paraffin sections and epidermal whole-mounts. In 2.5 months aged K15 $\Delta$ NLef1 skin (B and C line, n=2 mice/line), myc-tagged  $\Delta$ NLef1 was detected in the HF bulge compartment, but also in parts of the IFE, at the periphery of the multiplied SG and occasionally in the HF, indicating a stability of the transgene. Immunological detection of nuclear myc-tag in A\_K15 $\Delta$ NLef1 skin failed, probably due to low expression levels of the transgene. In wt skin, no immunofluorescent signal was observed with anti-myc-tag antibodies.

Most strikingly, B\_C\_K15 $\Delta$ NLef1 founder mice developed spontaneous skin tumours

with the age of 16 months (C\_line) and 19 months (B\_line). Histological analyses and immunostainings (Nöbel, 2009) revealed strong expression of the sebocyte marker SCD1 within the tumours. K14 was detected in the basal layer of keratinocytes of tumour lobules and within thickened and invaginated areas of the IFE. Furthermore, transgene expression was detected in the tumours as demonstrated by immunofluorescent analysis

These studies demonstrate that sebaceous adenomas had emerged in K15 $\Delta$ NLef1 animals, the same tumour types that K14 $\Delta$ NLef1 mice develop spontaneously.

To investigate whether  $\Delta$ NLef1 acts as tumour promotor in the HF bulge, we subjected B\_C\_K15 $\Delta$ NLef1-animals (F1 and F2 generation) to a one-step carcinogenesis protocol. A single treatment of B\_C\_K15 $\Delta$ NLef1-animals with subcritical dose of DMBA resulted in the formation of sebaceous adenomas, whereas DMBA-treated control littermates never developed tumours.

Notably, tumour growth and frequency in DMBA-treated K15 $\Delta$ NLef1 mice was similar to age matched DMBA-treated K14 $\Delta$ NLef1 animals, albeit the number of tumours per mouse was decreased and the incidence slightly delayed in K15 $\Delta$ NLef1 by 1-2 weeks (B\_K15 $\Delta$ NLef1, n=5) and 4 weeks (C\_K15 $\Delta$ NLef1, n=3).

Further immunological analyses (Nöbel, 2009) revealed that induced tumours in B\_C\_K15 $\Delta$ NLef1-animals (n=17 tumours of 4 B\_K15 $\Delta$ NLef1-animals, n=7 tumours of 3 C\_K15 $\Delta$ NLef1-animals) and tumours derived from K14 $\Delta$ NLef1-animals express similar epidermal markers, such as SCD1, K14 and K10. Additionally, tumours of B\_C\_K15 $\Delta$ NLef1 and K14 $\Delta$ NLef1-animals displayed the same number of proliferating (Ki67<sup>+</sup>ve) keratinocytes at the periphery of the tumour lobules.

Thus, dominant-negative Lef1 expressed in the HFSC compartment promoted sebaceous tumorigenesis.

## 4 Discussion

Multiple stem and progenitor cell populations are responsible for spontaneous regeneration of mammalian epidermis consisting of an IFE with associated HF and SG (Cotsarelis, 2006; Fuchs and Horsley, 2008; Jaks et al., 2008; Jaks et al., 2010).

It has been well documented that long-lived stem cells from the HF niche (bulge) are capable to sustain hair growth (Blanpain et al., 2004; Jaks et al., 2008; Liu et al., 2003; Morris et al., 2004). Although there are implications that uni- or bipotent progenitors (Horsley et al., 2006; Jensen et al., 2009; Jensen et al., 2008; Nijhof et al., 2006; Snippert et al., 2010) are involved to regenerate the upper integral parts of the epidermis, the cellular mechanism of SG renewal during tissue homeostasis still has to be uncovered. Over the last years, several SC/progenitor compartments have been identified within the pilosebaceous unit, but it is not clear if these stem and progenitor cells act autonomously or are related to each other.

To investigate a potential function of SC from the bulge HF niche, we have developed an tamoxifen-inducible Cre-mouse model. We aimed to specifically target HFSC by using the K15 regulatory sequence (Liu et al., 2003) to drive the inducible Cre-recombinase fused to the mutated estrogen receptor (Indra et al., 1999), thereby generating the K15CreER(G)T2-mice. By crossing K15CreER(G)T2 strain to Cre-sensitive reporter mice R26RLacZ (Soriano, 1999) and R26REYFP (Srinivas et al., 2001), bulge SCs as well as all descending cell lineages could be visualised.

In this PhD project a mouse model was generated providing a powerful tool to monitor the fate of HFSC on a single cell level under homeostatic and pathophysiological conditions (e.g. epidermal tumourigenesis).



#### **4.1 Development of a transgenic mouse model to trace the fate of HFSC-derived progeny on a single cell level**

Eight K15CreER(G)T2 lines were generated and two founder lines A\_K15CreER(G)T2 and C\_K15CreER(G)T2 were specific for Cre activation in the HF bulge and differed only in the number of targeted cells:

i. C\_K15CreER(G)T2 founder line exhibited high levels of activated Cre-recombinase in the bulge region and Cre-reporter gene activation was monitored in many keratinocytes within the HFSC compartment. This high expressing C\_K15CreER(G)T2 strain represents an excellent tool to genetically target the HFSC compartment and will be suitable for the specific manipulation of the HFSC niche. Indeed, the number of labelled bulge cells using C\_K15CreER(G)T2 was very similar to previously published conditional K15Cre mouse models (K15CrePR or K15CrePR\*), which can be induced by the application of the progesterone analgon RU486 (Morris et al., 2004).

ii. In contrast to the former generated inducible K15Cre strains (Malanchi et al., 2008; Morris et al., 2004; Youssef et al., 2010), individual cells could be targeted to the HFSC compartment using A\_K15CreER(G)T2-mice. Therefore, the A\_K15CreER(G)T2 line provides an excellent and novel tool to follow the fate of HFSC-derived progeny on a single cell resolution. In combination with the whole-mount technique (Braun et al., 2003), a three dimensional, complete and detailed lineage analysis of every genetically marked cell of the entire tail epidermis is now feasible.

The characterisation of targeted cells by A\_K15CreER(G)T2 mice at initial time points (day 1-2) confirmed that they were confined specifically to the bulge region since individually labelled keratinocytes co-localised with established HFSC markers such as K15 or an intense Itga6 signal and LRC.

## 4.2 Multipotency of individually labelled bulge cells

Previously, lineage analyses of HF regeneration have been performed applying the inducible K15CrePR and K15CrePR\* lines. These pioneer studies were among the first lineage tracing experiments conducted in the skin demonstrating that K15-targeted cells were multipotent to regenerate the entire HF including all different hair lineages (Morris et al., 2004).

Consistent with these reports, single HFSC-derived progeny labelled by A\_K15CreER(G)T2 mice participated in HF regeneration: Lineage tracing during the HFSC mobilisation phase demonstrated that HF were repopulated by HFSC-derived progeny, even after tracing through another hair cycle (28 days) or for 6 months in long-term studies. Taken together, these data demonstrated that the genetically targeted bulge cells utilising K15CreER(G)T2 mice indeed were long-lived and multipotent HFSC.

## 4.3 HFSC contribute to epidermal homeostasis

Until now, it was controversially discussed whether SC from the HF bulge actually contribute to spontaneous regeneration of other integral parts of the epidermis during skin homeostasis (Morris et al., 2004; Horsley et al., 2006; Blanpain et al., 2004; Levy et al., 2005; Blanpain and Fuchs, 2009; Jaks et al., 2010). It has been reported that SC from the bulge are able to reconstitute the IFE upon wounding or tissue damage (Ito et al., 2005; Ito et al., 2007; Langton et al., 2008; Levy et al., 2005; Levy et al., 2007).

The fate mapping analysis of single HFSC targeted by A\_K15CreER(G)T2-mice presented in this thesis now provides strong evidence that besides HF renewal, individual HFSC-derived progeny is also capable to regenerate the SG and IFE during skin homeostasis.

### 4.3.1 Regeneration of the SG

Lineage tracing experiments performed with A\_K15CreER(G)T2 mice during the resting phase of the hair cycle revealed that single HFSC-derived progeny drove SG renewal. First, YFP<sup>+</sup>ve keratinocytes were detected at the inner periphery of the SG which is located between SD and the lower tip of the SG. Subsequently, the entire

SG was repopulated by HFSC-derived progeny within a time frame of 5-7 days, thus implying a rather dynamic and fast turn-over of SG. In contrast, the HF compartment is replaced in a cyclic fashion with growth phases (anagen) lasting about 2 weeks (Alonso and Fuchs, 2006). Interestingly, the repopulation of one of the two glands by individual HFSC-derivates was observed in a high frequency, indicating that the renewal of both glands needs the activation of more than one HFSC.

Detailed statistical analyses of traced cells within a time frame of 7 days revealed that labelled keratinocytes were displaced from an exclusive localisation in the bulge to the SD and SG and a more complex pattern.

Thus, these data demonstrate that HFSC-derived progeny left the HF bulge region to contribute to the highly dynamic process of SG regeneration. In addition, many labelled bulge cells remained in the HF niche and will most likely be activated at a later time point for tissue regeneration and replenishment of the bulge SC pool. The spatial changes of HFSC-derived progeny towards the SG have been confirmed by FACS analyses. In the course of tracing (6 days of chase), a deprivation of YFP<sup>+</sup>/CD34 positive bulge cells (by 28 %) and an elevation of YFP/Lrig1<sup>+</sup> population (by 89 %) was detected (H. Brylka, personal communication and Petersson et al., submitted). These results were consistent with our observation that besides the persistence of LRC in the bulge, the BrdU label was also diluted upwards the UI and SG.

The possibility that the K15 promotor fragment itself was expressed in the SG or the CreER(G)T2 system was more sensitive to the hormone analogon tamoxifen in the SG could be ruled out, since Cre reporter gene activation in the higher expressing C\_K15CreER(G)T2-line was restricted to the bulge only at early tracing times. Furthermore, no increased number of labelled SG cells was observed over time of tracing demonstrating that SG homeostasis is not maintained by resident YFP<sup>+</sup> progenitors.

For future studies, it would be beneficial to perform live cell imaging to directly follow the migration, propagation and lineage commitment of individual HFSC-derived progeny. Therefore, cultivation of epidermal whole-mounts would not only allow time laps analyses of labelled HFSC-derived progeny, but also would open up the opportunities for manipulating growth and differentiation of whole-mounts *in vitro*. Addition of a distinct ligand or inhibitor of a certain pathway could be useful to study

the direct effects on individual cells and the consequences for homeostasis of the pilosebaceous unit.

Tracking HFSC-derived progeny at distinct phases of the hair cycle provided new insights into temporal control of SG renewal. Activation of HFSC for SG homeostasis occurred continuously and independently of the cyclic mobilisation of HFSC required for HF renewal. Thus, different signalling cues must exist to instruct HFSC either to move upwards to renew the SG or to migrate downwards to sustain hair growth. However, these signals are still elusive and need to be identified in the near future.

### 4.3.2 Regeneration of the IFE

HFSC-derived progeny additionally participated in the regeneration of the IFE. Intriguingly, YFP<sup>+</sup>ve keratinocytes were detected in clusters emanating from the JZ towards the IFE. Since no increase in YFP signal was seen at 28 days of tracing, it seems quite likely that labelled cells did not permanently reside in this compartment. Interestingly, a contribution of HFSC-derived progeny to IFE renewal was enhanced during HFSC mobilisation phase (telogen to anagen transition) compared to the initial telogen tracing experiment. Ongoing statistical analyses will help to quantify and validate these observations.

For the future, it will be challenging to investigate whether the regeneration of the SG and the IFE are interconnected and originate from the same HFSC. An elegant way to allow the visualisation of cell lineages derived from one particular SC *in vivo* was recently demonstrated for the nervous system. Livet et al. have generated a neuronal specific Cre reporter mouse model (Thy1-brainbow), which in response to active Cre recombinase expresses multiple fluorescent proteins in a mosaic fashion. This is achieved by the use of incompatible loxP sites to generate exclusive recombination events and by inserting loxP sites in opposite orientation positioned in series to induce several recombination events. This resulted in the expression of multiple fluorescent proteins from a single transgene upon Cre mediated recombination. Therefore, a reconstruction of hundreds of neighbouring axons and multiple synaptic contacts exhibiting approximately 90 colours was impressively demonstrated (Livet et al., 2007). With respect to our lineage tracing experiments these brainbow cassette could be adapted to a ubiquitous or skin specific promoter.

This would provide a powerful tool not only to perform clonal analyses derived from one particular labelled HFSC but also to isolate and analyse the molecular profile of clones derived from a single HFSC. With regard to the regeneration of the SG and the IFE, one could directly investigate whether progeny emanated from one HFSC gives rise to the IFE and the SG or whether renewal of the IFE and SG are achieved independently.

#### **4.4 A hierarchy of stem and progenitor cells drives epidermal renewal**

During the process of SG regeneration, single HFSC-derived progeny transits different SC/progenitor compartments of the pilosebaceous unit as verified by co-immunofluorescent analyses for marker molecules. They migrated through the MTS24antigen/Plet1<sup>+</sup>ve UI (Nijhof et al., 2006; Raymond et al., 2010), the JZ (Lrig1<sup>+</sup>ve) (Jensen et al., 2009) and the SD. At the inner periphery of the SG, Lrig1 seemed to mark the trail of genetically labelled keratinocytes towards the lower tip of the SG. FACS-analyses (performed by H.Brylka, Niemann lab, Petersson et al., submitted) verified and manifested that HFSC-derived progeny indeed gave rise to the SC/progenitor populations of the UI (MTS24) and JZ (Lrig1). Additional molecular analyses of SG-associated marker molecules revealed that both, YFP/Lrig1<sup>+</sup>ve and Itga6/Lrig1<sup>+</sup>ve cells, exhibited elevated expression levels of Blimp1, a marker for unipotent SG progenitors (Horsley et al., 2006) and the sebocyte marker SCD1 (Sampath et al., 2009). Thus, both populations had adopted sebaceous fate. Notably, the expressional change was quite similar comparing the subpopulation of YFP<sup>+</sup>ve keratinocytes in the Lrig1<sup>+</sup>ve compartment and the basal cell pool of the Lrig1<sup>+</sup>ve population. Of note, expression levels for bulge markers of YFP/Itga6 and CD34/Itga6 at 2 days chasing time were quite similar confirming that the initial genetically marked cells were indeed bulge stem cells.

Taken together, these data strongly imply that the different classes of SC/progenitor niches do not operate autonomously but are rather linked into a hierarchic system (Fig 35). Ongoing transplantation experiments and clonal analyses *in vitro* of YFP<sup>+</sup>ve keratinocytes isolated from different SC/progenitor compartments will prove this hierarchy on a more functional level.

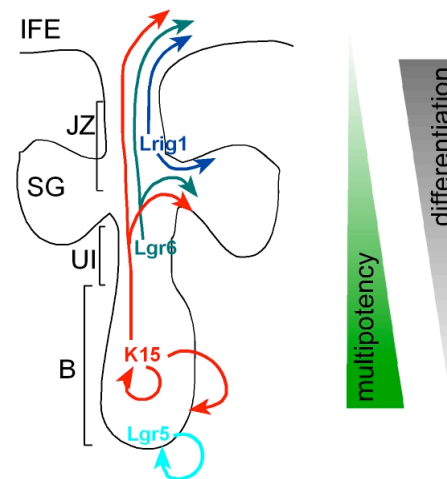


**Fig 35: Hierarchy of epidermal SC**

K15<sup>+</sup>ve SC population gives rise to HF, SG and the HF niche itself. Lgr6<sup>+</sup>ve (dark green) from the central isthmus and Lrig1<sup>+</sup>ve cells (blue) at the JZ contain bipotent progenitors that renew the SG or the IFE. Thus, multipotency decreases as cells move upwards, whereas the differentiation potential increases. A Lgr5-targeted SC population at the lower base of the HF is capable to only regenerate the HF.

Another emerging issue is how the different niches and the hierarchy are established during early morphogenesis. Several data suggest that during early stages of HF morphogenesis (E18.5), a common founder population (being positive for Lgr5, Lgr6, Lrig1 and Sox9) exists which is confined to the ORS of the developing HF (Jaks et al., 2008; Jaks et al., 2010; Nowak et al., 2008; Snippert et al., 2010). To dissect a hierarchy potentially established during HF morphogenesis, it will be very interesting to investigate the relationship between K15-targeted cells and the other described markers during early HF morphogenesis.

But what is the functional significance of the different progenitor pools within the pilosebaceous units during adult life? Previously, functional assays of different isolated SC/progenitor populations of the pilosebaceous unit were performed by several laboratories to prove the stem cell identity and their regenerative potential. Isolated bulge stem cells as well as MTS24 and Lrig1<sup>+</sup>ve keratinocytes form an increased number of highly proliferative stem cell colonies (holoclones) *in vitro* (Nijhof et al., 2006; Jensen et al., 2008; Jensen et al., 2009). In addition, all three isolated cell populations gave rise to a multilayered IFE, HF and SG in transplantation experiments, thus containing multipotent SC. For the future, more sensitive assays have to be evolved to distinguish SC potential of different epidermal progenitor populations and to test a hierarchic relationship on a functional level. Therefore, it

would be quite challenging to specifically target and ablate Lrig1 or MTS24 positive progenitor populations in HFSC-derived progeny to investigate the functional implications of these diverse SC/progenitor compartments within the pilosebaceous unit.

## 4.5 Signalling cues governing epidermal homeostasis

It is intriguing to speculate that during epidermal homeostasis, signals sent from the surrounding microenvironment instruct SC and its derivatives to migrate into diverse directions to renew all integral parts of the epidermis. Based on our own results and recent reports by other laboratories (Greco et al., 2009; Horsley et al., 2006; Jaks et al., 2008; Jensen et al., 2009; Jensen et al., 2008; Nijhof et al., 2006; Snippert et al., 2010; Tumber et al., 2004; Zhang et al., 2009; Zhang et al., 2010) a model comprising 2 “fate determination centers” governing the renewal of the HF, SG, IFE and the HFSC niche itself could be proposed (Fig 36): The first signal center is located at the HF bulge, where the mobilisation of HFSC either to migrate towards the HF or upwards to the SG/IFE is controlled. Recently, a Lgr5<sup>+</sup>ve SC population targeted by Wnt signals and located at the lower part of the HF near to the secondary HG has been identified and Lgr5<sup>+</sup>ve progeny is involved HF renewal (Jaks et al., 2008). More recently, it has been shown that Lgr6<sup>+</sup>ve SC located above the HF bulge and below the MTS24<sup>+</sup>ve cell compartment give rise to the IFE and SG (Snippert et al., 2010). In contrast to Lgr5, Lgr6 is not a Wnt target, suggesting that an active Wnt signal below the bulge sustains hair growth and a repressed Wnt signalling above the bulge leads to renewal of the SG and IFE. Notably, K15ΔN<sup>Lef1</sup> mice, where β-catenin/Lef1 mediated signalling is repressed in the HFSC niche, display multiplied SG and hyperproliferative IFE, indicating that impaired Wnt/Lef1-signalling in the HF bulge directs the migration of HFSC upwards the HF. Thus, one could speculate that signals controlling lineage differentiation also govern migration.

Once they exit the HF bulge towards the upper integral parts of the epidermis, HFSC-derived progeny reaches the 2<sup>nd</sup> cell fate determination center, the JZ, where YFP/Lrig1<sup>+</sup>ve SC derivatives could be directed to either regenerate the SG or the IFE. It has been shown that Lrig1 is a c-myc target and Lrig1 expression resulted in a reduced c-myc activity. Therefore, at the 2<sup>nd</sup> cell fate determination center, c-myc mediated signals could govern proliferation and cell type specification into lineages of the IFE and/or SG. Previously, it has been shown that HFSC lacking Notch signalling

contribute to the homeostasis of the IFE, proposing that Notch signalling is required to prevent migration of HF bulge progeny to the IFE. So far, a role for Notch signalling in migration and SG renewal has not been reported (Demehri and Kopan, 2009).

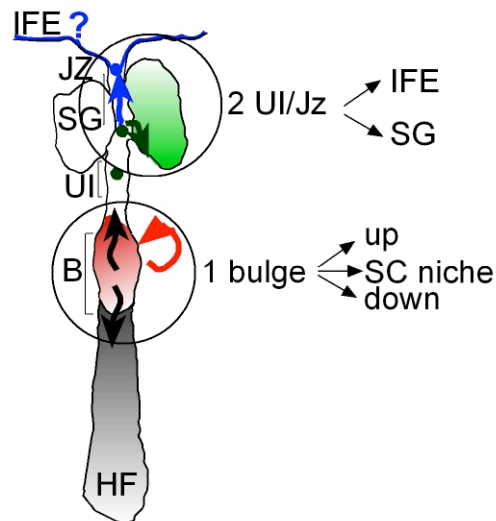


**Fig 36: Potential role of cell fate determination centers for epidermal regeneration**

4 independent signalling events are needed to renew the HF, SG, IFE and the HFSC niche itself. Fate determination is controlled in 2 centers. At the 1<sup>st</sup> center bulge cells are instructed either to move up- or downwards the HF or to replenish the HFSC niche. Fate decision for SG or IFE renewal is determined at the UI/JZ (2<sup>nd</sup> center).

## 4.6 Implications for ageing

Three important characteristics of aged skin are: shortened HF with reduced regenerative capacity enlarged SG and a thin IFE (Zouboulis et al., 2008a). Interestingly, despite an enhanced expression of cellular senescence markers such as INK4a (Jacobs et al., 1999), it has been shown that epidermal SC are maintained throughout adult life (Stern and Bickenbach, 2007). However, activity of surrounding/extrinsic signalling networks is altered in aged skin. For instance, it has been demonstrated that aged skin exhibits reduced expression levels of Igfbp3 (insulin-like growth factor binding protein3) (Giangreco et al., 2008). Furthermore, impaired Igf/Igfbp signalling has implications on the differentiation of the epidermis and HF shortening being indicative for premature ageing (Edmondson et al., 2003; Liu et al., 1993; Weger and Schlake, 2005).



Thus, these age-associated changes in signalling could lead to an imbalanced activation of bulge SC at the different cell fate determination centers (Fig 37). This could result in an enhanced mobilisation for SG renewal and reduced activation for HF or IFE regeneration. To investigate if HFSC mobilisation and activation is altered in aged skin, lineage tracing experiments could be conducted in old mice. Furthermore, it will be interesting to ablate or over-express age-associated factors such as INK4a or Igf/Igfbp signalling in the HFSC niche and to study the consequences on epidermal regeneration.

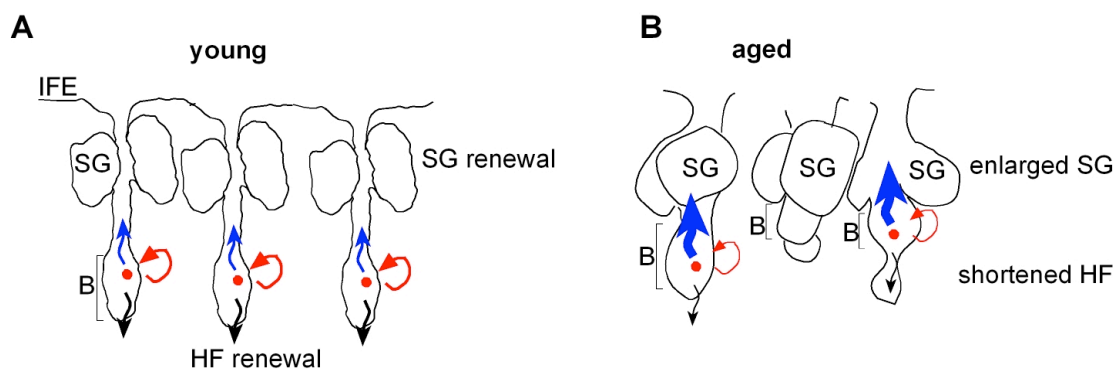


**Fig 37: Imbalanced activation of HFSC could be accompanied with ageing**

(A) HF and associated SG in young tail epidermis are organised in triplicates. The activation of HFSC for HF, SG, self-renewal and IFE are in a tight balance.

(B) HF of aged tail epidermis are shortened, possibly due to a reduced activation of HFSC for HF renewal. In contrast, enlarged SG could be a result of an enhanced mobilisation of HFSC for SG renewal. Additionally, the strict organisation of three HF in close proximity is lost in aged tail epidermis.

## 4.7 The HFSC niche exhibits a heterogeneous population

Our long term tracing experiments have shown that targeted HFSC were competent to replenish the HFSC niche itself. Notably, the HF bulge contained an elevated pool of labelled keratinocytes (3 fold) compared to the number of initially labelled HFSC. This could be a result of symmetric cell division at some stage of the long tracing period. Accordingly, a recently proposed model for HF renewal predicts that the self-renewing divisions within the HF bulge are symmetric in respect to their positioning towards the basement membrane. In contrast, divisions of short-lived progenitors in close proximity to the secondary HG seem to be orientated more asymmetrically (Zhang et al., 2010). This model would imply that the expansion of the SC pool and the mobilisation for the regeneration of the SG and IFE are assessed separately by

means of symmetric and asymmetric positioning towards the basement membrane. Furthermore, it is intriguing to speculate that the size of the SC pool might be controlled by an inhibitory feedback loop due to cell-cell contacts.

Our analyses clearly indicate that the HFSC niche exhibits a heterogeneous cell population consisting of a pool of SC dividing infrequently (silent SC) and more frequently (active SC). During SG renewal, some YFP<sup>+</sup>ve LRC were diluted towards the UI, whereas other LRC remain in the HFSC compartment. This is consistent with previous reports demonstrating that some bulge cells retained the label for longer periods indicating that they subsisted in a more quiescent state. In contrast, another population of LRC rapidly lost their label upon participation in epidermal regeneration (Blanpain et al., 2004; Tumber et al., 2004; Waghmare et al., 2008).

Taken together, the data support the “two SC population” hypothesis recently postulated (Li and Clevers, 2010). This model suggests that two SC populations reside within the same niche: (i.) A more primed and activated SC population that contributes to normal tissue homeostasis and (ii.) a highly competent quiescent SC population. The quiescent SC population can be activated in response to injury, safeguarding upon loss of the primed SCs. According to this model, maintenance and activation of the SC niche are balanced by secreted signalling proteins at segregated (“stimulatory” and “inhibitory”) zones. It has been demonstrated that Wnt and BMP signals are key players in these processes (Fuchs and Segre, 2000; Horsley et al., 2008; Kobiela et al., 2007; Rendl et al., 2008). To keep SC in a quiescent state, Wnt signalling is inhibited, whereas BMP-pathway is stimulated. The mirror image reflects the activated SC population. Besides the skin, there is compelling evidence for a heterogeneous composition of the SC niche from the hematopoietic system (Cheshier et al., 1999; Kiel et al., 2007; Wilson et al., 2008) and the intestine (Barker et al., 2007; Potten et al., 1997; Sato et al., 2009).

## **4.8 Impaired Lef1 signalling in the epidermis controls sebaceous commitment of HFSC-derived progeny**

Impairment of Lef1-signalling in the epidermis (K14 $\Delta$ NLef1 mice) promotes the development of ectopic SG along the deformed HF at expansion of HF differentiation (Niemann et al., 2002).

### **4.8.1 Composition of the HFSC niche**

Molecular and immunofluorescent analyses of K14 $\Delta$ NLef1 skin revealed that the expression levels of established HF bulge markers (K15, CD34) were decreased. In contrast, fate mapping experiments of HFSC-derived progeny in K14 $\Delta$ NLef1 mice clearly demonstrated that the targeted K15 promotor fragment was active in the deformed bulge at initial time points. Compared to the clonal analyses under homeostatic conditions, the number of labelled cells confined to the bulge region was elevated. This increase indicates that mutant Lef1 promotes the activation and proliferation of labelled HFSC.

Concomitant to the smaller size of the bulge compartment, a dramatic decrease in NFATc1 expression in K14 $\Delta$ NLef1 skin could be detected. NFATc1, a key regulator of SC quiescence, is activated by BMP signalling (Horsley et al., 2008) and our data indicate that the more silent SC population is deprived. It would be interesting to analyse if BMP signalling is altered in K14 $\Delta$ NLef1 mice. Long term tracing experiments within the K14 $\Delta$ NLef1 mouse model showed that small aggregates of labelled cells still remained in the bulge, thereby demonstrating that the SC pool in the HF bulge is not completely exhausted.

Taken together, our data suggest that the HFSC niche of K14 $\Delta$ NLef1 mice exhibits an enhanced pool of activated SC and that the reservoir of more dormant SC is diminished.

### **4.8.2 Ectopic SG originate from HFSC**

From our lineage tracing experiments within the K14 $\Delta$ NLef1 mouse model we have learned that HFSC-derived progeny not only contributes to the regeneration of the enlarged upper SG, but also drives formation of ectopic SG (Fig 38). Indeed, a

majority of labelled SC-derivates migrated towards the ectopic SG and were committed to sebaceous lineage as they co-expressed SCD1, a sebocyte differentiation marker.

Thus, HFSC from the bulge region could be identified as cellular source for ectopic SG development. In addition, mutant Lef1 not only determines the fate decision of HFSC but also affects the migration of HFSC-derived progeny. HFSC-derived progeny is instructed either to move upwards to repopulate the enlarged SG and downwards to drive formation of ectopic SG. The underlying mechanism how migration is controlled by Lef1 still remains elusive.

### 4.8.3 Establishment of new progenitor niches

The increase in SG fate in K14 $\Delta$ NLef1 mice was accompanied by an elevated number of progenitors directing SG differentiation. The molecules being associated with sebaceous lineage (Lrig1 and MTS24/Plet1) were also localised to the perimeter or branching ducts of the ectopic SG. These data imply that the induction of *de novo* SG by overexpressing dominant negative Lef1 required the establishment of new SG-associated progenitor niches. This finding was validated by qRT-PCR analysing marker molecules associated with SG fate specification. TenascinC, a known target of the UI (MTS24antigen<sup>+</sup>ve) compartment (Nijhof et al., 2006), is up-regulated in K14 $\Delta$ NLef1 mice. Additionally, Keratin6a, recently been discovered to be strongly expressed in the sebaceous duct (Gu and Coulombe, 2008), was upregulated in K14 $\Delta$ NLef1 epidermis. Future experiments will evaluate whether the expression levels of other described SG-associated progenitor marker such as Lrig1, Blimp1 and Lgr6 are also differentially regulated on a transcriptional level.

The presented fate mapping studies clearly show that HFSC-derived progeny transits the new established progenitor niches during development of ectopic SG in K14 $\Delta$ NLef1 mice. This again supports our view of a hierarchy of HFSC and MTS24/Plet1 and Lrig1<sup>+</sup>ve progenitors. One could speculate that SG morphogenesis is recapitulated during the process of ectopic SG formation, but this awaits further investigations.

Previous reports have delineated a crucial role for c-myc signalling in controlling proliferation and cell type specification of the IFE and SG (Watt et al., 2008). Interestingly, c-myc and its target Nucleolin were down-regulated in K14 $\Delta$ NLef1 epidermis. Therefore, Lef1 and c-myc might have an independent role in

controlling sebaceous fate specification. It seems possible that an elevated pool of Lrig1 could mediate c-myc signalling to regulate sebaceous fate decision.

## 4.9 Role of HFSC in epidermal tumourigenesis

Several studies provide evidence that de-regulated  $\beta$ -catenin signalling causes a variety of cancers, including skin tumours (Owens and Watt, 2003; Polakis, 2000). Activating mutations have been detected in human pilomatricomas (Chan et al., 1999) and mouse models stimulating  $\beta$ -catenin signalling form hair tumours (trichofolliculomas and pilomatricomas) (Gat et al., 1998). Conversely, mutations in the  $\beta$ -catenin binding domain of Lef1 have been found in a high frequency in human sebaceous tumours, indicating that also a repression of  $\beta$ -catenin-mediated Lef1 signalling results in cancer development (Takeda et al., 2006). Accordingly, our transgenic mouse model with an epidermal expression of mutant Lef1 ( $\Delta$ NLef1) lacking the  $\beta$ -catenin binding domain (K14 $\Delta$ NLef1) exhibits spontaneous tumourigenesis. These tumours are sebaceous adenomas and papillomas with sebocyte differentiation (Niemann et al., 2002). Since  $\Delta$ NLef1 itself acts as a tumour promotor, these tumours can also be induced by a single application of a carcinogen (DMBA) to initiate tumour growth (Niemann et al., 2007).

Therefore, the development of sebaceous adenomas following 4 weeks after tumour initiation provides an excellent tool to study distinct stages of tumour formation and origin and cause of tumourigenesis.

According to the rationale of cancer stem cells (CSC) (Bonnet and Dick, 1997; Lobo et al., 2007; Visvader and Lindeman, 2008; Wang, 2010; Wang and Dick, 2005) sebaceous tumour formation in K14 $\Delta$ NLef1 mice is initiated and driven by a subpopulation of self-renewing CSC.

To analyse whether HFSC and its derivatives were transformed into a CSC, label retention and fate mapping experiments were assayed within the K14 $\Delta$ NLef1 tumour model. Label retention studies revealed that LRC localised to the deformed HFSC niche showed an increased recruitment into the cell cycle upon tumour initiation, indicating that HF progenitors were activated in the process of tumour development (C. Niemann, unpublished data and data not shown).

The protocol to isolate epidermal whole-mounts derived from was adapted and enabled a three dimensional and detailed lineage analyses of HFSC-derived progeny at early and late stages of sebaceous tumourigenesis. At early stages, an elevated

number of labelled cells could be detected in the deformed HF bulge, indicating that DMBA treatment causes an enhanced mobilisation of HFSC. Concomitantly with tumour progression, HFSC-derived progeny was detected in early lesions and the entire sebaceous tumours including the more differentiated areas.

From these fate mapping studies we conclude that HFSC-derived progeny indeed contributes to sebaceous adenoma formation (Fig 38). In the future, we aim to isolate HFSC-derived progeny at different stages of tumour development. Subsequent serial transplantations and clonal analyses of the isolated cells will prove their tumourigenic potential. Important issues will be how many cells are required to recapitulate tumourigenesis and to calculate the number of self-renewing CSC within the isolated cell population.

Additionally, it will be interesting to investigate which tumour type is induced to gain information about multipotency and plasticity of the isolated cell fractions.

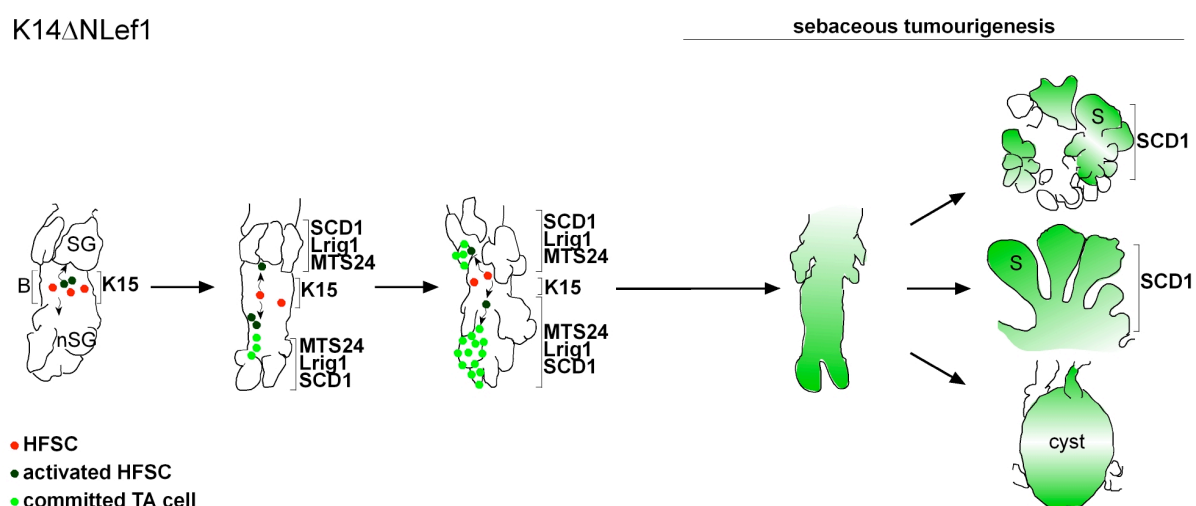


**Fig 38: HFSC-derived progeny contributes to ectopic SG and sebaceous adenoma formation.**

Mutant Lef1 mobilises HFSC from the deformed bulge region to drive ectopic SG renewal. HFSC-derived progeny transits different newly established progenitor compartments thereby creating a hierarchy of different classes of stem and progenitor cells. Upon tumour initiation, clonal expansion of labelled cells was found in early lesions and sebaceous tumours.

Here, we present data supporting the idea of CSC driving formation of skin tumours. It was found previously, that a large number of tumourigenic CD34-expressing cells reside in murine squamous cell carcinomas (SCC). Interestingly, the published data indicate that  $\beta$ -catenin was essential for maintaining the tumour-initiating potential of the CD34<sup>+</sup>ve tumour cells (Malanchi et al., 2008).

More recently, lineage tracing experiments utilising a Cre-sensitive tumour-mouse model for basal cell carcinoma (BCC) revealed that progenitor cells from the basal layer and not from the HFSC niche represent the cell of origin generating the bulk of the tumour (Youssef et al., 2010).

To this end, it is unclear whether labelled HFSC itself or HFSC-derived progeny is targeted by mutations resulting in tumour development.

Due to the high plasticity within the epidermal tissue, it is intriguing to speculate that all progenitors could adopt SC characteristics and therefore become CSC. Alternatively, a certain hierarchy of HFSC and SG progenitors could be established during sebaceous tumourigenesis. Therefore, we will analyse if labelled HFSC give rise to an elevated progenitor pool of Lrig1, MTS24 or Lgr6<sup>+</sup>ve cell populations within the tumour model. To investigate if the labelled HFSC itself serves as unique cellular source during sebaceous tumourigenesis, deletion experiments of K15-targeted cells at different stages of tumour development are planned.

## **4.10 Manipulating Lef1 signalling in the HFSC niche**

### **4.10.1 Impaired epidermal differentiation**

To investigate whether mutated Lef1 signalling in the HFSC niche affects epidermal regeneration and is sufficient to drive tumourigenesis, K15 $\Delta$ Lef1 transgenic mice were generated. K15 $\Delta$ Lef1 mice showed a normal development, but displayed a progressive reversible hair loss. Histological analyses revealed that the IFE was hyperproliferative. In addition, sebocyte differentiation was stimulated. All K15 $\Delta$ Lef1 mice displayed multiple sebaceous lobules attached to one HF, whereas the wt controls exhibited only two SG within one pilosebaceous unit (Nöbel, 2009). Notably, an augmentation of sebaceous lobules was seen from 7 months of age onwards. In contrast, HF were degenerated and deformed occasionally. Often, HF were shortened indicating that mobilisation of HFSC for HF renewal is reduced. Interestingly, the typical organisation of HF triplets was frequently lost in epidermal whole-mounts.

Taken together, these data imply that dominant negative Lef1 in the HFSC causes an imbalanced mobilisation of HFSC leading to an image which is typically seen in aged skin. Therefore, qRT-PCR analysing ageing-associated genes such as pINK4a will prove if the phenotype of K15 $\Delta$ Lef1 is coupled to premature ageing.

#### 4.10.2 Sebaceous tumourigenesis in K15 $\Delta$ NLef1 mice

Most strikingly, K15 $\Delta$ NLef1 mice developed spontaneous sebaceous tumours. Sebaceous tumours can also be induced by the application of a single subthreshold dose of DMBA (Nöbel, 2009).

These data proof that targeted expression of  $\Delta$ NLef1 within HFSC niche also acts as a tumour promotor and targeting  $\Delta$ Lef1 to the HFSC is sufficient to drive sebaceous tumour formation. Thus, it seems possible that cells from the HF bulge are transformed into a CSC.

#### 4.11 Perspectives

The data presented in this thesis provide novel insights into the cellular mechanisms of epidermal regeneration. HFSC are activated by at least 4 different signals to renew the SG, HF, IFE and to replenish the SC niche. Future experiments will focus on the molecular signals determining which epidermal compartment is regenerated thereby directing migration of HFSC-derived progeny. An imbalanced mobilisation of HFSC could promote an enhanced regeneration of one of these compartments, thereby allowing a certain plasticity within the tissue and responsiveness to damaging agents. This is not only important for tissue repair after injury, but also has major implications for ageing. Future fate mapping and manipulation experiments will address the question whether ageing is accompanied by an enhanced mobilisation of HFSC for SG renewal and reduced activation for HF regeneration. Our data demonstrated that HFSC-derived progeny gives rise to different epidermal progenitor compartments during SG homeostasis and ectopic SG formation. It will be challenging to identify which signals control the integration of the different SC/progenitor into a hierarchic system. Fate mapping studies within an inducible tumour model identified HFSC-derived progeny as cells of origin generating sebaceous tumours. Further analyses will be needed to characterise their tumourigenic potential in more detail. Ablation of HFSC-derived progeny will prove whether these cells serve as unique source driving sebaceous tumourigenesis. Analysing the molecular signature and crucial mutations of tumour-initiating cells might have a relevant diagnostic and therapeutic value. Mutant Lef1 in the HFSC niche drives sebaceous tumourigenesis, which raises the question whether tumour development is dependent on SC intrinsic mutations or is rather caused by an impaired crosstalk with signals provided by the microenvironment.



## 5 Summary

Mammalian epidermis is a highly dynamic epithelium comprising the interfollicular epidermis, hair follicles (HF) and associated sebaceous glands (SG). Spontaneous regeneration and cellular turn over of each of these compartments is maintained by multiple stem cell (SC) and progenitor populations (Cotsarelis, 2006; Fuchs and Horsley, 2008). Although there are implications that different SC/progenitors participate in SG regeneration, the cellular process of SG maintenance still needs to be uncovered (Blanpain and Fuchs, 2009). For instance, it is unknown whether different SC/progenitor reservoirs act autonomously or are interconnected and arranged within a certain hierarchy (Jaks et al, 2010). To investigate potential functions and epidermal contribution of SC from the HF bulge, we have developed an inducible Cre-mouse model enabling us to track the fate of single HFSC-derived progeny. From these lineage tracing experiments we have learned that HFSC-derived progenitors are not only essential for cyclic HF regeneration but also continuously reconstitute the SG. During this process of SG renewal, cells exit the HF bulge and transit through distinct epidermal progenitor compartments before finally repopulating the SG. Thus, our data imply a hierarchy of multipotent keratinocytes underlying epidermal homeostasis. Furthermore, tracking HFSC-derived progeny in long term studies revealed that the SC pool itself is replenished probably by symmetric cell division. Therefore, different signaling cues must exist to instruct HFSC to regenerate different integral parts of the epidermis or to replenish the SC pool.

By forcing basal keratinocytes into the sebocyte lineage through manipulation of Lef1 (Niemann et al., 2002), one of the crucial regulators of fate decision, we could identify HFSC as cells of origin for development of ectopic SG. Additionally, new sebocyte progenitor compartments are established adjacent to *de novo* formed SG. Intriguingly, fate mapping experiments within an inducible skin tumour model (Niemann et al., 2007) clearly demonstrated that HFSC-derived progeny contributes to sebaceous tumourigenesis. Finally, manipulation of Lef1 signalling within the HFSC niche in a transgenic mouse model results in formation of sebaceous adenoma, supporting the hypothesis that HFSC indeed are targeted by transformational events during skin tumour development.

## 6 Zusammenfassung

Das Hautepithel ist ein komplexes und stark kompartimentiertes Gewebe, bestehend aus interfollikulärer Epidermis und assoziierten Anhangsgeweben wie Haarfollikeln (HF) und Talgdrüsen (TD) (Cotsarelis, 2006; Fuchs and Horsley, 2008). Um die Barriere- und Schutzfunktion der Haut zu gewährleisten, müssen die verschiedenen Kompartimente kontinuierlich erneuert werden. Diese spontanen Regenerationsprozesse erfordern das Agieren mehrerer Stammzell (SZ)- und Progenitorpopulationen (Blanpain and Fuchs, 2009).

Obwohl Arbeiten der letzten Jahre darauf hindeuten, daß verschiedene SZ/Progenitoren im Prozeß der TD-Erneuerung involviert sind (Horsley et al. 2006, Jensen et al, 2009, Snippert et al., 2010), ist der zelluläre Mechanismus der TD-Homeöstase bisher noch ungeklärt. Weiterhin ist nicht untersucht, ob die diversen SZ/Progenitorzellreservoirs unabhängig voneinander wirken oder ob sie in ein hierarchisches Netzwerk integriert sind (Jaks et al, 2010). Um mögliche Funktionen von multipotenten SZ der HF Nische während der Hauthomeöstase zu untersuchen, haben wir ein induzierbares Cre-Mausmodell generiert, das uns ermöglicht, einzelne HFSZ und ihre Abkömmlinge unter physiologischen Bedingungen im Gewebe zu verfolgen. Diese "lineage"-Analysen ergaben, dass HFSZ-Abkömmlinge nicht nur für die zyklische Regeneration der HF essentiell sind, sondern auch zur kontinuierlichen Erneuerung der TD beitragen. Hierbei verlassen Tochterzellen die HFSZ-Nische und durchlaufen distinkte SZ/Progenitorkompartimente, um letztendlich die TD zu besiedeln. Unsere Ergebnisse schlagen eine hierarchische Anordnung von multi-kompetenten Keratinozyten im Prozeß der spontanen epidermalen Erneuerung vor. Darüber hinaus hat die Analyse der HFSZ-Nische in Langzeitexperimenten gezeigt, daß auch eine Selbsterneuerung des HFSZ-Reservoirs wahrscheinlich mittels symmetrischer Zellteilung erfolgt. Die Ergebnisse unterstreichen, dass HFSZ auf diverse Signalaktivitäten reagieren müssen, um die verschiedenen Kompartimente der Epidermis oder den SZ-Pool zu regenerieren. Durch die epidermis-spezifische Manipulation des Transkriptionsfaktors Lef1 werden die Entwicklung von ektopischen TD und die Bildung von TD-Tumoren stimuliert (Niemann et al., 2002). Die Verfolgung von HFSZ und allen hervorgehenden Tochterzellen innerhalb dieses transgenen Mausmodells hat gezeigt, daß HFSZ bzw. ihre Abkömmlinge maßgeblich zur Entstehung dieser ektopischen TD beitragen. Einhergehend mit der Entstehung neuer TD werden ebenfalls neue Progenitorzellnischen etabliert. "Lineage" Analysen

in einem induzierbaren TD-Tumormodell (Niemann et al., 2007) haben gezeigt, dass HFSZ-Abkömmlinge an der Entstehung von TD-Tumoren beteiligt sind. Darüber hinaus führt die Manipulation der Lef1 Signalgebung in der HFSZ Nische in einem neu generierten transgenen Mausmodell ebenfalls zu TD-Tumoren, was für eine Transformation von HFSZ als ursächlichen Mechanismus der Tumorigenese spricht.

## 7 References

- Adams, J.M., and Strasser, A. (2008). Is tumor growth sustained by rare cancer stem cells or dominant clones? *Cancer Res* 68, 4018-4021.
- Akagi, K., Sandig, V., Vooijs, M., Van der Valk, M., Giovannini, M., Strauss, M., and Berns, A. (1997). Cre-mediated somatic site-specific recombination in mice. *Nucleic Acids Res* 25, 1766-1773.
- Al-Hajj, M., Wicha, M.S., Benito-Hernandez, A., Morrison, S.J., and Clarke, M.F. (2003). Prospective identification of tumorigenic breast cancer cells. *Proc Natl Acad Sci U S A* 100, 3983-3988.
- Alberts, B. (2002). *Molecular biology of the cell*, 4th edn (New York, Garland Science).
- Alonso, L., and Fuchs, E. (2006). The hair cycle. *J Cell Sci* 119, 391-393.
- Ambler, C.A., and Maatta, A. (2009). Epidermal stem cells: location, potential and contribution to cancer. *J Pathol* 217, 206-216.
- Barrandon, Y., and Green, H. (1985). Cell size as a determinant of the clone-forming ability of human keratinocytes. *Proc Natl Acad Sci U S A* 82, 5390-5394.
- Barrandon, Y., and Green, H. (1987). Three clonal types of keratinocyte with different capacities for multiplication. *Proc Natl Acad Sci U S A* 84, 2302-2306.
- Behrens, J., von Kries, J.P., Kuhl, M., Bruhn, L., Wedlich, D., Grosschedl, R., and Birchmeier, W. (1996). Functional interaction of beta-catenin with the transcription factor LEF-1. *Nature* 382, 638-642.
- Binczek, E., Jenke, B., Holz, B., Gunter, R.H., Thevis, M., and Stoffel, W. (2007). Obesity resistance of the stearyl-CoA desaturase-deficient (*scd1*<sup>-/-</sup>) mouse results from disruption of the epidermal lipid barrier and adaptive thermoregulation. *Biol Chem* 388, 405-418.
- Blanpain, C., and Fuchs, E. (2006). Epidermal stem cells of the skin. *Annu Rev Cell Dev Biol* 22, 339-373.
- Blanpain, C., and Fuchs, E. (2009). Epidermal homeostasis: a balancing act of stem cells in the skin. *Nat Rev Mol Cell Biol* 10, 207-217.
- Blanpain, C., Lowry, W.E., Geoghegan, A., Polak, L., and Fuchs, E. (2004). Self-renewal, multipotency, and the existence of two cell populations within an epithelial stem cell niche. *Cell* 118, 635-648.
- Blanpain, C., Lowry, W.E., Pasolli, H.A., and Fuchs, E. (2006). Canonical notch signaling functions as a commitment switch in the epidermal lineage. *Genes Dev* 20, 3022-3035.
- Bonnet, D., and Dick, J.E. (1997). Human acute myeloid leukemia is organized as a hierarchy that originates from a primitive hematopoietic cell. *Nat Med* 3, 730-737.
- Carroll, J.M., Romero, M.R., and Watt, F.M. (1995). Suprabasal integrin expression in the epidermis of transgenic mice results in developmental defects and a phenotype resembling psoriasis. *Cell* 83, 957-968.
- Celis, J.E. (2006). *Cell biology: A laboratory handbook*. Elsevier Academic, Amsterdam, NL.
- Chan, E.F., Gat, U., McNiff, J.M., and Fuchs, E. (1999). A common human skin tumour is caused by activating mutations in beta-catenin. *Nat Genet* 21, 410-413.
- Chiang, C., Swan, R.Z., Grachtchouk, M., Bolinger, M., Litingtung, Y., Robertson, E.K., Cooper, M.K., Gaffield, W., Westphal, H., Beachy, P.A., *et al.* (1999). Essential role for Sonic hedgehog during hair follicle morphogenesis. *Dev Biol* 205, 1-9.
- Clayton, E., Doupe, D.P., Klein, A.M., Winton, D.J., Simons, B.D., and Jones, P.H. (2007). A single type of progenitor cell maintains normal epidermis. *Nature* 446, 185-189.

- Collins, A.T., and Maitland, N.J. (2006). Prostate cancer stem cells. *Eur J Cancer* 42, 1213-1218.
- Cotsarelis, G. (2006). Epithelial stem cells: a folliculocentric view. *J Invest Dermatol* 126, 1459-1468.
- DasGupta, R., Rhee, H., and Fuchs, E. (2002). A developmental conundrum: a stabilized form of beta-catenin lacking the transcriptional activation domain triggers features of hair cell fate in epidermal cells and epidermal cell fate in hair follicle cells. *J Cell Biol* 158, 331-344.
- Demehri, S., and Kopan, R. (2009). Notch signaling in bulge stem cells is not required for selection of hair follicle fate. *Development* 136, 891-896.
- Donovan, J. (2009). Review of the hair follicle origin hypothesis for basal cell carcinoma. *Dermatol Surg* 35, 1311-1323.
- Doupe, D.P., Klein, A.M., Simons, B.D., and Jones, P.H. (2010). The ordered architecture of murine ear epidermis is maintained by progenitor cells with random fate. *Dev Cell* 18, 317-323.
- Driskell, R.R., Giangreco, A., Jensen, K.B., Mulder, K.W., and Watt, F.M. (2009). Sox2-positive dermal papilla cells specify hair follicle type in mammalian epidermis. *Development* 136, 2815-2823.
- Edmondson, S.R., Thumiger, S.P., Werther, G.A., and Wraight, C.J. (2003). Epidermal homeostasis: the role of the growth hormone and insulin-like growth factor systems. *Endocr Rev* 24, 737-764.
- Enshell-Seijffers, D., Lindon, C., Kashiwagi, M., and Morgan, B.A. (2010). beta-catenin activity in the dermal papilla regulates morphogenesis and regeneration of hair. *Dev Cell* 18, 633-642.
- Estrach, S., Cordes, R., Hozumi, K., Gossler, A., and Watt, F.M. (2008). Role of the Notch ligand Delta1 in embryonic and adult mouse epidermis. *J Invest Dermatol* 128, 825-832.
- Fodde, R., and Brabletz, T. (2007). Wnt/beta-catenin signaling in cancer stemness and malignant behavior. *Curr Opin Cell Biol* 19, 150-158.
- Fuchs, E., and Green, H. (1980). Changes in keratin gene expression during terminal differentiation of the keratinocyte. *Cell* 19, 1033-1042.
- Fuchs, E., and Horsley, V. (2008). More than one way to skin. *Genes Dev* 22, 976-985.
- Fuchs, E., and Nowak, J.A. (2008). Building epithelial tissues from skin stem cells. *Cold Spring Harb Symp Quant Biol* 73, 333-350.
- Fuchs, E., and Segre, J.A. (2000). Stem cells: a new lease on life. *Cell* 100, 143-155.
- Gat, U., DasGupta, R., Degenstein, L., and Fuchs, E. (1998). De Novo hair follicle morphogenesis and hair tumors in mice expressing a truncated beta-catenin in skin. *Cell* 95, 605-614.
- Ghali, L., Wong, S.T., Tidman, N., Quinn, A., Philpott, M.P., and Leigh, I.M. (2004). Epidermal and hair follicle progenitor cells express melanoma-associated chondroitin sulfate proteoglycan core protein. *J Invest Dermatol* 122, 433-442.
- Ghazizadeh, S., and Taichman, L.B. (2001). Multiple classes of stem cells in cutaneous epithelium: a lineage analysis of adult mouse skin. *Embo J* 20, 1215-1222.
- Giangreco, A., Qin, M., Pinter, J.E., and Watt, F.M. (2008). Epidermal stem cells are retained in vivo throughout skin aging. *Aging Cell* 7, 250-259.
- Greco, V., Chen, T., Rendl, M., Schober, M., Pasolli, H.A., Stokes, N., Dela Cruz-Racelis, J., and Fuchs, E. (2009). A two-step mechanism for stem cell activation during hair regeneration. *Cell Stem Cell* 4, 155-169.

- Gu, L.H., and Coulombe, P.A. (2008). Hedgehog signaling, keratin 6 induction, and sebaceous gland morphogenesis: implications for pachyonychia congenita and related conditions. *Am J Pathol* 173, 752-761.
- Gupta, P.B., Chaffer, C.L., and Weinberg, R.A. (2009). Cancer stem cells: mirage or reality? *Nat Med* 15, 1010-1012.
- Hardy, M.H. (1992). The secret life of the hair follicle. *Trends Genet* 8, 55-61.
- Horsley, V., Aliprantis, A.O., Polak, L., Glimcher, L.H., and Fuchs, E. (2008). NFATc1 balances quiescence and proliferation of skin stem cells. *Cell* 132, 299-310.
- Horsley, V., O'Carroll, D., Tooze, R., Ohinata, Y., Saitou, M., Obukhanych, T., Nussenzweig, M., Tarakhovsky, A., and Fuchs, E. (2006). Blimp1 defines a progenitor population that governs cellular input to the sebaceous gland. *Cell* 126, 597-609.
- Ito, M., Liu, Y., Yang, Z., Nguyen, J., Liang, F., Morris, R.J., and Cotsarelis, G. (2005). Stem cells in the hair follicle bulge contribute to wound repair but not to homeostasis of the epidermis. *Nat Med* 11, 1351-1354.
- Ito, M., Yang, Z., Andl, T., Cui, C., Kim, N., Millar, S.E., and Cotsarelis, G. (2007). Wnt-dependent de novo hair follicle regeneration in adult mouse skin after wounding. *Nature* 447, 316-320.
- Jaks, V., Barker, N., Kasper, M., van Es, J.H., Snippert, H.J., Clevers, H., and Toftgard, R. (2008). Lgr5 marks cycling, yet long-lived, hair follicle stem cells. *Nat Genet* 40, 1291-1299.
- Jaks, V., Kasper, M., and Toftgard, R. (2010). The hair follicle-a stem cell zoo. *Exp Cell Res*.
- Jensen, K.B., Collins, C.A., Nascimento, E., Tan, D.W., Frye, M., Itami, S., and Watt, F.M. (2009). Lrig1 expression defines a distinct multipotent stem cell population in mammalian epidermis. *Cell Stem Cell* 4, 427-439.
- Jensen, U.B., Yan, X., Triel, C., Woo, S.H., Christensen, R., and Owens, D.M. (2008). A distinct population of clonogenic and multipotent murine follicular keratinocytes residing in the upper isthmus. *J Cell Sci* 121, 609-617.
- Jones, P., and Simons, B.D. (2008). Epidermal homeostasis: do committed progenitors work while stem cells sleep? *Nat Rev Mol Cell Biol* 9, 82-88.
- Jones, P.H., and Watt, F.M. (1993). Separation of human epidermal stem cells from transit amplifying cells on the basis of differences in integrin function and expression. *Cell* 73, 713-724.
- Kelly, P.N., Dakic, A., Adams, J.M., Nutt, S.L., and Strasser, A. (2007). Tumor growth need not be driven by rare cancer stem cells. *Science* 317, 337.
- Kim, C.F., Jackson, E.L., Woolfenden, A.E., Lawrence, S., Babar, I., Vogel, S., Crowley, D., Bronson, R.T., and Jacks, T. (2005). Identification of bronchioalveolar stem cells in normal lung and lung cancer. *Cell* 121, 823-835.
- Kobielak, K., Pasolli, H.A., Alonso, L., Polak, L., and Fuchs, E. (2003). Defining BMP functions in the hair follicle by conditional ablation of BMP receptor IA. *J Cell Biol* 163, 609-623.
- Kobielak, K., Stokes, N., de la Cruz, J., Polak, L., and Fuchs, E. (2007). Loss of a quiescent niche but not follicle stem cells in the absence of bone morphogenetic protein signaling. *Proc Natl Acad Sci U S A* 104, 10063-10068.
- Langton, A.K., Herrick, S.E., and Headon, D.J. (2008). An extended epidermal response heals cutaneous wounds in the absence of a hair follicle stem cell contribution. *J Invest Dermatol* 128, 1311-1318.
- Legg, J., Jensen, U.B., Broad, S., Leigh, I., and Watt, F.M. (2003). Role of melanoma chondroitin sulphate proteoglycan in patterning stem cells in human interfollicular epidermis. *Development* 130, 6049-6063.

- Legue, E., Sequeira, I., and Nicolas, J.F. (2010). Hair follicle renewal: authentic morphogenesis that depends on a complex progression of stem cell lineages. *Development* 137, 569-577.
- Levy, V., Lindon, C., Harfe, B.D., and Morgan, B.A. (2005). Distinct stem cell populations regenerate the follicle and interfollicular epidermis. *Dev Cell* 9, 855-861.
- Levy, V., Lindon, C., Zheng, Y., Harfe, B.D., and Morgan, B.A. (2007). Epidermal stem cells arise from the hair follicle after wounding. *Faseb J* 21, 1358-1366.
- Li, L., and Clevers, H. (2010). Coexistence of quiescent and active adult stem cells in mammals. *Science* 327, 542-545.
- Liu, J.P., Baker, J., Perkins, A.S., Robertson, E.J., and Efstratiadis, A. (1993). Mice carrying null mutations of the genes encoding insulin-like growth factor I (Igf-1) and type 1 IGF receptor (Igf1r). *Cell* 75, 59-72.
- Liu, Y., Lyle, S., Yang, Z., and Cotsarelis, G. (2003). Keratin 15 promoter targets putative epithelial stem cells in the hair follicle bulge. *J Invest Dermatol* 121, 963-968.
- Livet, J., Weissman, T.A., Kang, H., Draft, R.W., Lu, J., Bennis, R.A., Sanes, J.R., and Lichtman, J.W. (2007). Transgenic strategies for combinatorial expression of fluorescent proteins in the nervous system. *Nature* 450, 56-62.
- Lo Celso, C., Prowse, D.M., and Watt, F.M. (2004). Transient activation of beta-catenin signalling in adult mouse epidermis is sufficient to induce new hair follicles but continuous activation is required to maintain hair follicle tumours. *Development* 131, 1787-1799.
- Lobo, N.A., Shimono, Y., Qian, D., and Clarke, M.F. (2007). The biology of cancer stem cells. *Annu Rev Cell Dev Biol* 23, 675-699.
- Lyle, S., Christofidou-Solomidou, M., Liu, Y., Elder, D.E., Albelda, S., and Cotsarelis, G. (1998). The C8/144B monoclonal antibody recognizes cytokeratin 15 and defines the location of human hair follicle stem cells. *J Cell Sci* 111 ( Pt 21), 3179-3188.
- Mackenzie, I.C., and Bickenbach, J.R. (1985). Label-retaining keratinocytes and Langerhans cells in mouse epithelia. *Cell Tissue Res* 242, 551-556.
- Malanchi, I., Peinado, H., Kassen, D., Hussenet, T., Metzger, D., Chambon, P., Huber, M., Hohl, D., Cano, A., Birchmeier, W., *et al.* (2008). Cutaneous cancer stem cell maintenance is dependent on beta-catenin signalling. *Nature* 452, 650-653.
- Mancuso, M., Leonardi, S., Tanori, M., Pasquali, E., Pierdomenico, M., Rebessi, S., Di Majo, V., Covelli, V., Pazzaglia, S., and Saran, A. (2006). Hair cycle-dependent basal cell carcinoma tumorigenesis in *Ptc1*neo67/+ mice exposed to radiation. *Cancer Res* 66, 6606-6614.
- Mao, X., Fujiwara, Y., and Orkin, S.H. (1999). Improved reporter strain for monitoring Cre recombinase-mediated DNA excisions in mice. *Proc Natl Acad Sci U S A* 96, 5037-5042.
- Merrill, B.J., Gat, U., DasGupta, R., and Fuchs, E. (2001). Tcf3 and Lef1 regulate lineage differentiation of multipotent stem cells in skin. *Genes Dev* 15, 1688-1705.
- Millar, S.E. (2002). Molecular mechanisms regulating hair follicle development. *J Invest Dermatol* 118, 216-225.
- Milner, Y., Sudnik, J., Filippi, M., Kizoulis, M., Kashgarian, M., and Stenn, K. (2002). Exogen, shedding phase of the hair growth cycle: characterization of a mouse model. *J Invest Dermatol* 119, 639-644.
- Montagna, W., and Parakkal, P. (1974). <<The>> structure and function of skin, 3rd edn (New York, Academic Press).
- Morris, R.J., Liu, Y., Marles, L., Yang, Z., Trempus, C., Li, S., Lin, J.S., Sawicki, J.A., and Cotsarelis, G. (2004). Capturing and profiling adult hair follicle stem cells. *Nat Biotechnol* 22, 411-417.

- Morris, R.J., and Potten, C.S. (1994). Slowly cycling (label-retaining) epidermal cells behave like clonogenic stem cells in vitro. *Cell Prolif* 27, 279-289.
- Morris, R.J., Tacker, K.C., Baldwin, J.K., Fischer, S.M., and Slaga, T.J. (1987). A new medium for primary cultures of adult murine epidermal cells: application to experimental carcinogenesis. *Cancer Lett* 34, 297-304.
- Muller-Rover, S., Handjiski, B., van der Veen, C., Eichmuller, S., Foitzik, K., McKay, I.A., Stenn, K.S., and Paus, R. (2001). A comprehensive guide for the accurate classification of murine hair follicles in distinct hair cycle stages. *J Invest Dermatol* 117, 3-15.
- Nelson, W.G., and Sun, T.T. (1983). The 50- and 58-kdalton keratin classes as molecular markers for stratified squamous epithelia: cell culture studies. *J Cell Biol* 97, 244-251.
- Nguyen, H., Rendl, M., and Fuchs, E. (2006). Tcf3 governs stem cell features and represses cell fate determination in skin. *Cell* 127, 171-183.
- Niemann, C., Owens, D.M., Hulsken, J., Birchmeier, W., and Watt, F.M. (2002). Expression of DeltaNlcf1 in mouse epidermis results in differentiation of hair follicles into squamous epidermal cysts and formation of skin tumours. *Development* 129, 95-109.
- Niemann, C., Owens, D.M., Schettina, P., and Watt, F.M. (2007). Dual role of inactivating Lef1 mutations in epidermis: tumor promotion and specification of tumor type. *Cancer Res* 67, 2916-2921.
- Niemann, C., Uuden, A.B., Lyle, S., Zouboulis Ch, C., Toftgard, R., and Watt, F.M. (2003). Indian hedgehog and beta-catenin signaling: role in the sebaceous lineage of normal and neoplastic mammalian epidermis. *Proc Natl Acad Sci U S A* 100 Suppl 1, 11873-11880.
- Niemann, C., and Watt, F.M. (2002). Designer skin: lineage commitment in postnatal epidermis. *Trends Cell Biol* 12, 185-192.
- Nijhof, J.G., Braun, K.M., Giangreco, A., van Pelt, C., Kawamoto, H., Boyd, R.L., Willemze, R., Mullenders, L.H., Watt, F.M., de Gruijl, F.R., *et al.* (2006). The cell-surface marker MTS24 identifies a novel population of follicular keratinocytes with characteristics of progenitor cells. *Development* 133, 3027-3037.
- Nöbel, H. (2009). Analysen zur Regulation und Manipulation von epithelialen Progenitorzellen. diploma thesis, University of Cologne, germany.
- Nowak, J.A., Polak, L., Pasolli, H.A., and Fuchs, E. (2008). Hair follicle stem cells are specified and function in early skin morphogenesis. *Cell Stem Cell* 3, 33-43.
- Ntambi, J.M. (1995). The regulation of stearyl-CoA desaturase (SCD). *Prog Lipid Res* 34, 139-150.
- Nusse, R. (2005). Wnt signaling in disease and in development. *Cell Res* 15, 28-32.
- O'Brien, C.A., Pollett, A., Gallinger, S., and Dick, J.E. (2007). A human colon cancer cell capable of initiating tumour growth in immunodeficient mice. *Nature* 445, 106-110.
- Owens, D.M., and Watt, F.M. (2003). Contribution of stem cells and differentiated cells to epidermal tumours. *Nat Rev Cancer* 3, 444-451.
- Panteleyev, A.A., Rosenbach, T., Paus, R., and Christiano, A.M. (2000). The bulge is the source of cellular renewal in the sebaceous gland of mouse skin. *Arch Dermatol Res* 292, 573-576.
- Paus, R., Muller-Rover, S., Van Der Veen, C., Maurer, M., Eichmuller, S., Ling, G., Hofmann, U., Foitzik, K., Mecklenburg, L., and Handjiski, B. (1999). A comprehensive guide for the recognition and classification of distinct stages of hair follicle morphogenesis. *J Invest Dermatol* 113, 523-532.



- Peinkofer, G. (2008). Function of lymphoid enhancer factor1(Lef1) in skin tumorigenesis and epidermal stem cell regulation. diploma thesis, University of Cologne, Germany.
- Polakis, P. (2000). Wnt signaling and cancer. *Genes Dev* 14, 1837-1851.
- Potten, C.S. (1974). The epidermal proliferative unit: the possible role of the central basal cell. *Cell Tissue Kinet* 7, 77-88.
- Prince, M.E., and Ailles, L.E. (2008). Cancer stem cells in head and neck squamous cell cancer. *J Clin Oncol* 26, 2871-2875.
- Raymond, K., Richter, A., Kreft, M., Frijns, E., Janssen, H., Slijper, M., Praetzel-Wunder, S., Langbein, L., and Sonnenberg, A. (2010). Expression of the Orphan Protein Plet-1 during Trichilemmal Differentiation of Anagen Hair Follicles. *J Invest Dermatol*.
- Rendl, M., Polak, L., and Fuchs, E. (2008). BMP signaling in dermal papilla cells is required for their hair follicle-inductive properties. *Genes Dev* 22, 543-557.
- Rhee, H., Polak, L., and Fuchs, E. (2006). Lhx2 maintains stem cell character in hair follicles. *Science* 312, 1946-1949.
- Rheinwald, J.G. (1989). Human epidermal keratinocyte cell culture and xenograft systems: applications in the detection of potential chemical carcinogens and the study of epidermal transformation. *Prog Clin Biol Res* 298, 113-125.
- Rheinwald, J.G., and Green, H. (1975). Serial cultivation of strains of human epidermal keratinocytes: the formation of keratinizing colonies from single cells. *Cell* 6, 331-343.
- Sambrook, J., and Russel, R.B. (2001). *Molecular Cloning: A laboratory Manual*. Cold Spring Harb.
- Sampath, H., Flowers, M.T., Liu, X., Paton, C.M., Sullivan, R., Chu, K., Zhao, M., and Ntambi, J.M. (2009). Skin-specific deletion of stearyl-CoA desaturase-1 alters skin lipid composition and protects mice from high fat diet-induced obesity. *J Biol Chem* 284, 19961-19973.
- Schatton, T., Murphy, G.F., Frank, N.Y., Yamaura, K., Waaga-Gasser, A.M., Gasser, M., Zhan, Q., Jordan, S., Duncan, L.M., Weishaupt, C., *et al.* (2008). Identification of cells initiating human melanomas. *Nature* 451, 345-349.
- Schneider, M.R., and Paus, R. (2009). Sebocytes, multifaceted epithelial cells: Lipid production and holocrine secretion. *Int J Biochem Cell Biol*.
- Segre, J.A. (2006). Epidermal barrier formation and recovery in skin disorders. *J Clin Invest* 116, 1150-1158.
- Snippert, H.J., Haegebarth, A., Kasper, M., Jaks, V., van Es, J.H., Barker, N., van de Wetering, M., van den Born, M., Begthel, H., Vries, R.G., *et al.* (2010). Lgr6 marks stem cells in the hair follicle that generate all cell lineages of the skin. *Science* 327, 1385-1389.
- Soriano, P. (1999). Generalized lacZ expression with the ROSA26 Cre reporter strain. *Nat Genet* 21, 70-71.
- Sotiropoulou, P.A., Candi, A., and Blanpain, C. (2008). The majority of multipotent epidermal stem cells do not protect their genome by asymmetrical chromosome segregation. *Stem Cells* 26, 2964-2973.
- Srinivas, S., Watanabe, T., Lin, C.S., Williams, C.M., Tanabe, Y., Jessell, T.M., and Costantini, F. (2001). Cre reporter strains produced by targeted insertion of EYFP and ECFP into the ROSA26 locus. *BMC Dev Biol* 1, 4.
- St-Jacques, B., Dassule, H.R., Karavanova, I., Botchkarev, V.A., Li, J., Danielian, P.S., McMahon, J.A., Lewis, P.M., Paus, R., and McMahon, A.P. (1998). Sonic hedgehog signaling is essential for hair development. *Curr Biol* 8, 1058-1068.

- Stern, M.M., and Bickenbach, J.R. (2007). Epidermal stem cells are resistant to cellular aging. *Aging Cell* 6, 439-452.
- Taipale, J., and Beachy, P.A. (2001). The Hedgehog and Wnt signalling pathways in cancer. *Nature* 411, 349-354.
- Takeda, H., Lyle, S., Lazar, A.J., Zouboulis, C.C., Smyth, I., and Watt, F.M. (2006). Human sebaceous tumors harbor inactivating mutations in LEF1. *Nat Med*.
- Taylor, G., Lehrer, M.S., Jensen, P.J., Sun, T.T., and Lavker, R.M. (2000). Involvement of follicular stem cells in forming not only the follicle but also the epidermis. *Cell* 102, 451-461.
- Trempus, C.S., Morris, R.J., Bortner, C.D., Cotsarelis, G., Faircloth, R.S., Reece, J.M., and Tennant, R.W. (2003). Enrichment for living murine keratinocytes from the hair follicle bulge with the cell surface marker CD34. *J Invest Dermatol* 120, 501-511.
- Tumbar, T., Guasch, G., Greco, V., Blanpain, C., Lowry, W.E., Rendl, M., and Fuchs, E. (2004). Defining the epithelial stem cell niche in skin. *Science* 303, 359-363.
- Vidal, V.P., Chaboissier, M.C., Lutzkendorf, S., Cotsarelis, G., Mill, P., Hui, C.C., Ortonne, N., Ortonne, J.P., and Schedl, A. (2005). Sox9 is essential for outer root sheath differentiation and the formation of the hair stem cell compartment. *Curr Biol* 15, 1340-1351.
- Visvader, J.E., and Lindeman, G.J. (2008). Cancer stem cells in solid tumours: accumulating evidence and unresolved questions. *Nat Rev Cancer* 8, 755-768.
- Waghmare, S.K., Bansal, R., Lee, J., Zhang, Y.V., McDermitt, D.J., and Tumbar, T. (2008). Quantitative proliferation dynamics and random chromosome segregation of hair follicle stem cells. *Embo J* 27, 1309-1320.
- Wang, J.C. (2010). Good cells gone bad: the cellular origins of cancer. *Trends Mol Med* 16, 145-151.
- Wang, J.C., and Dick, J.E. (2005). Cancer stem cells: lessons from leukemia. *Trends Cell Biol* 15, 494-501.
- Watt, F.M. (1994). Cultivation of human epidermal keratinocytes with a 3T3 feeder layer. In *Cell biology: A laboratory handbook* Cambridge University Press, Cambridge, UK, 83-89.
- Watt, F.M., Frye, M., and Benitah, S.A. (2008). MYC in mammalian epidermis: how can an oncogene stimulate differentiation? *Nat Rev Cancer* 8, 234-242.
- Watt, F.M., and Hogan, B.L. (2000). Out of Eden: stem cells and their niches. *Science* 287, 1427-1430.
- Watt, F.M., and Jensen, K.B. (2009). Epidermal stem cell diversity and quiescence. *EMBO Mol Med* 1, 260-267.
- Weger, N., and Schlake, T. (2005). Igf-I signalling controls the hair growth cycle and the differentiation of hair shafts. *J Invest Dermatol* 125, 873-882.
- Youssef, K.K., Van Keymeulen, A., Lapouge, G., Beck, B., Michaux, C., Achouri, Y., Sotiropoulou, P.A., and Blanpain, C. (2010). Identification of the cell lineage at the origin of basal cell carcinoma. *Nat Cell Biol* 12, 299-305.
- Zhang, L., Li, W.H., Anthonavage, M., and Eisinger, M. (2006). Melanocortin-5 receptor: a marker of human sebocyte differentiation. *Peptides* 27, 413-420.
- Zhang, Y.V., Cheong, J., Ciapurin, N., McDermitt, D.J., and Tumbar, T. (2009). Distinct self-renewal and differentiation phases in the niche of infrequently dividing hair follicle stem cells. *Cell Stem Cell* 5, 267-278.
- Zhang, Y.V., White, B.S., Shalloway, D.I., and Tumbar, T. (2010). Stem cell dynamics in mouse hair follicles: A story from cell division counting and single cell lineage tracing. *Cell Cycle* 9.

- Zheng, Y., Eilertsen, K.J., Ge, L., Zhang, L., Sundberg, J.P., Prouty, S.M., Stenn, K.S., and Parimoo, S. (1999). *Scd1* is expressed in sebaceous glands and is disrupted in the *asebia* mouse. *Nat Genet* 23, 268-270.
- Zouboulis, C.C. (2004). Acne and sebaceous gland function. *Clin Dermatol* 22, 360-366.
- Zouboulis, C.C., Adjaye, J., Akamatsu, H., Moe-Behrens, G., and Niemann, C. (2008a). Human skin stem cells and the ageing process. *Exp Gerontol* 43, 986-997.
- Zouboulis, C.C., Baron, J.M., Bohm, M., Kippenberger, S., Kurzen, H., Reichrath, J., and Thielitz, A. (2008b). Frontiers in sebaceous gland biology and pathology. *Exp Dermatol* 17, 542-551.

## 8 Figure index

Fig 1: Organisation of the skin.....	1
Fig 2: Structure of the pilosebaceous unit.....	3
Fig 3: Structure of the SG.....	4
Fig 4: The HFSC niche and its markers .....	7
Fig 5: Epidermal SC/ progenitor niches of the UI and JZ.....	8
Fig 6: Cyclic renewal of the HF .....	11
Fig 7: Scheme depicting the Wnt/ $\beta$ -catenin pathway in repressed (left) and active state (right) (Fodde and Brabletz, 2007) .....	13
Fig 8: Manipulation of canonical Wnt signalling affects epidermal homeostasis.....	14
Fig 9: Formation of ectopic SG in K14 $\Delta$ NLef1 mice.....	15
Fig 10: Scheme depicting cloning procedure for generating pK15CreER(G)T2 (see also text).....	23
Fig 11: Schematic representation of cloning of K15 $\Delta$ NLef1 .....	24
Fig 12: Different SC/progenitor compartments within the epidermis.....	34
Fig 13: Generation of K15CreER(G)T2 mice to target HFSC and to map HFSC-derived progeny.....	36
Fig 14: Scheme depicting the K15CreER(G)T2 construct.....	36
Fig 15: Generation of pK15CreER(G)T2 .....	37
Fig 16: pK15CreER(G)T2 is inducible and active <i>in vitro</i> .....	38
Fig 17: Identification of K15CreER(G)T2 founder lines .....	39
Fig 18: Optimisation of tamoxifen application procedure and detection methods .....	41
Fig 19: Targeting of bulge cells using K15CreER(G)T2 .....	43
Fig 20: Genetically targeted cells co-localise with established HFSC/progenitor markers .....	44
Fig 21: Targeted bulge cells are capable to regenerate all hair lineages.....	47
Fig 22: Commitment of bulge-derived progeny to sebaceous lineage .....	49
Fig 23: Epidermal regeneration during different stages of the hair cycle .....	51
Fig 24: Labelled bulge-derived progeny is competent to regenerate all epidermal compartments after 6 months of tracing.....	53
Fig 25: Traced bulge-derived cells co-express different progenitor markers .....	55

---

Fig 26: HFSC derived progeny at the periphery of the SG expressed markers for sebaceous lineage .....	57
Fig 27: Epidermal SC and SG-associated markers are differentially expressed in K14 $\Delta$ NLef1 mice. ....	59
Fig 28: Bulge-derived progeny contributes to ectopic SG formation in K14 $\Delta$ NLef1 mice.....	60
Fig 29: Ectopic SG formation is accompanied with the establishment.....	62
Fig 30: Development of skin lesions and sebaceous adenomas in K14 $\Delta$ NLef1-mice.....	64
Fig 31: Optimisation of the detection protocols for lineage tracing experiment during sebaceous tumour formations .....	66
Fig 32: Bulge-derived progeny contributes to sebaceous adenoma formation .....	68
Fig 33: pK15 $\Delta$ NLef1 was cloned and linearised for subsequent microinjection .....	70
Fig 34: Characterisation of K15 $\Delta$ NLef1-mice (F0-F2 generation) .....	73
Fig 35: Hierarchy of epidermal SC .....	81
Fig 36: Potential role of cell fate determination centers for epidermal regeneration ..	83
Fig 37: Imbalanced activation of HFSC could be accompanied with ageing.....	84
Fig 38: HFSC-derived progeny contributes to ectopic SG and sebaceous adenoma formation. ....	89

## 9 Table index

Table 1: Identification of several marker molecules at different epidermal SC/progenitor compartments .....	1
Table 2: Molecular biological enzymes .....	19
Table 3: Used plasmids.....	20
Table 4: Oligonucleotides used for genotyping .....	20
Table 5: Oligonucleotides used for qRT-PCR .....	21
Table 6: Used antibodies.....	25
Table 7: Analysis of Cre expression, number of labelled cells and intensity of Cre-reporter gene activation in K15CreER(G)T2/Cre reporter mice .....	42
Table 8: Detection of EYFP <sup>+</sup> ve keratinocytes in early lesions and sebaceous tumours derived from DMBA treated A_K15CreER(G)T2/R26REYFP/K14 $\Delta$ NLef1 mice (n= 6 mice).....	69

## 10 List of abbreviations

APC	Adenomatous Polyposis Coli
A	adenine
amp	ampicillin
B	Bulge
bp	base pair
BLIMP1	B-lymphocyte-induced maturation protein 1
BM	basement membrane
BMP	Bone Morphogenetic Protein
BrdU	5-bromo-2`desoxyuridine
BD	binding domain
°C	temperature in degree Celsius
cDNA	complementary DNA
CK1 $\alpha$	Casein Kinase 1 $\alpha$
CMV	cytolomegavirus
CO <sub>2</sub>	carbon dioxide
Cre	site specific recombinase from bacteriophageP1 causes recombination
c-myc	cellular myelo cytomatosis oncogene
CSC	cancer stem cell
ddH <sub>2</sub> O	double distilled water
DE	dermis
DMBA	dimethylbenz-[a]-anthracene
CMMC	Center for Molecular Medicine Cologne
DP	dermal papilla
DSH	Dishevelled
EPU	epidermal proliferative unit
for	forward
g	gram/gravitation
GSK-3 $\beta$	glycogen synthase kinase 3 $\beta$
EDTA	ethylenediaminetetraacetic acid
EGFP	enhanced gree fluorescent protein
EGTA	ethylenediaminetetraacetic acid
EtBr	ethidiumbromide
EtOH	ethanol
EYFP	enhanced yellow fluorescent protein
FCS	fetal calf serum
h	hour
HCl	hydrochloric acid
H_E	haematoxyline and eosin
HEPES	4-(2-hydroxyethyl)-1piperazineethanesulfonic acid
HG	secondary hair germ
Hh	Hedgehog
HF	hair follicle
HS	hair shaft
IFE	interfollicular epidermis
i.p.	intraperitoneal
IFE	interfollicular epidermis
IRS	inner root sheath

Itga6	$\alpha$ 6-integrin
JZ	junctional zone
K14	Keratin 14
K15	Keratin 15
KPP	potassium phosphate-buffer
l	liter
LacZ	gene encoding for $\beta$ -galactosidase
Lef1	lymphoid enhancer factor 1
Lgr5/6	leucine-rich repeat-containing G-protein coupled receptor 5/6
LRC	label retaining cells
Lrig1	leucine rich immunoglobuline-like factor 1
m	milli/meter
M	molar
MgCl <sub>2</sub>	magnesium chloride
min	minute
MTS24	murine thymic stroma24
Mx	hair matrix
n	nano
NaCl	sodium chloride
NaOH	sodium hydroxide
ORS	outer root sheath
p	pico
PCR	polymerase chain reaction
PFA	paraformaldehyde
PD	post natal day
Plet1	glycoylphosphatidylinositol-anchored glycoprotein1
PBS	phosphate buffered saline
RNA	ribonucleic acid
rev	reverse
rpm	rounds per minute
RT	reverse transcriptase/room temperature
SA	sebaceous adenoma
Sca-I	Stem cell antigen1
SC	stem cell
SCC	squamous cell carcinoma
SCD1	Stearoyl-Coenzym A Desaturase 1
S.D.	standard deviation
SD	sebaceous duct
SDS	sodiumdodecylsulfate
sec	second
TAE	Tris-acetic acid-EDTA-buffer
TA	transit amplifying
Tam	tamoxifen
Tris	2-amino-2(hydroxymethyl)1,3-propandiole
Tween	polyoxethylene-sorbitan-monolaureate
TCF	T-cell factor
tg	transgenic
U	unit
UI	upper isthmus



V	volt
VDR	Vitamin D receptor
wt	wildtype
%(v/v)	volume-volume percentage
5'	five prime-end of DNA sequences
3'	three prime-end of DNA sequences
Δ	deleted / mutated allele
μ	micro

## ***Acknowledgements***

I sincerely thank Catherin Niemann for the excellent supervision, tremendous support and for providing me with this interesting and challenging project.

I would like to thank Prof. Dr. Jens Brüning, Prof. Dr. Thomas Krieg and Prof. Dr. Matthias Hammerschmidt for agreeing to form my thesis committee, and Dr. Debora Grosskopf-Kroiher for her continuous help.

I would like to thank all former and present members of the Niemann and Niessen lab for their help and the good time in and outside the lab. I thank Susan John, Gilles Séquaris, Parisa Kakanj, Claudia Wodtke and Michaela Niessen for the stimulating discussions and general advice. Special thanks to Heike Brylka, Gabriel Peinkofer and Heike Nöbel for their support.

I particularly appreciate the support and endless encouragement of Andreas Kraus, Dagmar Fehrenschild and Peter Schettina.

I am especially thankful to Chantal Brüggemann and Klaus Kruttwig (MPI for neurological research, Cologne) and Daniela Bobermien for their support, friendship and critically reading my thesis.

Furthermore, I would like to thank Pierre Chambon and George Cotsarelis for providing us with the constructs and general advice.

Finally, I remain indebted to my parents, my brother, Cornelia Nell and Thomas Nagy for their patience, love and encouragement.

## ***Eidesstattliche Erklärung***

Ich versichere, dass ich die von mir vorgelegte Dissertation selbständig angefertigt, die benutzten Quellen und Hilfsmittel vollständig angegeben und die Stellen der Arbeit – einschließlich Tabellen, Karten und Abbildungen –, die anderen Werken im Wortlaut oder dem Sinn nach entnommen sind, in jedem Einzelfall als Entlehnung kenntlich gemacht habe; dass diese Dissertation noch keiner anderen Fakultät oder Universität zur Prüfung vorgelegen hat; dass sie – abgesehen von unten angegebenen Teilpublikationen – noch nicht veröffentlicht worden ist sowie, dass ich eine solche Veröffentlichung vor Abschluss des Promotionsverfahrens nicht vornehmen werde. Die Bestimmungen der Promotionsordnung sind mir bekannt. Die von mir vorgelegte Dissertation ist von Herrn Prof. Dr. Jens Brüning betreut worden.

Köln, im Mai 2010

Monika Petersson

Teilpublikationen im Rahmen dieser Arbeit:

# 11 Curriculum vitae

## Bildungsweg

---

seit 2004	Promotion am Zentrum für Molekulare Medizin (ZMMK) der Universität zu Köln  NGIV Niemann: Mechanismen der Morphogenese und Differenzierung des Hautepithels  Teilnahme am Interdisziplinären Postgraduierten Programm „Molekulare Medizin“
2003-2004	Wissenschaftliche Hilfstätigkeit am Lehrstuhl für Molekulare Genetik (Prof. Dr. R. Knippers)
1998-2003	Biologiestudium an der Universität Konstanz  Mündliches Abschlusskolloquium in den Fachgebieten Genetik und Biochemie  Diplomarbeit am Lehrstuhl für Molekulare Genetik (Prof. Dr. R. Knippers) Thema :“Effekte von genotoxischen Verbindungen auf den Prä-Replikationskomplex in eukaryotischen Zellen in Kultur“ Abschluss Diplom
1989-1998	Helmholtz-Gymnasium Hilden  Erwerb der allgemeinen Hochschulreife
1985-1989	Gemeinschafts-Grundschule Zur Verlach, Hilden

## Publikationen

---

**Petersson M.**, Brylka H., Kraus A., Niemann C. A hierarchy of stem and progenitor cells drives renewal of mammalian epidermis (manuscript submitted)

Schettina P., **Petersson M.**, Fehrenschild D., Sequaris G., Siebolts U., Munro P., Daniels J., Watt FM, Niemann C. Functional Lef1 is required for corneal cell fate and lens differentiation of the eye (manuscript submitted)

## **Vorträge**

---

- 2010      Ausgewählt für eine Präsentation auf der Jahrestagung der  
            "International Society for Stem Cell Research" im Juni, 2010, San  
            Francisco, USA
- 2010      "Crossroads in Biology"-Symposium, Köln
- 2009      Combined meeting of "XVII<sup>th</sup> Annual Congress of the European  
            Society of Gene and Cell Therapy (ESGCT), 4<sup>th</sup> Annual  
            Congress of the German Society for Stem Cell Research and  
            International Society for Cellular Therapy (ISCT)", Hannover